2022

Directly Polymerizable CO Releasing Molecules

Jackson Snow
University of Denver

Directly Polymerizable CO Releasing Molecules

Abstract

Despite the commonly held consensus that carbon monoxide (CO) is toxic, it has been shown to be an essential signaling molecule in the human neuronal system and has been noted to have anti-inflammatory properties, act as a vasodilator, have anti-proliferative impacts on tumors, and many other beneficial effects. The current limitation to using CO as a therapeutic molecule is delivering the proper dosages using CO releasing molecules (CORMs) without exhibiting toxicity. The first chapter of this thesis will review the biological significance of CO in biological systems, the limitations of existing CORMs, and the properties of diphenylcyclopropenone (DPCP) that make it a promising CORM. The second chapter of this thesis will describe our work to develop a new class of directly polymerizable organic CORMs based on DPCP.

Document Type

Thesis

Degree Name

M.S.

Department

Chemistry and Biochemistry

First Advisor

Brady T. Worrell

Second Advisor

Brian Michel

Third Advisor

Sunil Kumar

Keywords

Carbon monoxide releasing molecules (CORM), Diphenylcyclopropenone, Quantum Chain Reaction

Subject Categories

Chemistry | Polymer Chemistry

Directly Polymerizable CO Releasing Molecules

_____

A Thesis

Presented to

the Faculty of the College of Natural Sciences and Mathematics

University of Denver

_____

In Partial Fulfillment

of the Requirements for the Degree

Master of Science

_____

by

Jackson Snow

November 2022

Advisor: Brady Worrell

Author: Jackson Snow
Title: Directly Polymerizable CO Releasing Molecules
Advisor: Brady Worrell
Degree Date: November 2022

Abstract

Despite the commonly held consensus that carbon monoxide (CO) is toxic, it has been shown to be an essential signaling molecule in the human neuronal system and has been noted to have anti-inflammatory properties, act as a vasodilator, have anti-proliferative impacts on tumors, and many other beneficial effects. The current limitation to using CO as a therapeutic molecule is delivering the proper dosages using CO releasing molecules (CORMs) without exhibiting toxicity. The first chapter of this thesis will review the biological significance of CO in biological systems, the limitations of existing CORMs, and the properties of diphenylcyclopropenone (DPCP) that make it a promising CORM. The second chapter of this thesis will describe our work to develop a new class of directly polymerizable organic CORMs based on DPCP.

Acknowledgements

I would like to begin by thanking Dr. Ivan Novitskiy for always having chemicals we need to try new experiments. I have been fortunate to have a wonderful support network throughout my time at DU. Fortunately, I had Casey Patrick, Kelby Johnson, and Ben Wingo here when I arrived in Denver. My mother Paula and stepfather Jeremy weren't too far from Denver either. Shortly after arriving, I began spending a huge piece of my life with Sophia Todorov. Jeshurun Small deserves a huge shout out for all the fun Zwift conversations about chemistry. Finally, I would like to acknowledge my father Jimmy and sister Emma. I appreciate you all and I don't think I would have made it this far without you! I have saved some of the longer acknowledgements for last: The Worrell Lab. I would like to thank Nick Bagnall for dealing with me on a daily basis, teaching me a lot about chemistry, and helping me out around the lab. Thank you thank you thank you Meredith Jones for being yourself. You've become a wonderful friend of mine and I am already cherishing our memories both inside and outside of lab. I look forward to more good times! Cole Jernigan. What a guy. I think he has dice in his pocket. Thank you so much for providing comedic relief during desperate times. And very importantly, thank you for the work you've done on this project. Specifically, optimizing and scaling up a lot of the synthesis. Last but least, thank you Brady Worrell. I owe you many random thank yous that would take up too much space, so I will keep it brief. Thank you for being a friend and an advisor. You have really sculpted the way I think about science and the way that I think about life. I appreciate how you supported me through my journey. I've changed and grown a lot over these last two years and I'm realizing now that it is probably your fault.

Table of Contents

List of Figures

List of Tables

List of Schemes

Abbreviations

°C	Degrees Celsius
AIBN	azobisisobutyronitrile
$AlCl_3$	aluminum trichloride
ATP	adenosine triphosphate
BBr_3	Boron tribromide
cGMP	cyclic guanosine monophosphate
CO	Carbon monoxide
CORM	CO Releasing Molecule
CPDB	2-Cyano-2-propyl benzodithioate
CTAB	cetrimonium bromide
Đ	dispersity
DCM	dichloromethane
DMAP	Dimethylaminopyridine
DMF	dimethylformamide
DMSO	dimethylsulfoxide
DoPAT	(Dodecylthiocarbonothioylthio)propionic acid
DPA	diphenylacetylene
DPCP	diphenylcyclopropenone
DTB-2PA	2-[(Phenylthioxomethyl)thio]propanoic acid
EtOAc	Ethyl Acetate
GPC	Gel permeation chromatography

HbCO	Carboxyhemoglobin
HO	Heme oxygenase
HO-1	Heme oxygenase-1
HO-2	Heme oxygenase-2
HO-3	Heme oxygenase-3
KOtBu	Potassium tert-butoxide
M	molarity
MeCN	Acetonitrile
MeOH	Methanol
n-BuLi	n-butyllithium
NMR	Nuclear Magnetic Resonance
PEG	Poly ethylene glycol
Ppb	Parts per billion
RAFT	Reversible Addition-Fragmentation Chain Transfer
TEA	Triethylamine
THF	tetrahydrofuran
TLC	Thin layer chromatography
UV	ultraviolet
Φ	Quantum yield

1. Introduction

1.1 Carbon Monoxide

Carbon monoxide (CO) is a colorless, odorless, and tasteless gas that is commonly considered a hazardous chemical.[1] CO contains one carbon atom and one oxygen connected by a triple bond comprised of two pi bonds and one sigma bond. CO is the simplest oxide of carbon and contains 10 valence electrons, making it isoelectronic with other triple bonded diatomic molecules such as cyanide and molecular nitrogen. Small amounts (about 100 ppb) of CO are found in unpolluted parts of Earth's atmosphere, and pollution in urban areas can result in the concentration of CO increasing up to tenfold.[2] The most common sources of CO are anthropogenic and natural combustion of carbon containing compounds.[3] Other natural sources of CO include photochemical reactions within Earth's troposphere and various geologic activity.[4] When CO is emitted into the atmosphere, it affects several processes that contribute to climate change.[5] CO is industrially and biologically relevant because it plays an important role in producing plastics, pharmaceuticals, and other products that benefit humanity.[6]

1.2 CO in Biological Systems

The common consensus is that CO is a toxic molecule. This is because it has a very strong affinity for heme, which is a precursor to hemoglobin that binds and transports molecular oxygen throughout the bloodstream. CO's affinity for heme is about 220 times stronger than oxygen's affinity for heme, therefore, when CO is present it will

preferentially bind to hemoglobin to produce carboxyhemoglobin (HbCO), reducing the capacity for oxygen transport.[7] CO poisoning is considered severe when HbCO levels reach 30% and levels above 56% are typically fatal.[8] Despite CO toxicity at high concentrations, this gas is produced endogenously in small quantities. About 86% of endogenously produced CO is through the oxidative breakdown of heme while the other 14% is produced by the reduction of cytochromes, enzymatic and photo-oxidation of organic compounds, ascorbate-catalyzed lipid peroxidation of lipids and phospholipids.[9]

Three isoforms of heme oxygenase (HO) enzymes are responsible for catalyzing the first step in degrading heme to produce CO, biliverdin, and iron (**Figure 1**). Heme

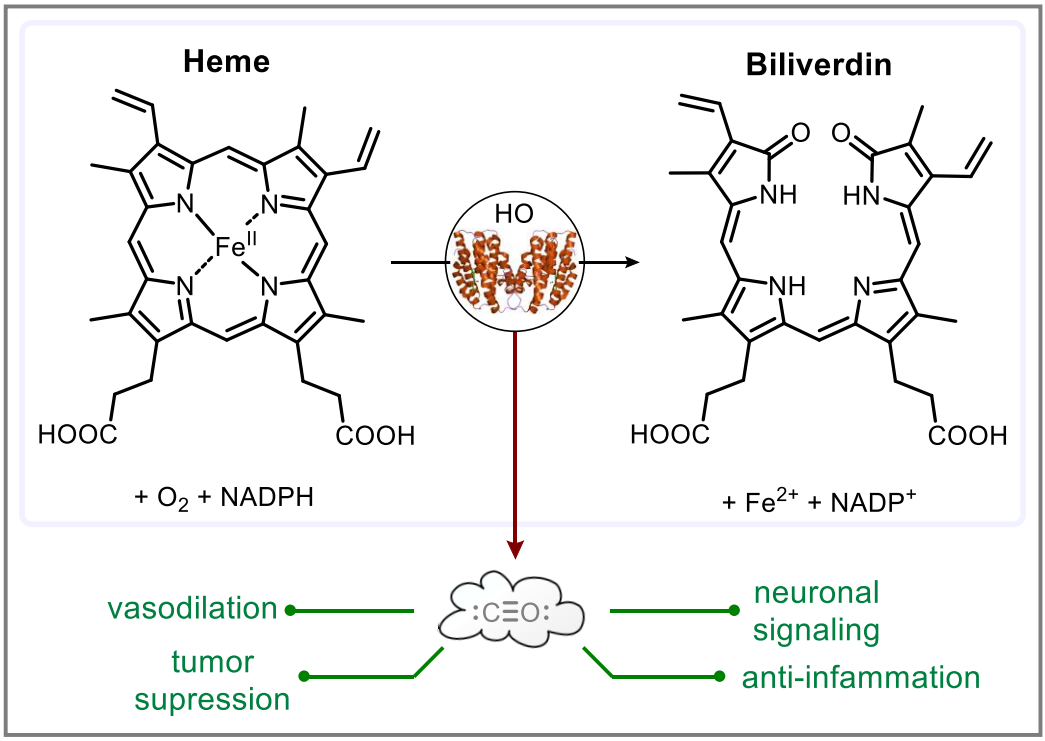

Figure 1: Methods for generation of endogenous CO in biological settings. *Green lines:* Known biological responses to CO gas.

oxygenase-1 (HO-1) is induced by stress and heme oxygenase-2 (HO-2) is expressed constitutively. Heme oxygenase-3 (HO-3) has been identified as a significantly less

catalytic homologue of HO-2.[10] HOs are often thought of as cytoprotectants because their catalytic product, CO, has many important biological roles.[11] Once CO is produced endogenously, it diffuses across tissue and activates soluble guanylyl cyclase, producing cyclic guanosine monophosphate (cGMP), which acts as a secondary messenger in a variety of cellular functions.

Since CO was identified as an endogenous gaseous neurotransmitter, many studies manipulating HOs have shown that CO is an essential signaling molecule throughout the human body.[12] For example, removal of the gene that encodes for HO-2, the isoform of HO responsible for nearly all constitutive production of CO in the central nervous system, increases neurotoxicity in brain cells and exacerbates oxidative stress which leads to neurodegenerative disease, tissue damage, and inflammation.[13] A different study showed that CO gas has been noted to have anti-inflammatory properties as oxidative stress can induce the upregulation of HO-1. After HO-1 catalyzes the breakdown of heme, CO inhibits expression of pro-inflammatory proteins and escalates expression of anti-inflammatory proteins such as interleukin-10.[14] Studies observing vascular constriction upon inhibition of HO-1 has shown that CO acts as a vasodilator.[15,16] Using antibodies against HO-1 in tumor cells has shown that CO increases cancer cell sensitivity to chemotherapeutics 1,000-fold.[17] Manipulation of HOs provides plentiful insight in to the role of endogenous CO production, deeming CO a promising therapeutic molecule. Unfortunately, clinical applications of inhaled CO are limited due of the difficulty of delivering gaseous CO and potential hazards related with administering and handling this toxic gas.

1.3 Controlled Release of CO

Given the vast research and therapeutic potentials of CO, many molecules that selectively produce CO gas when triggered by various stimuli have been designed and synthesized, which are referred to as CO Releasing Molecules, or **CORMs** (**Figure 2**).[18,19] **CORMs**, as originally reported in 2002, have given researchers a new set of tools to generate CO gas and directly study its effects on biological systems.[20] Application of **CORMs** not only allow researchers to quantitatively and temporally control dosages of CO, they avoid CO delivery by inhalation which greatly reduces the probability of encountering the toxic effects of CO.

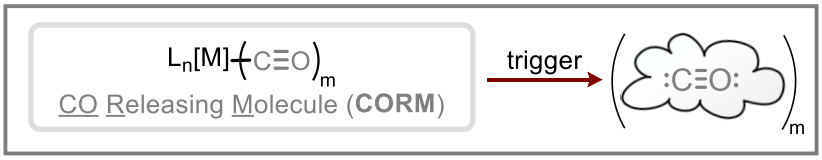

Figure 2: A simplified model of a carbon monoxide-releasing molecule (**CORM**).

CORMs have been utilized in multiple model animal studies to corroborate the beneficial effects of CO.[21–27] **CORMs** such as **1a** (**Figure 3A**) have been used to show that CO may be a beneficial treatment for inflammatory diseases such as arthritis. A study showed that treating arthritis in mice with **1a** reduced the expression of pro-inflammatory proteins.[21] **CORMs** such as **1a** and **1c** have been used to study the role of CO in cardiovascular disease. A mouse model designed to have a coronary occlusion had blood infusions of **1a**, which showed that CO reduced the size and number of heart attacks.[22] A second model transplanted HO-1 deficient mouse abdominal aorta to show the importance of CO in cardiovascular disease. This study found that treating these mice with **1c** significantly increased survival rate by reducing platelet aggregation.[23] Moreover, studies

utilizing **1a** as a **CORM** have showed that CO has antimicrobial properties[24] and can act as a bactericide, limiting cellular respiration in bacteria by interfering with and cutting off ATP supplies.[25] Lastly, **CORMs** have been shown to inhibit cancer metastasis,[26] and **1c**, specifically, has been shown to inhibit the expression of proteins that contribute to cancer progression in mice.[27] Although this section only briefly touches on the many roles of CO in animal models, **CORMs** have been shown to serve as promising therapeutic research molecules.

1.3.1 Inorganic CORMs

A large majority of **CORM** design has been based on transition metal carbonyl compounds (Mn, Fe, Ru, Mo, etc.) (**Figure 3**). Many of these compounds, such as **1a**, release CO spontaneously through solvent induced ligand exchange (**Figure 3A**). For example, when **1a** is added to water, it spontaneously releases CO with a half-life of about 1 minute.[28] The disadvantage of spontaneous **CORMs** is the inability temporally control the release of CO. To combat this pitfall, metal carbonyl compounds were synthesized to release CO only when triggered by specific stimuli including pH change (**Figure 3B**), ligand exchange (**Figure 3C**), and direct photolysis (**Figure 3D**). It has been shown that half-lives of rhenium^{II}-based **CORMs** containing bromide anions **1b** can range from 1 to 6 min as the pH increases from 5.8 to 7.4 (**Figure 3B**).[29] Another method commonly used to liberate CO from **CORMs**, specifically tricarbonyldichlororuthenium(II) dimer **1c** (**Figure 3C**), is to trigger a ligand exchange process by the addition of a stronger sigma donating ligand, such as dimethylsulfoxide (DMSO).[30] This example is similar to **1a**, but

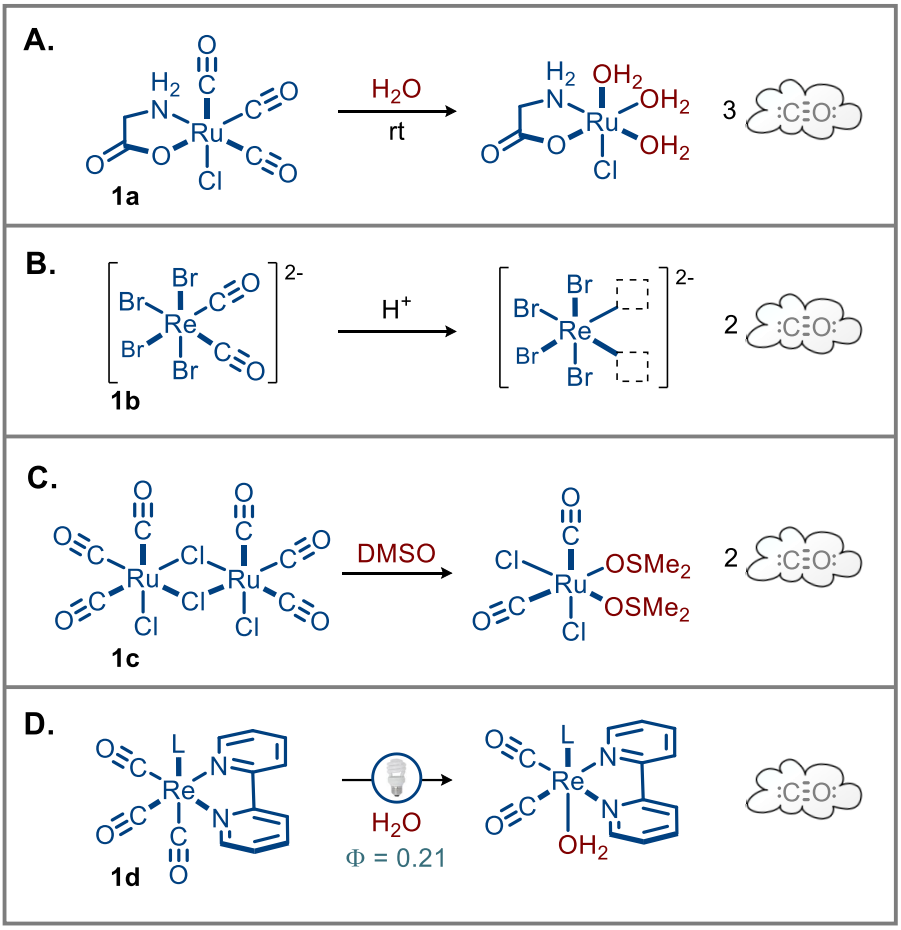

Figure 3: A. Spontaneous CO release through solvent induced ligand exchange. **B**. CO release triggered by increased acidity. **C**. CO release triggered by ligand exchange upon the addition of dimethylsulfoxide (DMSO). **D**. CO release triggered by direct irradiation.

1c was designed to be insoluble in physiological media and CO release only occurred after the addition of DMSO, which adds an element of control. **CORMs** triggered by irradiation with UV or visible light are commonly referred to as ***photo*-CORMs.** Compound **1d** is an example of a ***photo*-CORM** that is stable in the dark in aqueous media and releases CO upon irradiation with an appropriate wavelength of light, despite having a relatively low quantum yield of 0.21 (**Figure 3D**).[31] ***Photo*-CORMs** are undoubtedly the most popular

CORMs used in CO research because they easy to handle and grant practitioners inherent control over the spatial and temporal (spatiotemporal) release of CO..

1.3.2 Polymeric CORMs

As can be noted from the surveyed inorganic **CORMs** discussed above (**Figure 3**), at a maximum three molecules of CO can be release per atom of transition metal. To increase the amount of CO that can be produced by a **CORM**, metal carbonyl complexes have been ligated to organic polymers to create ***poly*-CORMs**.[32–35]

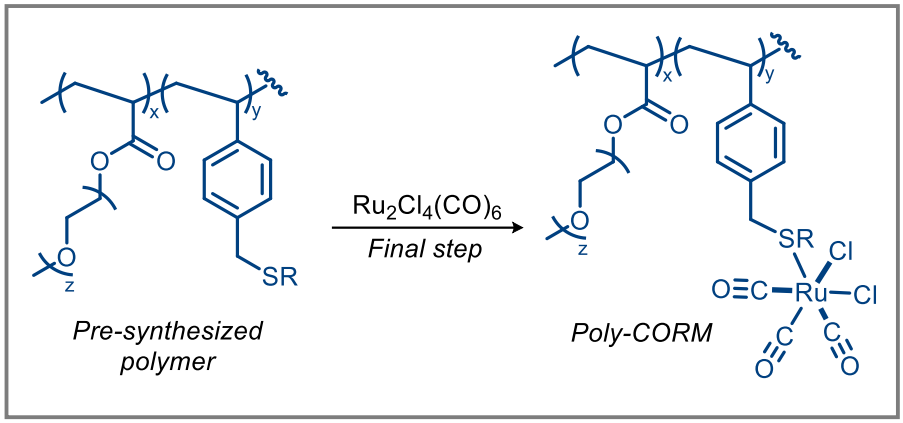

Figure 4: The strategy currently used to synthesize ***poly*-CORMs**: a polymer architecture is designed before ligating to an inorganic **CORM**.

As transition metals inhibit free-radical polymerizations, the CO releasing metal carbonyl must be ligated to the macromolecule following polymerization, rendering this method for the creation and engineering of truly complex polymer architectures infeasible (**Figure 4**).[33] Moreover, ***poly*-CORMs** based on metal carbonyl complexes were found to be cytotoxic before and following the release of CO,[35] greatly limiting their utility in research or therapeutic applications. Finally, the use of metal carbonyl-based **CORMs**, either monomeric or polymeric, are inherently flawed as they produce poorly defined and

coordinatively unsaturated transition metal complexes,[36] which could have significant downstream effects in biological systems following release of CO.

1.3.3 Organic CORMs

To avoid toxicity associated with metal-based **CORMs**, many organic, small molecule **CORMs** have been designed with biocompatibility in mind.[37–39] An example of a biocompatible organic **CORM** is **2a**, which exhibits no cytotoxicity before or after CO liberation and can successfully release CO under physiological conditions (**Figure 5A**).

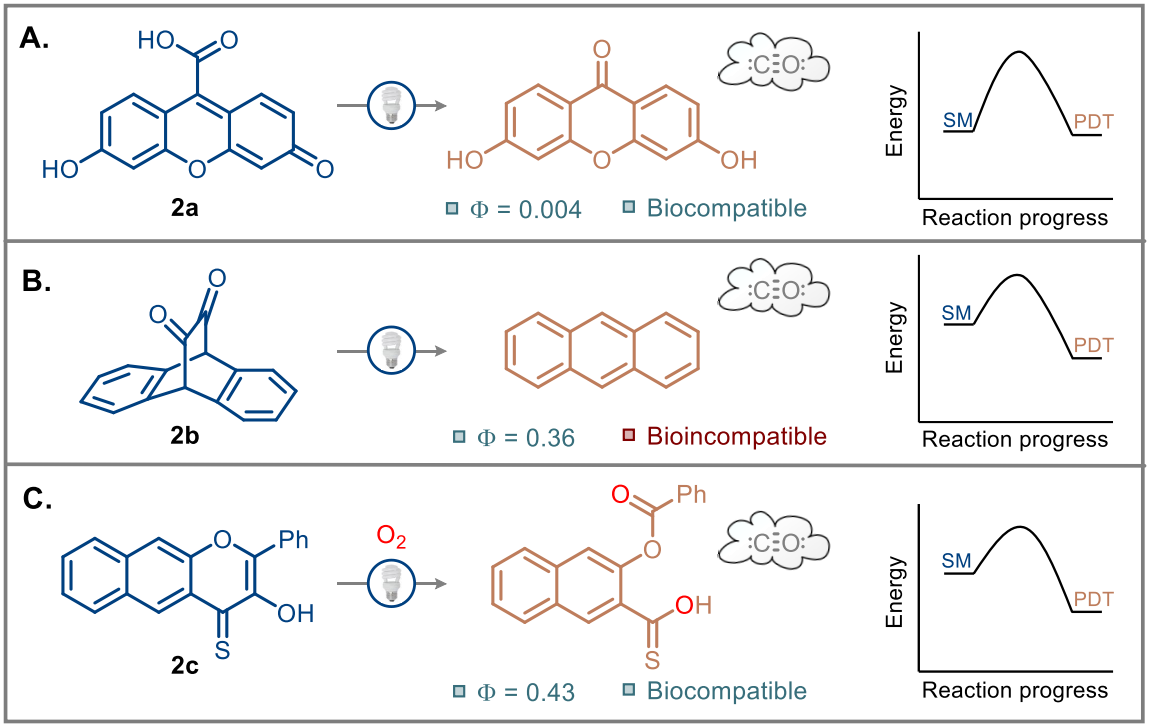

Figure 5: A. An organic **CORM** that inefficiently releases CO in biological conditions. **B.** An organic **CORM** that efficiently releases CO, but only in organic solvents. **C.** An organic **CORM** that efficiently releases CO in biological conditions, but forms potentially reactive byproducts and requires photolysis and oxygen to release CO.

The downside to this particular **CORM** and its variants is that they have low synthetic and quantum yields, resulting in inefficient production on large scales and underwhelming quantities of CO release.[37] Organic **CORMs** such as **2b** have higher reported quantum

yields than **2a** when irradiated in organic solvents, but lose the ability to liberate CO entirely when irradiated in aqueous environments (presumably due to their hydrolytic instability, **Figure 5B**).[38] A new generation of organic **CORMs**, including **2c**, were introduced to undergo fluorescent changes upon CO release to monitor CO release in real time (**Figure 5C**).[39] These **CORMs** were determined to have slightly better quantum yields than **2b**, but are only able to release CO in aerobic conditions, limiting their application in hypoxic experiments. Although organic **CORMs** are promising in terms of biocompatibility, they are limited by low quantum yields and CO production. Polymerization of an organic **CORM** could combat these limitations, but the synthesis of an organic ***poly*-CORM** has not yet been reported.

1.4 Diphenylcyclopropenone as a CORM

Cyclopropenones are highly strained three-membered cycloalkanes containing a carbonyl and an unsaturated double bond.[40] Although cyclopropenones have considerable ring strain, they are remarkably stable; they exist as ketones (not hydrates) in aqueous solution,[41] are resistant to thermal decomposition to 130°C,[41] and do not react with naturally occurring functional groups (**Figure 6A**).[42–44] It has been suggested that the peculiar stability of cyclopropenones is derived from its major contributing resonance form as an aromatic oxyanion pendant cyclopropenyl cation.[40] Moreover, cyclopropenones have been used as a tool to examine biomolecules in their native state. Prescher and co-workers reported successful bioorthogonal ligation of cyclopropenones mediated by functionalized phosphines,[42] showing the stability of cyclopropenones in physiologically relevant environments (**Figure 6B**). The photolysis of diphenylcyclopropenone (**DPCP, 2d**) has been extensively studied and was shown to occur with high quantum yields (1.0),

generating only diphenylacetylene and CO gas (**Figure 6C**).[45] Although the mechanism of CO release from **DPCP** is still debated, it is widely considered that it proceeds through an ionic, non-radical mechanism, meaning that this process is not retarded by the presence of functional groups with abstractable hydrogens (thiols, phenols, etc.), oxygen, or aqueous

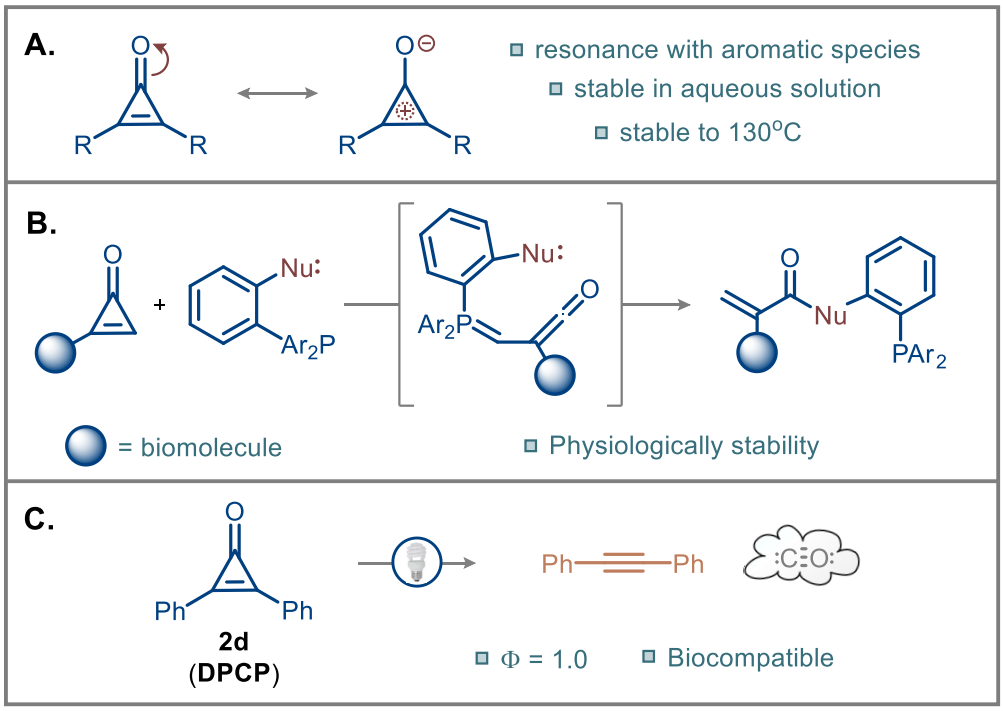

Figure 6: A. The physical chemistry of cyclopropenones. **B.** Bioorthogonal ligation between cyclopropenones and functionalized phosphines displaying the physiological stability of cyclopropenones. **C.** The highly efficient photorelease of CO from diphenylcyclopropenone that produces CO gas and forms innocuous byproducts and operates under anaerobic conditions.

media. Aside from its photolysis, **DPCP** has been topically administered to treat alopecia areata and multiple studies have shown that it promotes hair regrowth among patients.[46–48] Despite the appealing chemical properties of **DPCP**, its use as a therapeutic **CORM** has never been reported.

1.5 Amplificative Decarbonylation of DPCP

As stated above, the solution photochemistry of **DPCP** has been extensively studied and leads to the rapid, clean, and efficient (Φ = 1.0) release of CO gas upon irradiation (**Figure 5D**). In this context, at a maximum, 1 photon of light would result in 1 molecule of CO being released. However, in 2008, Garcia-Garibay and co-workers reported that the excitation of crystalline suspensions of **DPCP** in water/cetrimonium bromide (CTAB) to their second excited state (S2) with UV light (~330 nm) resulted in crumbling of the crystals to powders consisting solely of diphenylacetylene within minutes.[49]

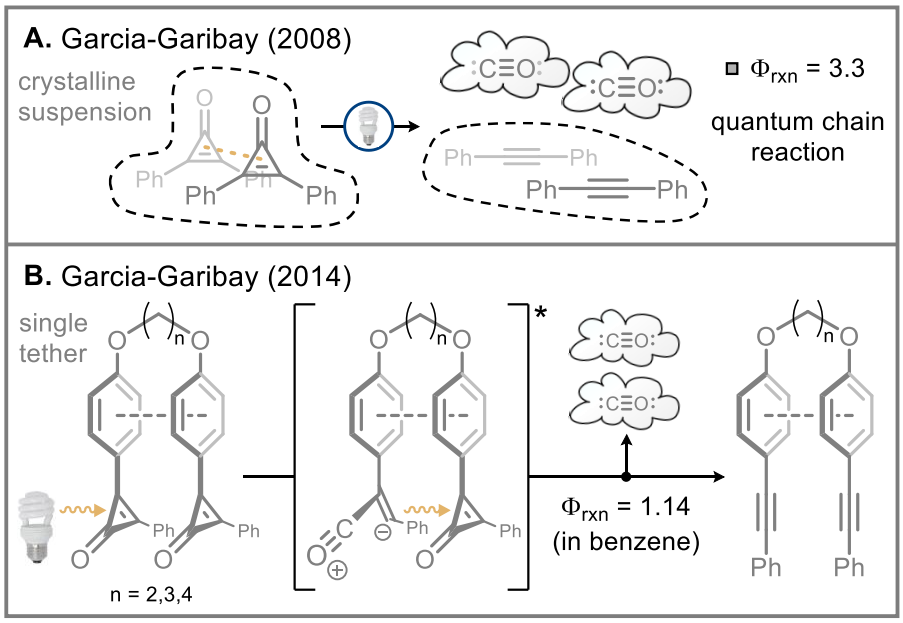

Figure 7: A. Quantum chain reaction for the photodecarbonylation of **DPCP** in a solid state; **B**. quantum chain behavior of tethered **DPCPs**.

Further inspection revealed that this photoreaction had a quantum yield of 3.3; meaning that every 1 photon absorbed by the crystalline suspension of **DPCP** resulted in the release of 3.3 molecules of CO gas![49,50] This phenomenon is referred to as a quantum chain reaction because it proceeds through energy transfer from an excited molecule (that

releases CO) to another proximal molecule in its ground state (that subsequently releases CO) and so forth. As energy transfer can occur on a sub-picosecond time scale in crystalline solids, this amplificative effect was initially evidenced in crystalline suspensions (**Figure 7A**). In a second study, Garcia-Garibay and co-workers synthesized three different tethered **DPCP**s: dimers with 2, 3, and 4 carbons separating **DPCP** moieties (**Figure 7B**). They irradiated each molecule in solution (benzene) at 365 nm and 312 nm to determine

	Φ in Benzene	
n	**365 nm**	**312 nm**
2	0.73 ± 0.03	1.14 ± 0.03
3	0.74 ± 0.06	1.02 ± 0.04
4	0.74 ± 0.04	0.70 ± 0.04

Table 1: Quantum yields of each tethered **DPCP** in benzene at 365 nm and at 312 nm.

quantum yields (**Table 1**). They found that increasing the distance between **DPCP** molecules decreases quantum yields in benzene, and that irradiation with shorter wavelengths of UV light result in higher quantum yields. Therefore, they were able to synthetically control the effect of quantum amplification.

1.6 Direct Polymerization of DPCP to Form Poly-CORMs

Inspired by the works of Garcia-Garibay, we considered that a polymer backbone is, in effect, a tether that could hold many **DPCP** units in very close proximity independent of the polymer's overall concentration. We looked through the literature and found that the

only example of polymeric **DPCP** is a **DPCP** centered polymer that only contained one equivalent of **DPCP** and thus, one equivalent of CO per polymer.[51] We thought that the best way to utilize **DPCP** as a **CORM** would be to synthesize a **DPCP** attached to a polymerizable functional group (**3a**), enabling its free-radical polymerization (**Figure 8**). The product of its polymerization is a linear polymer containing many repeating **DPCP** units (***poly*-DPCP**, **3b**). To the best of our knowledge, ***poly*-DPCP** is the first example of

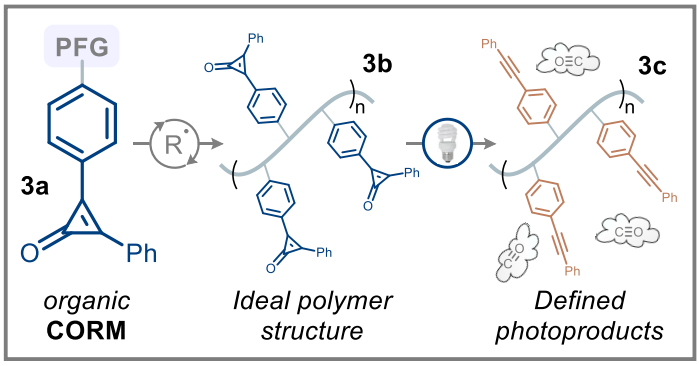

Figure 8: The polymerization of a **DPCP** containing monomer followed by its photodecarbonylation.

an organic ***poly*-CORM**. The liberation of CO from ***poly*-DPCP** will be achieved by direct irradiation. ***Poly*-DPCP** serves as an excellent **CORM** because large amounts of CO can be released, and the clean photolysis of **DPCP** results in well-defined photoproducts such as polymeric diphenylacetylene (***poly*-DPA**, **3c**).

1.7 Amplificative CO Release from a poly-CORM

We believe that irradiation of ***poly*-DPCP** with a proper wavelength of light would excite a singular **DPCP** unit within the polymer to the S2 state, initiating a quantum chain reaction and resulting in the amplified release of CO gas (**Figure 9**). This quantum chain process would not only increase the quantum yield of the photoreaction, but also would

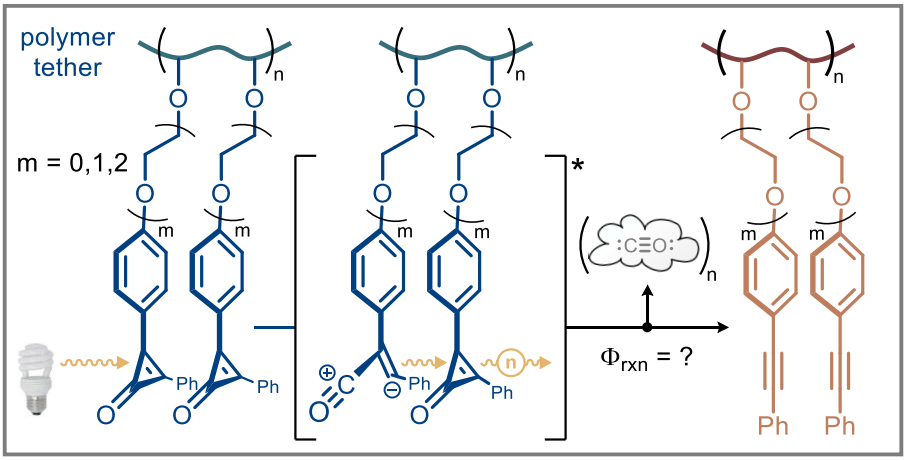

Figure 9: The use of ***poly*-DPCPs** to study quantum chain reactions.

lead to an increased rate of CO formation, making ***poly*-DPCP** a very desirable **CORM**. Garcia-Garibay's tethered **DPCPs** inspired us to synthesize multiple **DPCP** polymers using ethylene glycol units to vary lengths between **DPCP** moieties and the polymer backbone to further investigate the amplificative decarbonylation of **DPCP**. Ultimately, we sought to synthesize a new class of organic ***poly*-CORMs** that can be used to deliver therapeutic dosages of CO and serve as a model to study quantum chain reactions.

2. Research

2.1 Hypothesis

The goal of the work in this thesis is to develop a new class of organic **CORMs** based on **DPCP.** We believe that this new class of **CORMs** can be directly polymerized, are non-cytotoxic before and following photolysis, efficiently release CO gas, and create well-defined and, ideally, readily metabolizable photoproducts. This new class of **CORMs** would offer practitioners a powerful set of tools with significant impacts in the areas of research, therapeutics, and human health. Moreover, our ***poly*-CORMs** will be a useful tool to study quantum chain reactions. Specifically, in this thesis, we hypothesize that: 1) **DPCP** with polymerizable functionality can be successfully synthesized, 2) the polymerization of **DPCP** monomers can be controlled using RAFT polymerization, and 3) CO can be successfully liberated from ***poly*-DPCP**.

2.2 Synthesis of DPCP Acrylates

Due to the high reactivity of the acrylate functional group to free-radical polymerization, the first type of **DPCP** monomers we synthesized were **DPCPs** with acrylates attached in the para-position (**Scheme 1**). From commercially available tetrachlorocyclopropene, **4a** was synthesized in good yields (69%) by a Friedel-Crafts type reaction mediated by aluminum trichloride ($AlCl_3$). De-methylation of this material by boron tribromide (BBr_3) formed phenol **4b** in quantitative yields.[52] From here, we

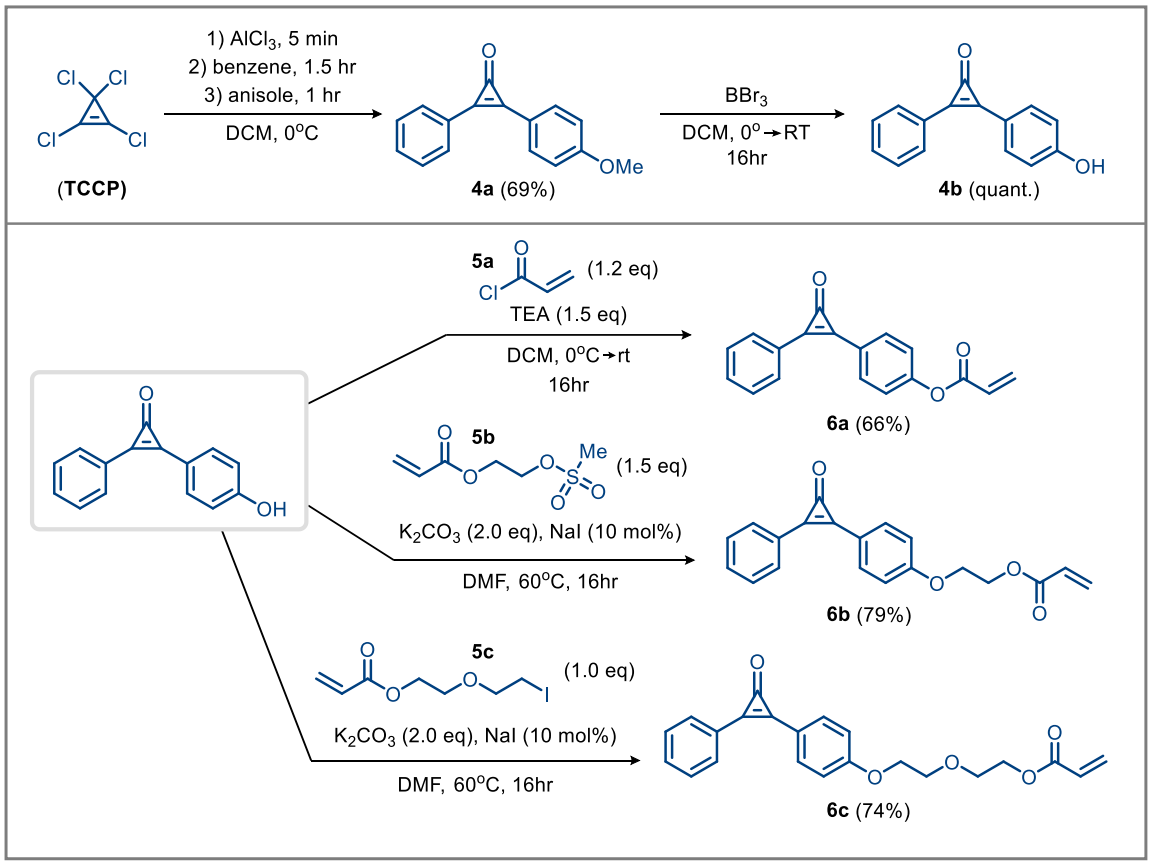

Scheme 1: Synthesis of acrylated **DPCP** with 0, 1, and 2 PEG units.

synthesized acrylates with 0, 1, and 2 ethylene glycol units with hopes to append them to phenol **4b** (**Scheme 1**). Specifically, phenol **4b** was reacted with triethylamine and acryloyl chloride (**5a**) to obtain 0-PEG acrylated **DPCP** (**6a**) in a 66% yield. A mesylate leaving group was added to 2-hydroxyethyl acrylate[53] to form **5b** before preforming a nucleophilic substitution with phenol **4b** to obtain 1-PEG acrylated **DPCP** (**6b**) in a 79% yield. The third acrylate was synthesized by the addition of acryloyl chloride (**5a**) to 2-(2-chloroethoxy)ethanol[21], followed by a Finkelstein halide exchange to yield iodo **5c**, and finally nucleophilic substitution with phenol **4b** to obtain 2-PEG acrylated **DPCP** (**6c**) in a

74% yield. Overall, these acrylate substituted **DPCPs** were formed in overall good yields, high purities, and few steps from commercial substrates.

2.3 Polymerization of DPCP Acrylates

2.3.1 Reversible Addition-Fragmentation Chain Transfer Polymerization

The best way to utilize ***poly*-DPCPs** as **CORMs** and as tools to study quantum amplification reactions is to control their polymerization. Dispersity (Đ) is a measure of heterogeneity that can be calculated using the equation: $Đ = M_w/M_n$, where M_w is the weight-average molar mass and M_n is the number-average molar mass. Dispersity can significantly affect the properties of a given polymer. If a sample of ***poly*-DPCP** has a high dispersity it will be difficult to quantify CO release per polymer upon irradiation. Moreover, variation in polymer size may also influence quantum amplification. One technique widely used to control radical polymerizations is Reversible Addition-Fragmentation Chain Transfer (RAFT), a process discovered in 1998 at the Commonwealth Scientific and Industrial Research Organization (CSIRO) in Australia by several researchers.[54]

Addition of RAFT reagents (e.g. dialkyl dithiocarbonates) to free-radical polymerizations creates polymers with predicable molecular weights and low dispersity.[55] The RAFT mechanism, shown in **Scheme 1**, operates through 4 specific steps: 1. initiation of a monomer to form an activated radical, 2. addition of the activated radical to the RAFT agent which enters equilibrium between active and dormant species, 3. initiation of new polymer growth by the fragmentation of the R group from the RAFT agent, and 4. termination by combination of active radical species. Accordingly, RAFT agents have been

used in free-radical polymerizations with a variety of monomers to engineer complex polymer architectures which were previously inaccessible with such as linear block copolymers, star polymers, brush polymers, and dendrimers.[54,56]

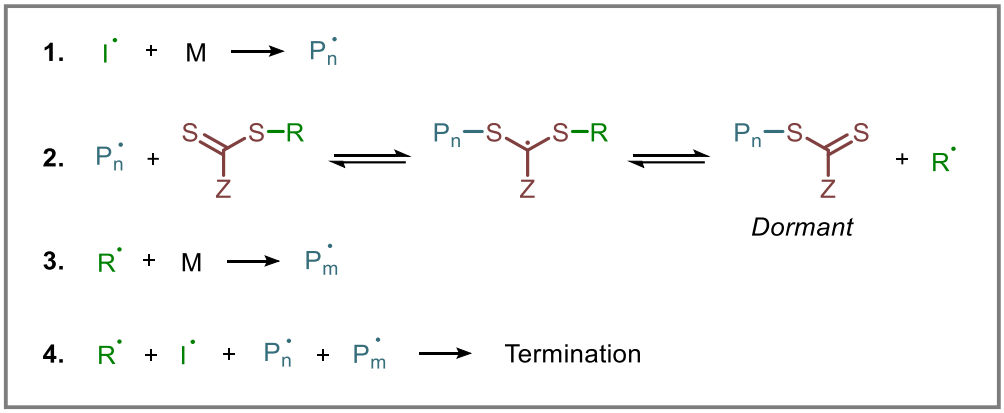

Scheme 2: Mechanism of RAFT polymerization.

The compatibility of RAFT reagents with an extensive range of monomers is what makes RAFT polymerization such a valuable technology. Most monomers compatible with free radical polymerization are compatible with RAFT. Furthermore, monomers that are difficult to polymerize under free-radical conditions can be successfully polymerized upon the addition of a compatible RAFT reagent. For example, dienes typically cross-link quite rapidly when polymerized free radically, but the addition of RAFT reagent results in much higher conversion before eventual crosslinking.[57] The compatibility between RAFT polymerization with many monomers is due to the reactivity of the RAFT reagent. A RAFT polymerization is successful when the carbon sulfur double bond is more reactive with radical addition than the carbon-carbon double bond on the monomer. Many RAFT agents have been synthesized with variable R and Z groups to alter the reactivity of the carbon-sulfur double bond, and to stabilize the radical intermediates. The RAFT agents we

experimented with in this thesis are shown in **Figure 10.** 2-(Dodecylthiocarbonothioylthio)propionic acid (DoPAT) is a popular, commercially available

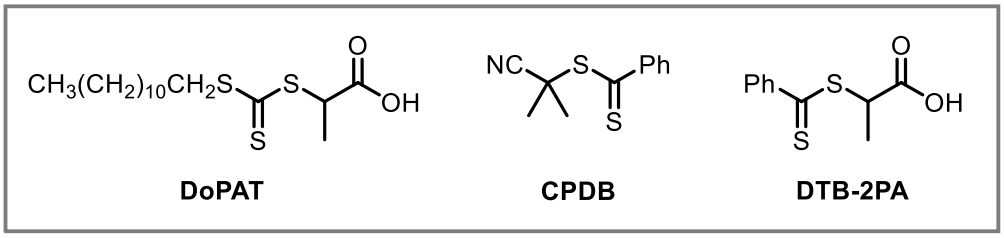

Figure 10: The structures of the RAFT agents used in this thesis.

trithiocarbonate designed to balance activity and hydrolytic stability that is commonly used with styrenes, acrylates, and acrylamides.[58] 2-Cyano-2-propyl benzodithioate (CPDB) and 2-[(Phenylthioxomethyl)thio]propanoic acid (DTB-2PA) are versatile, commercially available, dithiocarbonates that are most compatible with methacrylates and methacrylamides.[59] Compatibility is important because if the RAFT agent is incompatible with a monomer, the polymerization is entirely unsuccessful or the conversion is drastically reduced.

For the work in this thesis, we began experimenting with RAFT by synthesizing polymers containing 50 **DPCP** units from acrylate appended **DPCPs**. Using Equation 1, we were able to calculate the concentration of RAFT

$$M_n = \frac{[M]_o p M_m}{[RAFT]_o} + M_{RAFT} \textbf{ (Equation 1)}$$

$$[M]_o = initial\ concentration\ of\ monomer$$

$$p = theoretical\ conversion$$

$$M_m = molar\ mass\ of\ monomer$$

$[RAFT]_o$ = concentration of RAFT agent

$M_{RAFT} = molar\ mass\ of\ RAFT\ agent$

reagent required to synthesize a 50 **DPCP** unit (M_n = 14,150 g/mol) polymer. We typically set our theoretical conversion to 95% to account for error or incomplete double bond conversions. Equation 1 can be simplified to quickly solve for the concentration of RAFT agent required to synthesize a polymer with a theoretical number of monomer units (Equation 2).

$$[RAFT]_o = \frac{1}{(m_{th} \div p)} \quad \textbf{(Equation 2)}$$

$m_{th} = theoretical\ number\ of\ monomer\ units$

For example, if we aim to synthesize a polymer containing 50 repeats of **DPCP** that goes to 95% theoretical conversion, 0.019 stoichiometric equivalents of RAFT agent are required. **Table 2** illustrates the importance of experimentally determined conversion (p_{exp}) in this system and how it effects the number of monomer units (m_{units}) in the polymer. If the polymerization does not go to completion, the polymer will not be the desired length, demonstrating the livingness of this polymerization process.[60]

m_{th}	$[RAFT]_o$	p_{exp}	m_{units}
50	0.019	95%	50
50	0.019	100%	52.6
50	0.019	90%	47.3
50	0.019	75%	39.4
50	0.019	50%	26.3

Table 2: Hypothetical data showing the importance of conversion in controlled RAFT polymerizations.

There are many variables other than RAFT agent compatibility with monomers that effect the success of RAFT polymerizations. Indeed, variables such as concentration, time, and solvent are necessary to be optimized to result in a successful controlled polymerization. Typically, RAFT polymerizations are performed overnight in dimethylformamide (DMF), toluene, acetonitrile, or anisole at high concentrations. Variables pertaining to the radical initiator are more difficult to screen for. In all our experiments we used azobisisobutyronitrile (AIBN) as our radical initiator because it is inexpensive, crystalline, and readily gives off free radicals at temperatures above 40°C. The concentration of initiator in RAFT polymerizations is typically displayed as a ratio of RAFT:AIBN and ranges anywhere from 3:1 to 20:1, but ratios of 5:1 and 10:1 are most

commonly used. A lack of radicals may result in the rate of the polymerization decreasing, and too many radicals may result in the livingness of the system decreasing due to the formation of dead chain ends (resulting from bimolecular termination with an initiating radical).

2.3.2 RAFT Polymerization of DPCP Acrylates

With **DPCP** acrylates (**6a**, **6b**, **6c**) in hand, we began to assess their compatibility with the RAFT agent DoPAT. As our monomers have been previously reported nor have been evaluated in a living radical polymerization, we performed many experiments to determine the optimal conditions for their controlled polymerization. Our results, displayed in **Table 3,** show that polymerizations in DMF had superior conversions over anisole,

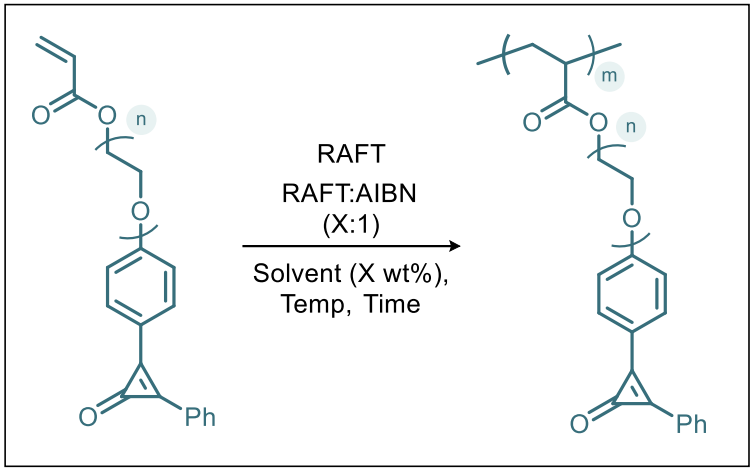

Scheme 3: Optimization experiment for the RAFT polymerization of DPCP acrylates.

acetonitrile, and 1,4-dioxane. We found that 300 wt% results in high conversion and that reaction mixtures exhibit partial insolubility in concentrations less than 300 wt%. Our results also show that 24 hours at 70°C is a sufficient reaction time and temperature, respectively. We found that using DoPAT as a RAFT reagent resulted in higher

conversions when compared to DTB-2PA. Our highest conversions for 0-PEG acrylate (**6a**)**,** 1-PEG acrylate (**6b**)**,** and 2-PEG acrylate (**6c**) were 78%, 94%, and 91% respectively. We found the most crucial variable that contributed to higher observed monomer conversions were the ratio of RAFT to AIBN. The optimal ratio for these experiments, based solely on observed conversion, was 3:1 RAFT:AIBN. We noticed another increase in polymerization success when we changed our reaction vessels from 6 mL microwave vials with Teflon caps to 2 mL glass ampoules. After learning that oxygen can readily diffuse through Teflon, we began performing three freeze pump-thaw-cycles with glass ampoules and flame sealing under vacuum, which likely resulted in reducing the amount of oxygen in the system.

entry	n	m_{th}	temp °C	Hrs.	solvent	RAFT reagent	RAFT: AIBN	Conc. wt%	P_{th}	p_{exp}
1	**0**	50	80	48	dioxane	DoPAT	5:1	100	95	50
2	**0**	50	80	24	dioxane	DoPAT	5:1	100	90	55
3	**0**	50	80	24	anisole	DoPAT	5:1	100	75	49
4	**0**	50	80	24	anisole	DoPAT	5:1	100	90	36
5	**0**	50	70	24	DMF	DoPAT	3:1	300	95	62
6	**0**	50	70	24	DMF	DoPAT	3:1	400	95	55
7	**0**	50	70	24	DMF	DoPAT	3:1	300	95	56
8	**0**	50	70	48	DMF	DoPAT	3:1	300	95	57
9	**0**	50	70	72	DMF	DoPAT	2:1	300	95	78
10	**0**	50	70	72	DMF	DoPAT	2.5	300	95	56
11	**0**	50	70	72	DMF	DTB-2PA	3:1	300	95	45
12	**0**	50	70	72	dioxane	DoPAT	3:1	300	95	38
13	**1**	50	70	24	DMF	DoPAT	5:1	200	95	80
14	**1**	50	70	48	DMF	DoPAT	5:1	200	95	80
15	**1**	50	70	24	DMF	DoPAT	20:1	200	95	14
16	**1**	50	70	24	Anisole	DoPAT	20:1	200	95	10

17	**1**	50	70	24	DMF	DoPAT	20:1	200	95	40
entry	*n*	m_{th}	temp °C	Hrs.	solvent	RAFT reagent	RAFT: AIBN	Conc. wt%	P_{th}	p_{exp}
18	**1**	50	70	24	DMF	DoPAT	15:1	200	95	57
19	**1**	50	70	24	DMF	DoPAT	10:1	200	95	56
20	**1**	50	70	24	DMF	DoPAT	20:1	200	95	56
21	**1**	50	70	24	DMF	DoPAT	15:1	200	95	56
22	**1**	50	70	24	DMF	DoPAT	10:1	200	95	59
23	**1**	50	70	24	DMF	DoPAT	2:1	300	95	94
24	**1**	50	70	24	DMF	DoPAT	5:1	300	95	93
25	**1**	50	70	24	DMF	DTB-2PA	20:1	200	95	28
26	**1**	50	70	24	DMF	DTB-2PA	15:1	200	95	43
27	**1**	50	70	24	DMF	DTB-2PA	10:1	200	95	55
28	**1**	50	70	24	DMF	DoPAT	5:1	300	95	85
29	**1**	50	70	24	DMF	DoPAT	5:1	400	95	78
30	**1**	50	70	24	DMF	DoPAT	5:1	1000	95	63
31	**1**	50	70	48	DMF	DoPAT	3:1	300	95	87
32	**1**	100	70	24	DMF	DoPAT	3:1	300	95	19
33	**1**	58.8	70	24	DMF	DoPAT	5:1	300	85	73
34	**1**	50	70	24	DMF	DoPAT	3:1	300	95	78

35	**1**	100	70	24	DMF	DoPAT	5:1	300	95	59
entry	*n*	m_{th}	temp °C	Hrs.	solvent	RAFT reagent	RAFT: AIBN	Conc. wt%	P_{th}	p_{exp}
36	**1**	50	70	24	DMF	DoPAT	3:1	300	95	93
37	**1**	50	70	24	DMF	DoPAT	3:1	300	95	94
38	**2**	50	70	24	DMF	DoPAT	5:1	200	95	77
39	**2**	50	70	48	DMF	DoPAT	5:1	200	95	77
40	**2**	50	70	48	DMF	DoPAT	3:1	300	95	87
41	**2**	62.5	70	24	DMF	DoPAT	5:1	300	80	68
42	**2**	100	70	24	DMF	DoPAT	5:1	300	95	29
43	**2**	50	70	24	DMF	DoPAT	3:1	300	95	91

Table 3: Optimization experiments for RAFT polymerization of **DPCP** acrylates. ***n*** = number of ethylene glycol units; $\boldsymbol{m_{th}}$ **=** theoretical number of monomer units per polymer; $\boldsymbol{p_{th}}$ = theoretical converstion; $\boldsymbol{p_{exp}}$ = experimental conversion. Rows highlighted in gold show the conditions that resulted in our highest conversions.

Upon optimizing RAFT polymerizations of **DPCP** acrylates, we attempted to use gel permeation chromatography (GPC) to analyze the polymers with the highest conversion. Initially, our GPC was equipped with a refractive index detector and a column that was compatible with a tetrahydrofuran (THF) mobile phase. We quickly learned that our ***poly*-DPCP** acrylates were completely insoluble in THF. To remedy this, our mobile phase was switched to chloroform, a solvent that readily solubilizes our polymers, only to find that our polymers are isorefractive with chloroform, giving a very weak or non-

existent RI signal. Ultimately, we were unable to determine the molecular weights and dispersities of our samples utilizing our instrument. Installation of a UV detector on our GPC, which we anticipate will be able to detect the strong UV signal of **DPCP**, is currently ongoing and future work will be related to analysis of these polymers by size exclusion with UV detection.

The difficulties encountered while optimizing and analyzing RAFT polymerizations of **DPCP** acrylate monomers inspired the investigation of a slightly less reactive monomer: methacrylates. Controlling the polymerization of methacrylates is more

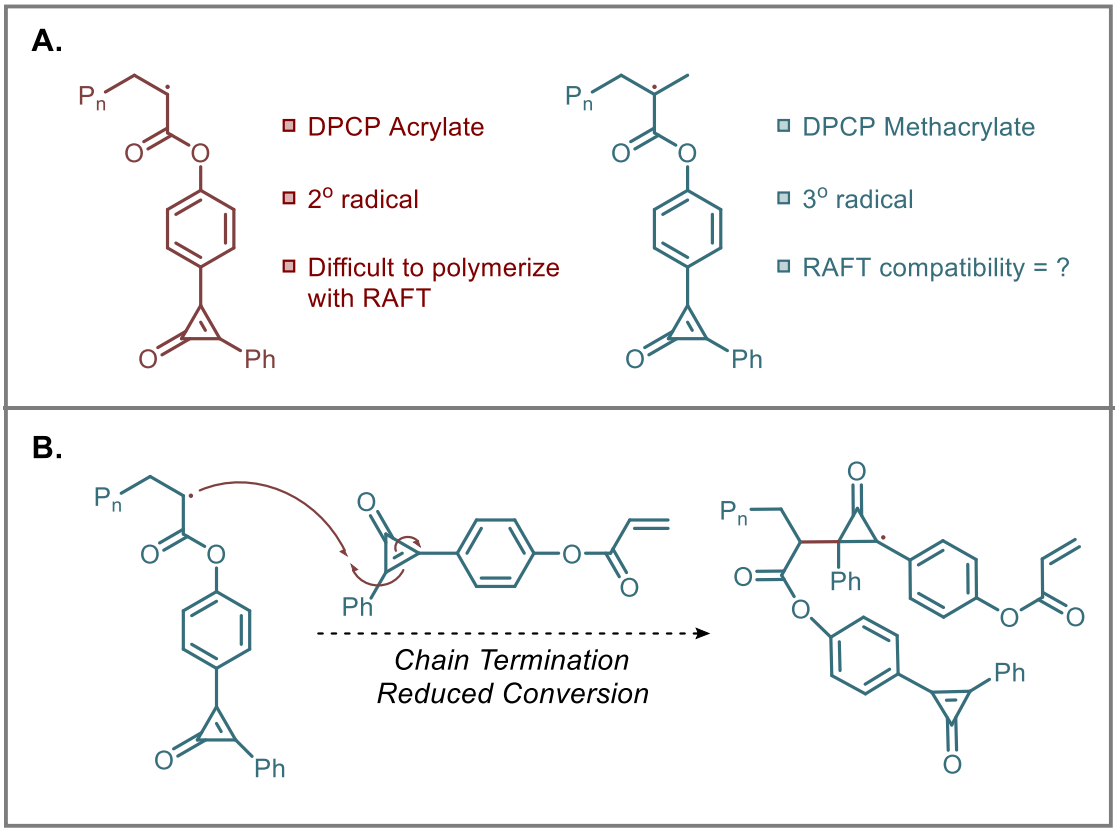

Figure 11: A. Comparison of **DPCP** acrylates and **DPCP** methacrylates as activated monomers, **B.** Proposed mechanism of chain termination between an activated **DPCP** acrylate monomer and the cyclopropenone moiety of another **DPCP** acrylate monomer.

promising than controlling the polymerization of acrylates because when the methacrylate monomer is activated it forms a tertiary radical rather than a secondary radical like the acrylate monomer (**Figure 11A**). The high reactivity of acrylates may be causing the activated radical to chain transfer to the alkene belonging to the cyclopropenone moiety rather than the acrylate (**Figure 11B**). This could result in reduced conversions and high dispersities. Moreover, this is a potential explanation for the requirement for higher concentrations of initiator being responsible for the highest observed conversions.

2.4 Synthesis of DPCP Methacrylates

The synthesis of **DPCP** methacrylates followed a similar synthetic path as the acrylated **DPCPs**. We began with the synthesis of a large batch of **DPCP** phenol (**4b**) using the previously described methods. From here, phenol **4b** was reacted with triethylamine

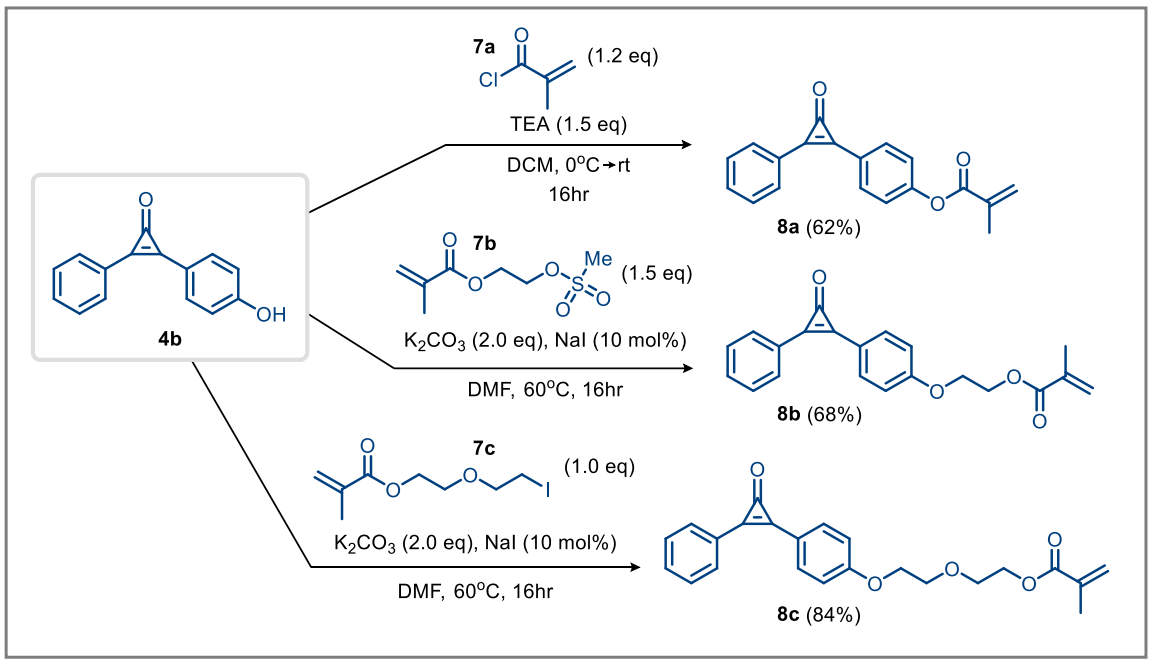

Scheme 4: Synthesis of **DPCP** methacrylates with 0, 1, and 2 PEG units.

and methacryloyl chloride (**7a**) to obtain 0-PEG methacrylated **DPCP** (**8a**) in a 62% yield. Secondly, a mesylate leaving group was added to 2-hydroxyethyl methacrylate[53] to form **7b** before preforming a nucleophilic substitution with phenol **4b** to obtain 1-PEG methacrylated **DPCP** (**8b**) in a 68% yield. The third methacrylate was synthesized by the addition of methacryloyl chloride (**7a**) to 2-(2-chloroethoxy)ethanol,[21] followed by a Finkelstein halide exchange to yield iodo methacrylate **7c**, and finally nucleophilic substitution with phenol **4b** to obtain 2-PEG methacrylated **DPCP** (**8c**) in an 84% yield.

2.5 Polymerization of DPCP Methcrylates

2.5.1 RAFT Polymerization of DPCP Methcrylates

With **DPCP** acrylates in hand, we began to assess their compatibility with RAFT polymerization (**Scheme 5**). Given the extensive optimization conducted with acrylated **DPCPs**, we had excellent general conditions to begin our evaluations. The main variable we needed to change for these polymerizations was the RAFT reagent. We started by assessing the compatibility of CPDP with **DPCP** methacrylates (**8a**, **8b**, **8c**) and quickly determined that this pair consistently showed

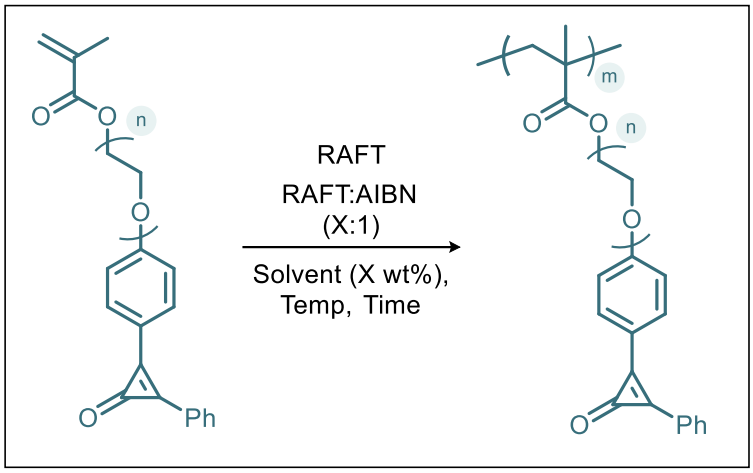

Scheme 5: Optimization experiments for the RAFT polymerization of DPCP methacrylates.

better conversions than RAFT polymerization of acrylated **DPCPs**. The optimization data for RAFT polymerizations of **DPCP** methacrylates are shown in **Table 4.** The conversions were consistently equal to or higher than the theoretical conversion of 95%, so we altered our calculations to account for 100% theoretical conversion. Our highest conversion (98%) was the polymerization of 0-PEG methacrylated **DPCP** (**8a**; **Table 4**, entry **15**). Although the majority of our experiments were conducted on **8a**, we found that polymerization of 1-PEG methacrylated DPCP (**8b**) and 2-PEG (**8c**) had lower conversions (93% and 79% respectively). This may be due to m_{th} of 2-PEG methacrylated **DPCP** (**8c**) being set to 200 to test the upper limit of the RAFT system with our monomers, which resulted in high viscosity, poor diffusion of monomers, and lower observed conversion. Overall, the controlled polymerization of methacrylated **DPCP** monomers need further optimization, but, in general, were found to perform more adequately than acrylated **DPCPs**.

entry	n	m_{th}	temp °C	Hrs.	solvent	RAFT reagent	RAFT: AIBN	Conc. wt%	P_{th}	p_{exp}
1	**0**	50	70	24	DMF	CPDB	10	300	95	96
2	**0**	50	70	24	MeCN	CPDB	10	300	95	93
3	**0**	100	70	24	DMF	CPDB	10	300	95	94
4	**0**	25	70	24	DMF	CPDB	10	300	95	96
5	**0**	200	70	24	DMF	CPDB	10	500	95	92
6	**0**	50	70	24	DMF	CPDB	10	300	100	96
7	**0**	100	70	24	DMF	CPDB	10	300	100	95
8	**0**	200	70	24	DMF	CPDB	10	300	100	93
9	**0**	50	70	24	DMF	CPDB	10	400	100	98
10	**0**	50	70	24	DMF	CPDB	10	500	100	98
11	**0**	50	60	24	DMF	CPDB	10	500	100	93
12	**0**	50	50	24	DMF	CPDB	10	500	100	78
13	**0**	50	70	24	DMF	CPDB	15	500	100	91
14	**0**	50	70	24	DMF	CPDB	20	500	100	89
15	**0**	50	70	24	DMF	CPDB	10	300	100	98
16	**1**	100	70	24	DMF	CPDB	10	300	100	83
17	**1**	200	70	24	DMF	CPDB	10	300	100	66

18	**1**	50	70	24	DMF	CPDB	10	300	100	93
entry	*n*	m_{th}	temp °C	Hrs.	solvent	RAFT reagent	RAFT: AIBN	Conc. wt%	P_{th}	p_{exp}
19	**2**	200	70	48	DMF	CPDB	10	300	100	73
20	**2**	200	70	90	DMF	CPDB	10	300	100	79

Table 4: Optimization experiments for RAFT polymerization of **DPCP** methacrylates. ***n*** = monomer used; $\boldsymbol{m_{th}}$ **=** theoretical number of monomer units per polymer; $\boldsymbol{p_{th}}$ = theoretical converstion; $\boldsymbol{p_{exp}}$ = experimental conversion. The row highlighted in gold shows the conditions used to achieve our highest conversion.

Curious about the control of our polymerizations but still lacking the instrumentation to analyze them ourselves, we sent samples to the Gutekunst lab at the Georgia Institute of Technology for GPC analysis. We analyzed samples of 50, 100, and 200 **DPCP** methacrylate unit polymers (entries 9, 7 and 8 respectively) and found that RAFT did influence the M_n and distribution of our samples (**Figure 12**). The M_n for the 50-unit polymer was 15,900 Da and was quite disperse ($Đ$ = 2.90). Dividing the experimental M_n by the monomeric molecular weight showed that this polymeric sample contained 54 **DPCP** units. The M_n for the 100-unit polymer was 22,500 which also had a high dispersity ($Đ$ = 2.24). Dividing the experimental M_n by the monomeric molecular weight showed that this polymeric sample was 77 **DPCP** methacrylate units. The M_n for the 200-unit polymer was 38,100 with even higher dispersity ($Đ$ = 3.94). These results show that this polymeric sample was 131 **DPCP** methacrylate units.

Although we were able to optimize the RAFT polymerization conditions to achieve high conversions, our results indicate poor control over the living polymerization. This

resulted in high dispersity (>1.2) and poor control over the degree of polymerization (DP). For example, we evaluated the RAFT polymerization of simple monomers such as methyl methacrylate using CPDB as a RAFT agent which consistently went to 98% conversions while giving a dispersity of 1.09.[61] Although our GPC spectra show that we have some control over M_n, the M_n of our 100 and 200 **DPCP** unit polymers are inconsistent compared to the theoretical M_n. Overall, the GPC results in this thesis show that the RAFT polymerization of **DPCP** methacrylate monomers require further optimization of the parameters. Many variables including time, temperature, and concentration have been evaluated; however, we are still awaiting the installation of a UV monitoring system for our GPC to properly analyze these polymers.

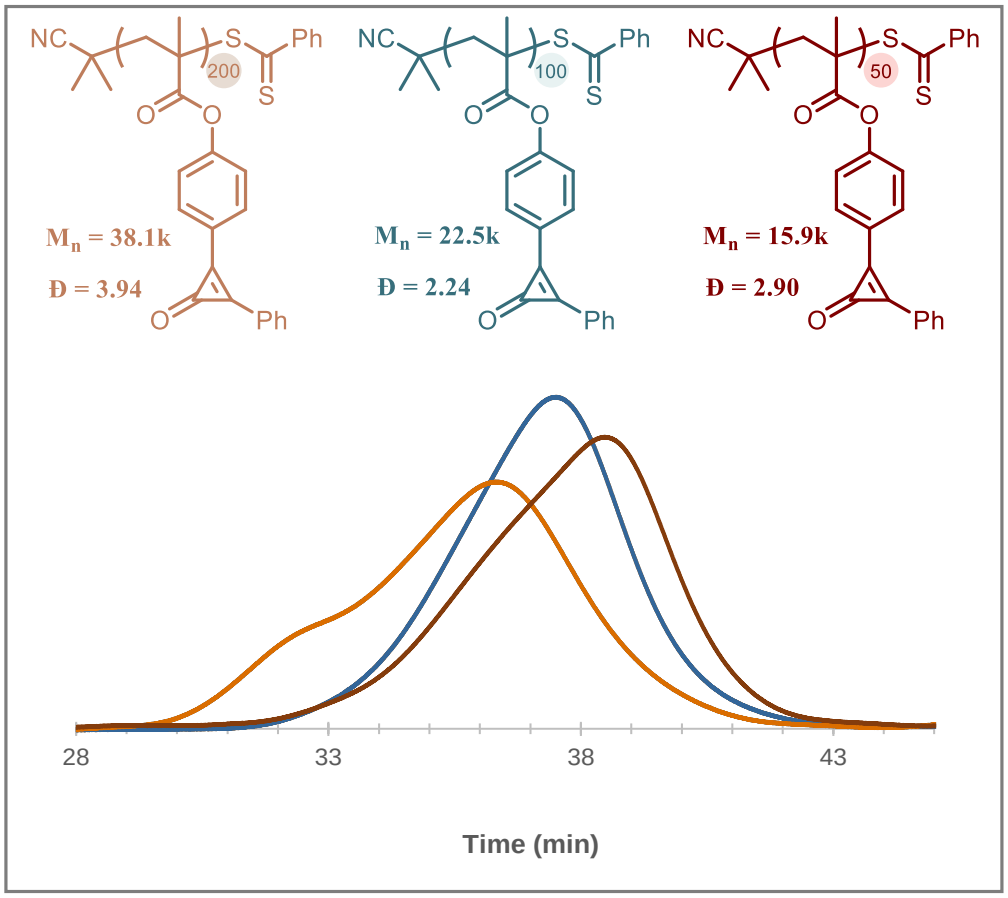

Figure 12: GPC spectra of 50, 100, and 200 **DPCP** methacrylate unit polymers.

2.5.2 Synthesis and Polymerization of DPA Methacrylate

To conduct a proof-of-concept experiment to confirm that the photoproduct formed upon irradiation of ***poly*-DPCP** methacrylates to release CO gas is indeed ***poly*-DPA**, we needed to independently synthesize and polymerize a methacryalted **DPA**. As the 0-PEG ***poly*-DPCP** methacrylate was most easily synthesized and polymerized, we decided that synthesizing 0-PEG methacryalted **DPA** would be sufficient for this study and that synthesizing 1 and 2-PEG **DPA** methacrylates was unnecessary. The two-step synthesis of **DPA** methacrylate, outlined in **Scheme 5**, began with a Sonogashira coupling between

phenylacetylene and 4-iodophenol using tetrakis(triphenylphosphine)palladium and copper(I) iodide to obtain **DPA** phenol (**4c**) in a 95% yield.[62] This material was reacted with 4-dimethylaminopyridine (DMAP) and methacrylic anhydride to form **DPA** methacrylate (**8d**) in a 75% yield. Finally, we polymerized **DPA** methacrylate using CPDB as the RAFT reagent using the conditions from entry 15 in **Table 4.** This polymerization went to 96% conversion and yielded 106 mg of pure ***poly*-DPA.**

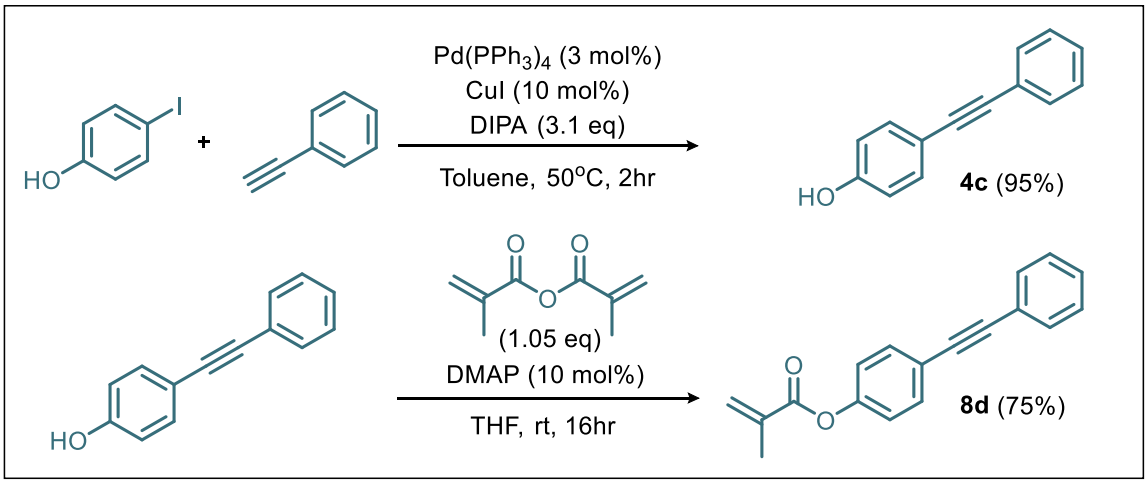

Scheme 6: The two-step synthesis of **DPA** methacrylate.

2.5.3 Decarbonylation of DPCP Methcrylates

After obtaining ***poly*-DPCP** and its theoretical photoproduct ***poly*-DPA**, we investigated the photo-decarbonylation of ***poly*-DPCP**. All of our experiments were conducted on the polymer that was synthesized under the conditions underlined in **Table 4**. We irradiated (365 nm, ~10 mW/cm^2, 30 min, RT) our 0-PEG methacrylated **DPCP** 50-unit polymer (**Figure 13A**) and monitored its CO release via ^{1}H NMR and FTIR using a horizontal curing station. We found that the CO release from the decarbonylation was remarkably clean and went to completion in under 30 minutes of irradiation. The ^{1}H NMR

spectrum of the irradiated polymer photoproduct overlayed perfectly with the ^{1}H NMR spectrum of independently synthesized ***poly*-DPA (Figure 13B).** Moreover, a solution of ***poly*-DPCP** in DCM was drop-cast onto a salt plate, the solvent was allowed to fully evaporate, and the resultant thin film was analyzed by FTIR. Via this method we observed the disappearance of the carbonyl (~1850 cm^{-1}) and alkene (~1620 cm^{-1}) stretches belonging to **DPCP** and the appearance of a alkyne stretch (~2220 cm^{-1}) belonging to **DPA** upon irradiation. We also observed that the FTIR spectrum of the irradiated polymer photoproduct overlayed perfectly with the FTIR spectrum of independently synthesized ***poly*-DPA (Figure 13C**). These results indicate that ***poly*-DPCP** can successfully liberate CO gas upon photolysis even under mild irradiation to form only ***poly*-DPA**. Of note, no special precautions (dry solvent, use of inert atmosphere, etc.) were taken for the photolysis of ***poly*-DPCP** to ***poly*-DPA**, evidencing the spring-loaded nature of the cyclopropenone functionality and the robustness of CO release by an anionic, non-radical mechanism.

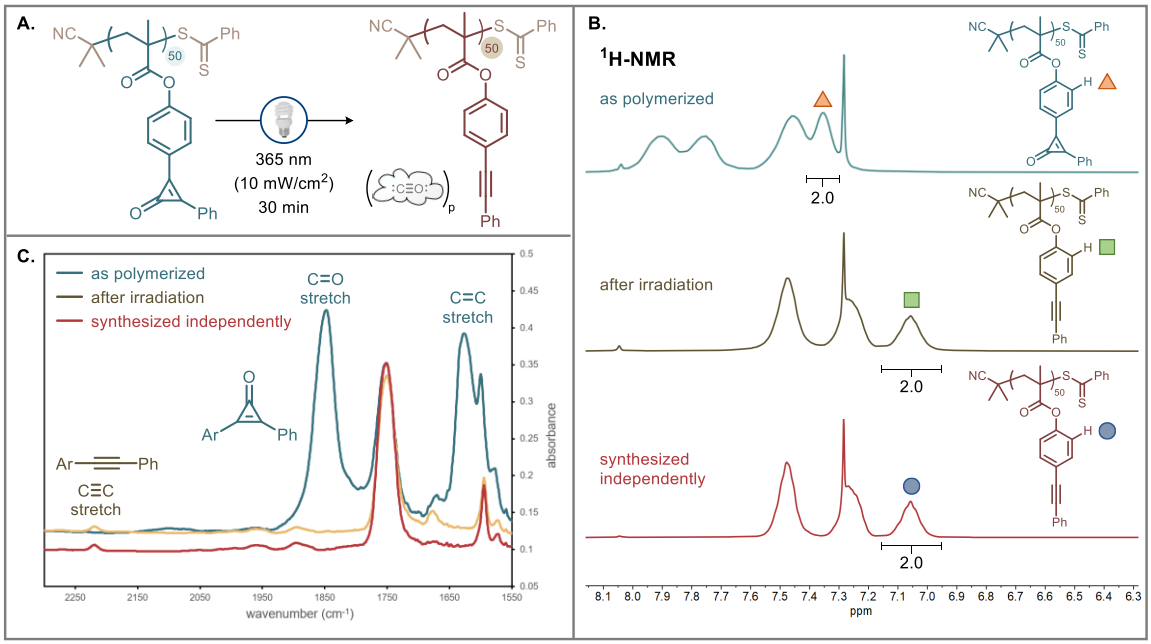

Figure 13: A. Photolysis of a **DPCP** methacrylate 50-unit polymer to yield CO and ***poly*-DPA**, **B.** The clean photolysis of a **DPCP** methacrylate 50-unit polymer monitored by ^{1}H NMR, **C.** FTIR monitoring of the photolysis in real time.

2.6 Synthesis of Styrene DPCP

After synthesizing and polymerizing both acrylated and methacrylated **DPCP** monomers, we sought to synthesize a new **DPCP** monomer based on styrene (***sty*-DPCP)**. Polymerization of ***sty*-DPCP** will bring intermolecular **DPCP** moieties 1Å closer than Garcia-Garibay's tethered **DPCPs** and much closer than ***poly*-DPCPs** derived from either acrylates or methacrylates. Theoretically, due to the close proximity of the repeat units ***poly*-DPCPs** based on styrene will exhibit stronger quantum amplificative effects than ***poly*-DPCPs** based on acrylates and methacrylates, as well as Garcia-Garibay's tethered **DPCPs.** Although ***poly*-DPCPs** based on styrene could have improved photolytic CO release, we found the synthesis of this monomer to be quite challenging and ultimately

required us to evaluate several synthetic routes and methods. Ultimately, we prevailed and our optimized synthesis is detailed below.

The synthesis of ***sty*-DPCP** (**Scheme 7**) begins from commercially available ethyl phenylacetate (**9**) and 4-bromophenylacetonitrile (**10**) which undergo a modified cross-Claisen condensation to form a β-ketonitrile under basic conditions.[63] This β-ketonitrile was submitted to an optimized acidic hydrolysis to form a β-ketoacid, which spontaneously decarboxylated to form ketone **11a** in a moderate overall yield (48% over 2 steps).[64] Ketone **11a** was then protected as the ketal (**11b**) under standard conditions in quantitative yield. Ketal **11b** was subsequently reacted with bromine (Br_2) in ether (Et_2O), to form the di-α-brominated ketal **11c** in quantitative yield.[65] The brominated ketal **11c** was reacted with excess potassium *tert*-butoxide (KO*t*Bu) to undergo an intramolecular S_N2 followed by elimination (presumably via an E1 mechanism)[66] to afford the cyclopropenone ketal **11d**

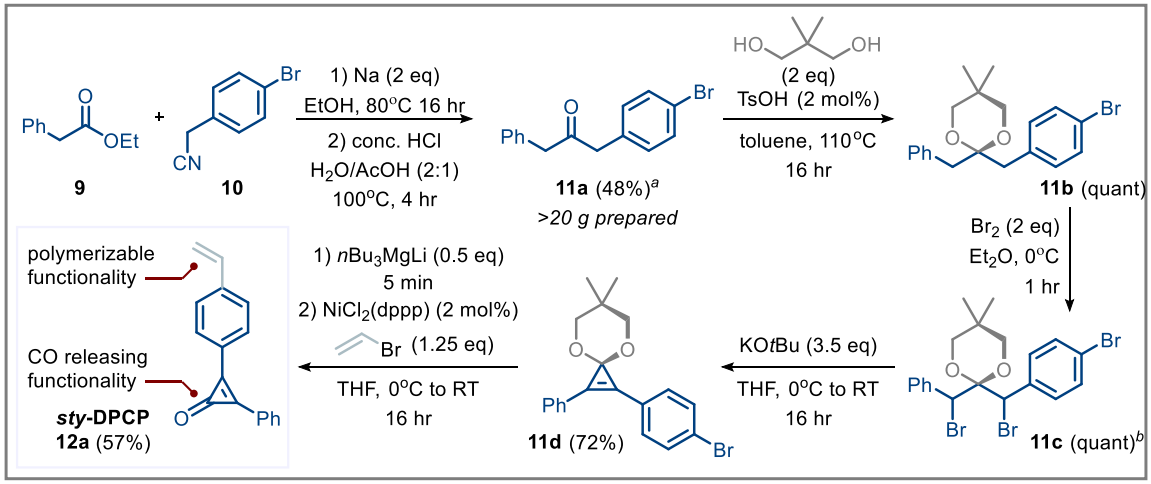

Scheme 7: A modular, scalable 6-step synthesis of ***sty*-DPCP**. a. Yield over 2 steps. b. Isolated as a mixture of brominated structural isomers that are resolved in the subsequent step.

in good yield (75%) and high purity (>99%) after trituration with cold hexanes. This 5-step sequence was scalable and operationally simple; it has yielded many grams of cyclopropenone ketal **11d** (>5 grams to date) and required only one purification by column chromatography. Finally, the vinyl group was attached by first reacting cyclopropenone ketal **11d** with lithium tri-*n*-butylmagnesate followed by a nickel-catalyzed Kumada coupling with vinyl bromide.[67] Upon quenching this cross-coupling with an aqueous solution of HCl, it was discovered that the deprotected ***sty*-DPCP** (**12a**) was obtained directly in good yield (57%).[68]

2.7 Polymerization of Styrene DPCP

2.7.1 Radical and RAFT Polymerizations of Styrene DPCP

With ***sty*-DPCP** in hand, we began to explore its compatibility with RAFT polymerizations (**Scheme 8**). Although we are currently in the early stages of optimizing the controlled polymerization of ***sty*-DPCP**, the results from the existing optimization

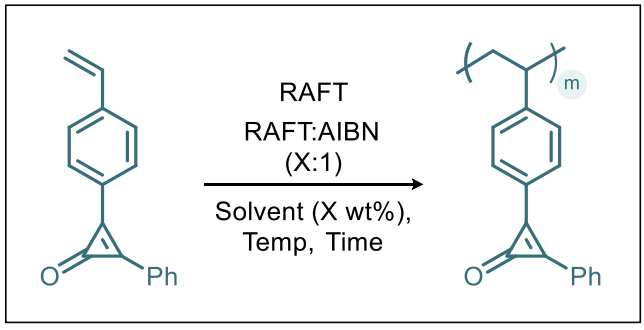

Scheme 8: Optimization experiments for the RAFT polymerization of **sty-DPCP**.

experiments are shown in **Table 5.** The results from this study were similar to the results from the **DPCP** acrylate optimization experiments. We found that increasing the

concentration of initiator resulted in higher conversions, but, given our previous experience with acrylated and methacrylated **DPCPs,** significant further optimization to control this polymerization will need to be conducted. Likely other controlled methods for the polymerization of ***sty*-DPCP** that are, in general, more compatible with styrene-based monomers such as nitroxide-mediated polymerization (NMP)[69] or atom transfer radical polymerization (ATRP)[70] should be evaluated.

entry	m_{th}	temp °C	Hrs.	solvent	RAFT reagent	RAFT: AIBN	Conc. wt%	P_{th}	p_{exp}
1	50	70	24	DMF	DoPAT	5	300	95	43
2	50	70	24	DMF	DTB-2PA	5	300	95	38
3	50	70	96	DMF	DoPAT	5	300	95	72
4	50	70	24	DMF	DoPAT	3	400	95	82
5	50	70	48	DMF	DoPAT	3	400	95	85
6	50	70	96	DMF	DoPAT	3	400	95	89
7	25	70	24	DMF	DoPAT	10	300	95	75
8	50	70	24	DMF	DoPAT	10	300	95	60
9	100	70	24	DMF	DoPAT	10	300	95	57

Table 5: Optimization experiments for RAFT polymerization of **DPCP** methacrylates. ***n*** = monomer used; $\boldsymbol{m_{th}}$ **=** theoretical number of monomer units per polymer; $\boldsymbol{p_{th}}$ = theoretical converstion; $\boldsymbol{p_{exp}}$ = experimental conversion.

Next, we attempted the direct polymerization of this molecule. Accordingly, ***sty*-DPCP** was reacted overnight at 60°C with a catalytic quantity of AIBN (0.5 mol%) in

DMF (1M), which resulted in the smooth homo-polymerization of ***sty*-DPCP** (**12a**) to ***poly*-DPCP** (**12b**, **Figure 14A**). Analysis by GPC verified the existence of the styrene-based polymer which was found to have a number average molecular weight of 19.6 kDa (an ~84-mer of ***sty*-DPCP**) and a dispersity of 2.08 (**Figure 14B**, *blue line*).

2.7.2 Decarbonylation of Styrene DPCP

Irradiation (365 nm, ~10 mW/cm^2, 30 min, RT) of a sample of ***poly*-DPCP** with low intensity light in $CDCl_3$ (1 wt%) and analysis of the product by SEC showed retention of the polymer backbone with no photochemical crosslinking or cleavage (**Figure 14B**, *brown line*). Given the slightly higher molecular weight (21.9 kDa) and dispersity (2.29), it is likely that the hydrodynamic volume of **12c** was marginally larger than ***poly*-DPCP**

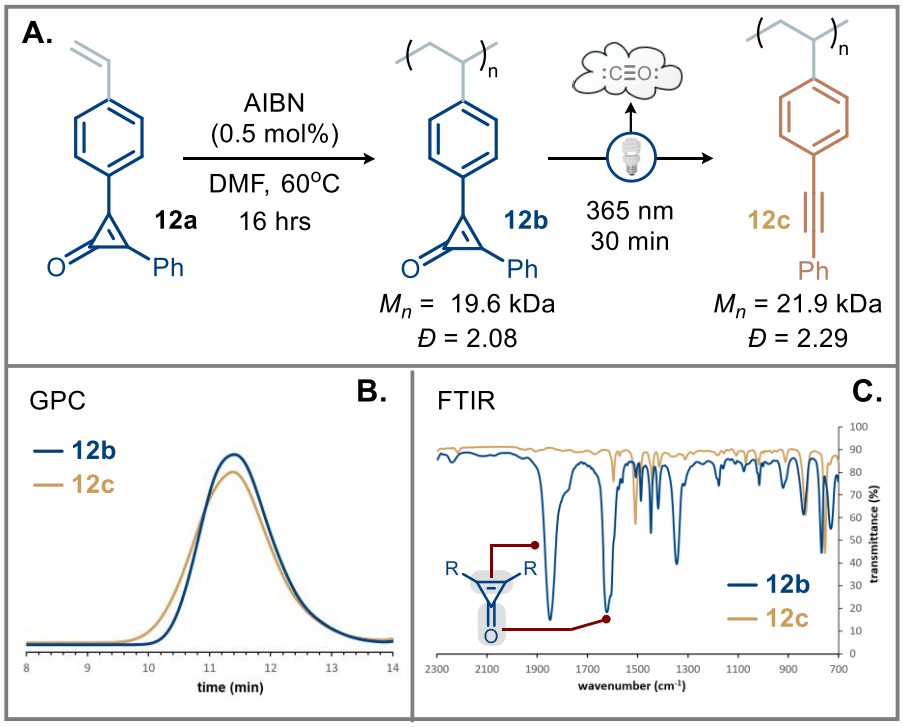

Figure 14: A. Direct free-radical polymerization of ***sty*-DPCP** (**12a**) to ***poly*-DPCP** (**12b**) and photolysis to CO gas and **12c**; **B.** SEC of polymers **12b** and **12c**; **C.** FTIR of polymers **12b** and **12c** showing loss of the cyclopropenone functionality.

(**12b**) leading to inflation of these values. Furthermore, a solution of ***poly*-DPCP** in DCM was drop-cast onto a salt plate, the solvent was allowed to fully evaporate, and the resultant thin film was analyzed by FTIR, showing that the cyclopropenone functionality (carbonyl peak at 1618 cm^{-1} and alkene at 1853 cm^{-1}) survived free-radical polymerization (**Figure 14C**, *blue line*). Irradiation of this salt plate using UV light (365 nm, ~10 mW/cm^2, 30 minutes) showed disappearance of the cyclopropenone (**Figure 14C**, *brown line*), directly evidencing the ability of these polymeric materials to release CO once irradiated. Change in chemical structure of ***poly*-DPCP** was further evidenced by ^1H NMR, showing complete

change in the polymer after standard irradiation conditions (1 wt% in $CDCl_3$, 365 nm, ~10 mW/cm^2, 30 minutes).

2.8 Future Work

The work presented in this thesis shows the synthesis of ***poly*-DPCPs** and their ability to rapidly and cleanly release CO gas, effectively laying the foundation for the use of these molecules as **CORMs** and as tools to study quantum amplification reactions. The next step of this project begins with further optimization of controlled polymerizations of ***poly*-DPCP** based on methacrylate and styrene appended cyclopropenones. Fortunately, the Worrell lab has purchased a UV detector for our GPC that will enable detection of ***poly*-DPCPs** in chloroform, greatly aiding in our ability to further optimize these polymerizations. With the ability to rapidly analyze M_n and dispersity of ***poly*-DPCPs** in lab, the optimization of the RAFT system will be attainable. Upon achieving low dispersities and accurate molecular weights, the amplificative CO release of each ***poly*-DPCP** can be assessed by determining the quantum yields of decarbonylation upon irradiation with 365 nm and 312 nm wavelengths of light.

Long-term goals of this project are geared towards using ***poly*-DPCPs** as **CORMs** to study and treat inflammatory bowel diseases (IBD), where CO has already been shown to have a significant therapeutic role. Naturally, ***poly*-DPCPs** have poor solubility in water, limiting their use in biological systems. To remedy this, RAFT agents will enable the creation of block copolymers to reliably add hydrophilic blocks, forming polymers that are soluble in physiological conditions. To test the use of our polymers in biological systems,

future work will be done in collaboration experts in IBD, specifically the Colgan/Onyiah group at the University of Colorado.

2.9 Conclusion

The importance of CO in biological systems is clear but tools for its delivery are currently insufficient. In this thesis we have reported the synthesis and polymerization of multiple **DPCP** based monomers to form ***poly*-DPCPs** that successfully release CO upon irradiation. To the best of our knowledge, **DPCP-**based monomers are the first directly polymerizable **CORMs**, and ***poly*-DPCP** is the first example of an organic ***poly*-CORM**. However, the use of ***poly*-DPCPs** as **CORMs** is currently limited by heterogeneity within polymeric samples and limited control over molecular weight. Optimizing the RAFT polymerization of **DPCP** based monomers will enable their di-block co-polymerization with hydrophilic monomers to produce water soluble **DPCP**-based **CORMs**. Overall, the information in this thesis sets the stage for developing a new and improved class of **CORMs** that will potentially be utilized as tools to deliver therapeutic dosages of CO in humans and in biological systems.

3. Experimental

3.1 General methods

All chemical reactions were carried out under a nitrogen atmosphere with dry solvents using anhydrous conditions unless otherwise stated. ^{1}H NMR (400 MHz) and ^{13}C NMR (101 MHz) were recorded in C_6D_6 (internal standard: 7.15 ppm, ^{1}H; 128.26 ppm, ^{13}C), in THF-d4 (internal standard: 3.58 ppm, ^{1}H; 67.57 ppm, ^{13}C), in $CDCl_3$ (internal standard: 7.26 ppm, ^{1}H; 77.00 ppm, ^{13}C), in MeCN-d3 (internal standard: 1.94 ppm, ^{1}H; 118.3 ppm, ^{13}C), in DMSO-d6 (internal standard: 2.50 ppm, ^{1}H; 39.52 ppm, ^{13}C), in MeOD-d3 (internal standard: 3.31 ppm, ^{1}H; 49.15 ppm, ^{13}C), on a Bruker DRX-500 MHz spectrometer. Chemical shifts (d) were reported as parts per million (ppm) and the following abbreviations were used to identify the multiplicities: s = singlet, d = doublet, t = triplet, q = quartet, sept. = septet, m = multiplet, b = broad and all combinations thereof can be explained by their integral parts. Column chromatography was carried out employing silica gel (40-63 µm, 230-400 mesh, 60A, Ultrapure, Spectrum Chemical) with the indicated solvent mixtures. All chemicals were obtained from commercial sources and used as received unless otherwise noted within the context of use. Chemicals were obtained from commercial sources and were used as received unless otherwise specified. All bulk solvents were purchased from Fisher Scientific or VWR and were used as received unless otherwise stated. All deuterated solvents utilized in this study (C_6D_6, THF-d4, $CDCl_3$,

MeCN-d3, DMSO-d6, and MeOD-d3) were obtained from Cambridge Isotope Laboratories, Inc. and were used as received.

3.2 Synthesis

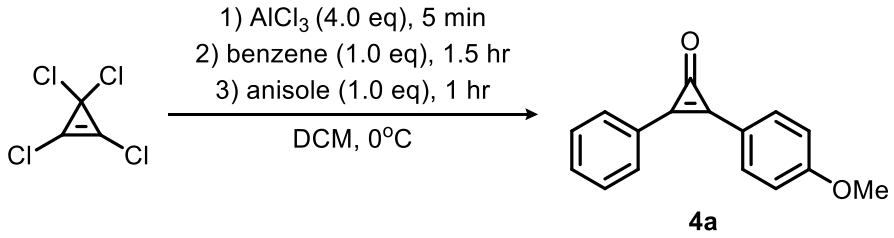

4a

To a flame dried 250 mL round-bottom flask under N_2 equipped with a magnetic stir bar was added 17.4 g (131 mmol, 4.00 equiv) aluminum trichloride ($AlCl_3$) which was diluted with ~110 mL of anhydrous DCM (~0.30 M). The flask was cooled to 0°C before adding 4.00 mL (5.80 g, 32.6 mmol, 1.00 equiv) tetrachlorocyclopropene over 30 minutes. After the tetrachlorocyclopropene was added, the homogeneous reaction mixture turned green. This mixture was allowed to stir for an additional 10 minutes at 0°C before 2.90 mL (2.55 g, 32.6 mmol, 1.0 equiv) benzene was added dropwise. The addition of benzene resulted in the reaction mixture turning dark orange/brown. After stirring at 0°C for 90 minutes, 3.55 mL (3.53 g, 32.6 mmol, 1.00 equiv) anisole was added to the reaction mixture. The reaction mixture was removed from the ice bath and continued stirring for 60 minutes. The reaction was transferred to a 500 mL Erlenmeyer flask equipped with a stir bar and cooled to 0°C before quenching with a saturated aqueous solution of ammonium chloride (NH_4Cl). The dark yellow mixture was transferred to a 500 mL separatory funnel and the aqueous layer was extracted with DCM (100 mL, 2x). The combined organics were washed with brine (~250 mL), dried over Na_2SO_4, filtered, and concentrated to yield a

crude yellow solid. The crude product was purified by column chromatography eluting with (40% acetone/hexanes). The chromatographed product was recrystallized from a solution of 20:1 hexanes:acetone which yielded 4.99 g (69% yield) of the title compound as white crystals.

DPCP-OMe (4a): white crystals; 69% yield; R_f = 0.47 (TLC conditions: 50% acetone/hexanes); ^{1}H NMR (500 MHz, $CDCl_3$) δ = 7.95 (dd, *J* = 7.5, 3.6 Hz, 4H), 7.60 – 7.54 (m, 3H), 7.07 (dd, *J* = 8.8, 2.5 Hz, 2H), 3.91 (s, 3H); ^{13}C NMR (126 MHz, $CDCl_3$) δ = 163.13, 155.56, 147.77, 144.46, 133.82, 132.23, 131.20, 129.32, 124.30, 116.80, 114.83, 77.41, 77.16, 76.90, 55.61.

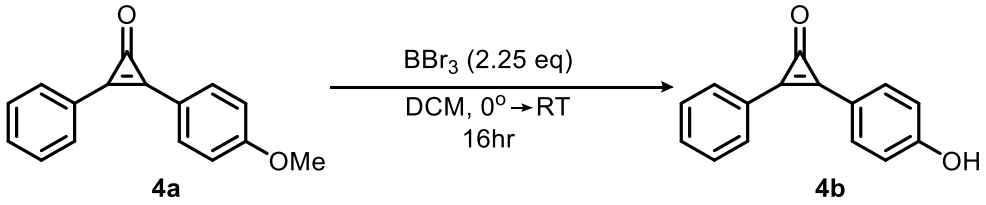

To a flame dried 250 mL round-bottom flask under N_2 equipped with a magnetic stir bar was added 3.30 g (14.0 mmol, 1.00 equiv) **DPCP-OMe** (**4a**) which was diluted with ~45.0 mL anhydrous DCM (~0.30 M). This solution was cooled to 0°C before adding 31.5 mL (1 M in DCM, 31.5 mmol, 2.25 equiv) of BBr_3 dropwise. The reaction was allowed to warm to room temperature while stirring overnight. After this time, the reaction was cooled to 0°C and quenched with a saturated ammonium chloride solution. The volatiles were removed under reduced pressure and the product was diluted in THF (~150 mL). The solution was transferred to a 500 mL separatory funnel, washed with a saturated

aqueous solution of ammonium chloride (~150 mL), water (~150 mL), brine (~150 mL), and dried

over sodium sulfate. The volatiles were removed under reduced pressure to afford 3.11 g (100% yield) of an off-white powder that was used without further purification.

DPCP-OH (**4b**): off-white powder; 100% yield; R_f = 0.25 (TLC conditions: 50% acetone/hexanes); ^{1}H NMR (500 MHz, MeOD-d3) δ = 8.03 (dt, *J* = 6.5, 2.2 Hz, 2H), 7.97 (dd, *J* = 8.8, 2.2 Hz, 2H), 7.67 (dq, *J* = 5.7, 3.5 Hz, 3H), 7.05 (dd, *J* = 8.6, 1.9 Hz, 2H); ^{13}C NMR (126 MHz, MeOD-d3) δ = 164.15, 157.91, 147.87, 142.94, 135.77, 133.88, 132.56, 130.67, 124.91, 117.59, 115.86.

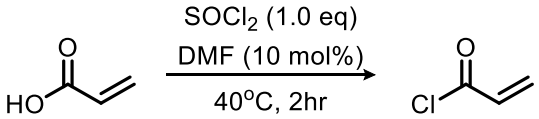

5a

To a flame-dried 50 mL round-bottom flask equipped with a magnetic stir bar was added 10.1 mL (16.5 g, 139 mmol, 1.00 equiv) thionyl chloride ($SOCl_2$), 76.0 mg (0.35 mmol, 2500 ppm) butylated hydroxytoluene (BHT) and 1.07 mL (1.01 g, 13.9 mmol, 0.10 equiv) dimethyl formamide (DMF). While stirring under N_2 at room temperature, 9.52 mL (10.0 g, 139 mmol, 1.00 equiv) acrylic acid was added dropwise. The reaction was heated to 40°C and after one hour of stirring, a short path distillation head was attached to the round-bottom flask. The oil bath temperature was increased to 130°C and the product distilled at 70°C (probe temp, atmospheric pressure) to afford 4.98 g (40% yield) of the acryloyl chloride as a clear liquid which was used directly in the next step with no further purifications.

Acryloyl Chloride (**5a**)**:** Clear liquid; 40% yield; R_f = 0.66 (TLC conditions: 50% ethyl acetate/hexanes); ^{1}H NMR (500 MHz, $CDCl_3$) δ = 6.66 (d, *J* = 16.8 Hz, 1H), 6.37 (dd, *J* = 16.8, 10.2 Hz, 1H), 6.20 (d, *J* = 10.2 Hz, 1H); ^{13}C NMR (126 MHz, $CDCl_3$) δ = 166.46, 136.74, 133.17.

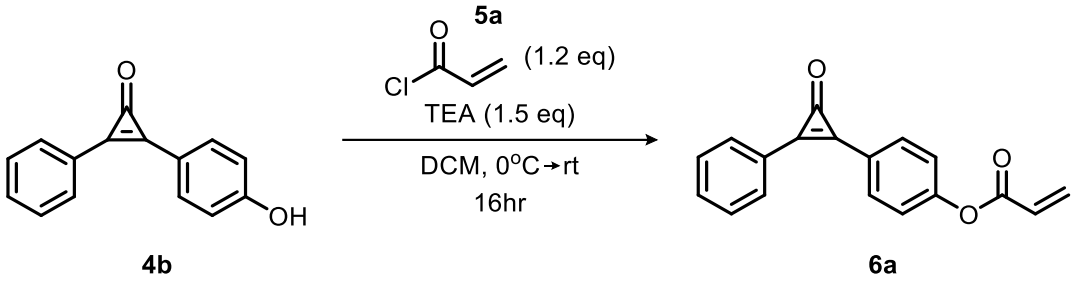

To a flame-dried 100 mL round-bottom flask under N_2 equipped with a magnetic stir bar was added 1.00 g (4.50 mmol, 1.00 equiv) of **DPCP-OH** (**4b**) which was diluted with 15.0 mL anhydrous DCM (0.30M). To this solution was added 0.94 mL (0.68 g, 6.75 mmol, 1.50 equiv) triethylamine (TEA) and the reaction was cooled to 0°C and was allowed to stir for 5 minutes before adding 490 mg (5.40 mmol, 1.20 equiv) **acryloyl chloride** (**5a**) dropwise. The reaction was allowed to warm to room temperature while stirring overnight. Following this period, the volatiles were removed under reduced pressure to yield a crude residue which was purified by column chromatography eluting with 40% acetone/hexanes. Evaporation of the fractions under reduced pressure yielded 660 mg (66% yield) of the title compound as yellow powder.

0-PEG acrylated DPCP (**6a**)**:** Yellow powder; 66% yield; R_f = 0.52 (TLC conditions: 50% acetone/hexanes); ^{1}H NMR (500 MHz, $CDCl_3$) δ = 8.05 (d, *J* = 8.6 Hz, 2H) 8.02 – 7.95 (m, 2H), 7.70 – 7.52 (m, 3H), 7.41 (d, *J* = 8.5 Hz, 2H), 6.68 (dd, *J* = 17.4, 1.1 Hz, 1H),

6.37 (dd, *J* = 17.4, 10.5 Hz, 1H), 6.11 (dd, *J* = 10.4, 1.1 Hz, 1H); ^{13}C NMR (126 MHz, $CDCl_3$) δ = 163.90, 155.52, 153.81, 148.14, 147.44, 133.69, 133.01, 132.88, 131.53, 129.52, 127.49, 124.07, 122.84, 121.79.

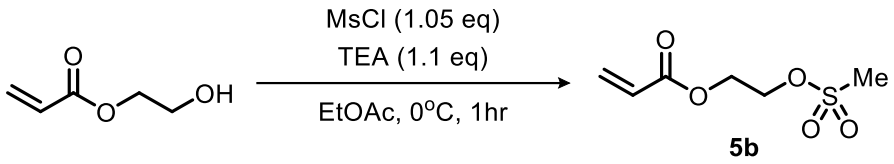

To a 100 mL flame-dried round-bottom flask under N_2 equipped with a magnetic stir bar was added 2.30 mL (2.32 g, 20.0 mmol, 1.00 equiv) 2-hydroxyethyl acrylate, which was diluted with 20.0 mL ethyl acetate (1.00 M). To this solution was added 3.06 mL (2.22 g, 22.0 mmol, 1.10 equiv) triethylamine (TEA) and the reaction mixture was cooled to 0°C. This reaction mixture was allowed to stir for 5 minutes before the adding 1.62 mL (2.40 g, 21.0 mmol, 1.05 equiv) methanesulfonyl chloride dropwise. This reaction was allowed to stir at 0°C for 1 hour before water (~50.0 mL) was added, the biphasic mixture was transferred to a 250 mL separatory funnel, and the aqueous layer was extracted with ethyl acetate (~30 mL). The combined organics were washed with water (~100 mL), dried over sodium sulfate, filtered, and approximately 1000 ppm butylated hydroxytoluene was added to the organic layer. The solvent was removed under reduced pressure to yield 3.88 g (100% yield) of the title compound as a clear liquid that was used in the next step with no further purifications.

1-PEG acrylated mesylate (5b): Clear liquid; 100% yield; R_f = 0.25 (TLC conditions: 50% ethyl acetate/hexanes); ^{1}H NMR (500 MHz, $CDCl_3$) δ = 6.46 (dd, J = 17.2, 1.3 Hz,

1H), 6.15 (dd, J = 17.3, 10.5 Hz, 1H), 5.90 (dd, J = 10.5, 1.3 Hz, 1H), 4.49 – 4.38 (m, 4H), 3.05 (s, 3H); ^{13}C NMR (126 MHz, $CDCl_3$) δ = 165.65, 132.05, 127.66, 67.22, 61.98, 37.75.

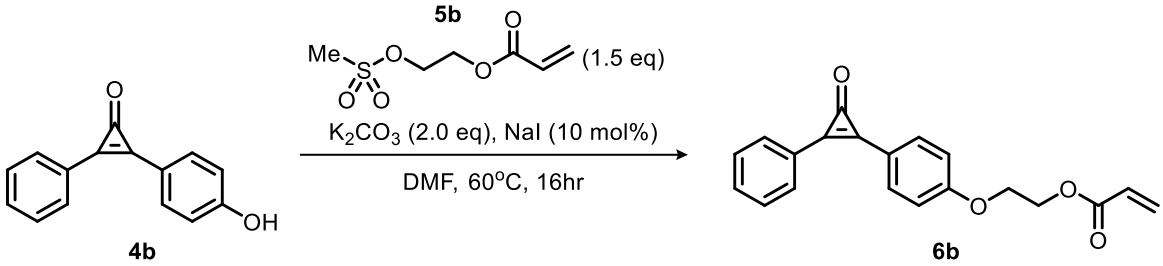

To a flame-dried 100 mL round-bottom flask under N_2 equipped with a magnetic stir bar was added 2.50 g (11.3 mmol, 1.00 equiv) of **DPCP-OH** (**4b**) which was diluted with 22.5 mL DMF (~0.50 M). To this solution was added 3.28 g (16.9 mmol, 1.50 equiv) of**1-PEG acrylated mesylate** (**5b**) via syringe followed by 170 mg (1.13 mmol, 0.10 equiv) sodium iodide (NaI). Finally, 3.11 g (22.5 mmol, 2.00 equiv) potassium carbonate (K_2CO_3) was added to the reaction mixture, the round-bottom flask was equipped with a reflux condenser, and the reaction was heated to 60°C for 16 hours. After this period, the flask was cooled to room temperature and the reaction mixture was transferred to a 500 mL separatory funnel. The reaction was diluted with ethyl acetate (~200 mL), washed with water (~250 mL), brine (~250 mL), dried over sodium sulfate, filtered, and submitted to column chromatography (20% acetone/hexanes → 50% acetone/hexanes). Evaporation of the fractions containing the desired material yielded 2.83 g (79%) of the title compound as a yellow solid.

1-PEG acrylated DPCP (**6b**)**:** Yellow powder; 79% yield; R_f = 0.44 (TLC conditions: 50% acetone/hexanes); ^{1}H NMR (500 MHz, $CDCl_3$) δ = 7.95 (dt, *J* = 7.5, 2.7 Hz, 4H), 7.60

– 7.53 (m, 3H), 7.09 (d, *J* = 9.0 Hz, 2H), 6.46 (dd, *J* = 17.3, 1.4 Hz, 1H), 6.17 (dd, *J* = 17.3, 10.5 Hz, 1H), 5.88 (dd, *J* = 10.4, 1.4 Hz, 1H), 4.56 (t, *J* = 4.6 Hz, 2H), 4.32 (t, *J* = 4.7 Hz, 2H); ^{13}C NMR (126 MHz, $CDCl_3$) δ = 166.08, 162.03, 155.65, 147.74, 145.00, 133.93, 132.41, 131.75, 131.35, 129.44, 127.99, 124.37, 117.38, 115.44, 66.26, 62.59.

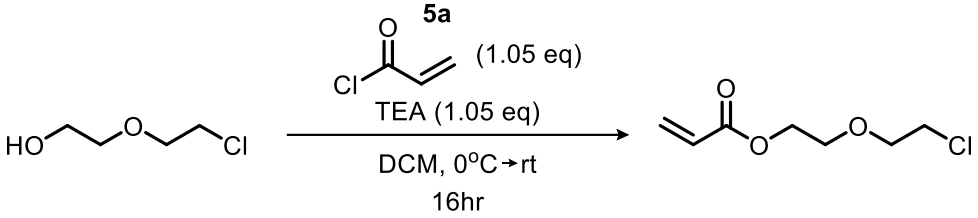

To a flame-dried100 mL round-bottom flask under N_2 equipped with a magnetic stir bar was added 2.12 mL (2.50 g, 20.2 mmol, 1.00 equiv) 2-(2-chloroethoxy)ethanol, which was diluted with 25.0 mL anhydrous THF (0.80 M). To this solution was added 2.95 mL (2.14 g, 21.2 mmol, 1.05 equiv) triethylamine (TEA). The reaction mixture was cooled to 0°C before adding 1.91 g (21.2 mmol, 1.05 equiv) **acryloyl chloride** (**5a**) dropwise via syringe. The reaction was allowed to warm to room temperature while stirring overnight. After this period, the volatiles were removed under reduced pressure to yield a crude residue that was diluted in ethyl acetate (~100 mL), transferred to a 250 mL separatory funnel, washed with water (~150 mL), washed with brine (~150 mL), dried over sodium sulfate, filtered, and purified by column chromatography (20% EtOAc/hexanes). Evaporation of the fractions containing the desired material yielded 1.51 g (42% yield) of the title compound as a clear liquid.

2-PEG acrylated chloro: Clear liquid; 42% yield; R_f = 0.39 (TLC conditions: 20% ethyl acetate/hexanes); ^{1}H NMR (500 MHz, $CDCl_3$) δ = 6.46 (dd, *J* = 17.3, 1.5 Hz, 1H), 6.18

(dd, *J* = 17.4, 10.5 Hz, 1H), 5.87 (dd, *J* = 10.4, 1.5 Hz, 1H), 4.35 (t, *J* = 4.7 Hz, 2H), 3.83 – 3.76 (m, 4H), 3.65 (t, *J* = 5.8 Hz, 2H); ^{13}C NMR (126 MHz, $CDCl_3$) δ = 166.14, 131.21, 128.26, 71.34, 69.20, 63.56, 60.44, 42.70, 14.27.

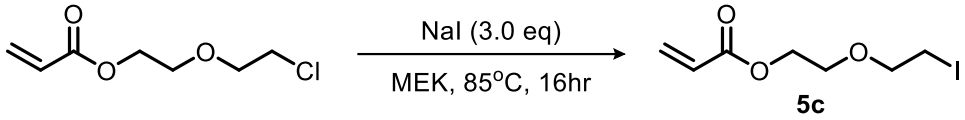

5c

To a 100 mL round-bottomed flask equipped with a magnetic stir bar was added 1.60 grams (8.97 mmol, 1.00 equiv) of **2-PEG acrylated chloro** and this was diluted with 30.0 mLs (0.30 M) of reagent grade methyl ethyl ketone (MEK). To this solution was added 4.03 grams (26.9 mmol, 3.00 equiv) of sodium iodide (NaI), the flask was equipped to a reflux condenser, heated to 85°C, and refluxed at this temperature overnight. After this time, the reaction mixture was concentrated under reduced pressure and the resultant crude residue was dissolved in EtOAc (~150 mLs), transferred to a 500 mL separatory funnel, and the organic layer was washed with water (~100 mLs), a saturated solution of $Na_2S_2O_3$ (~100 mLs), and brine (~100 mLs). The combined organics were then dried over sodium sulfate, filtered, and concentrated under reduced pressure to yield 2.01 g (83% yield) of the title compound as a clear liquid that was used in the next step with no further purifications. **2-PEG acrylated iodo (5c):** Clear liquid; 83% yield; R_f = 0.41 (TLC conditions: 20% ethyl acetate/hexanes); ^{1}H NMR (500 MHz, $CDCl_3$) δ = 6.44 (dd, *J* = 17.4, 1.4 Hz, 1H), 6.16 (dd, *J* = 17.4, 10.4 Hz, 1H), 5.85 (dd, *J* = 10.4, 1.4 Hz, 1H), 4.33 (t, *J* = 4.5 Hz, 2H), 3.80 – 3.72 (m, 4H), 3.26 (t, *J* = 6.8 Hz, 2H); ^{13}C NMR (126 MHz, $CDCl_3$) δ = 166.23, 131.33, 128.32, 71.98, 68.81, 63.65, 2.61.

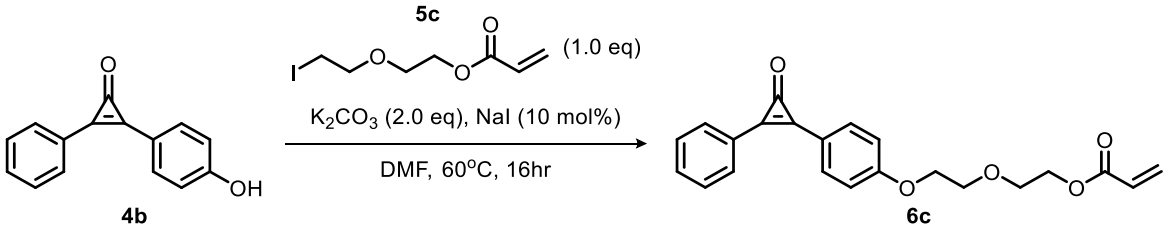

To a flame dried 100 mL round-bottom flask under N_2 equipped with a magnetic stir bar was added 1.00 g (4.50 mmol, 1.00 equiv) of **2-PEG acrylated iodo** (**5c**) which was diluted with 9.00 mL of DMF (0.5M). To this solution was added 1.22 g (4.50 mmol, 1.00 equiv) of **5c** via syringe followed by 67.5 mg (1.13 mmol, 0.10 equiv) sodium iodide (NaI). Finally, 1.25 g (9.0 mmol, 2.00 equiv) potassium carbonate (K_2CO_3) was added to the reaction mixture, the round-bottom flask was equipped with a reflux condenser, and the reaction was heated to 60°C for 16 hours. After this period, the reaction was cooled to room temperature and transferred to a 500 mL separatory funnel. The reaction was diluted with ethyl acetate (~200 mL), washed with water (~250 mL), brine (~250 mL), dried over sodium sulfate, filtered, and submitted to column chromatography (20% acetone/hexanes → 50% acetone/hexanes). Evaporation of the fractions containing the desired material yielded 1.45 g (74% yield) of the title compound as a light brown solid.

2-PEG acrylated DPCP (**6c**)**:** Light brown solid; 74% yield; R_f = 0.40 (TLC conditions: 50% acetone/hexanes); ^{1}H NMR (500 MHz, $CDCl_3$) δ = 7.98 – 7.91 (m, 4H), 7.57 (p, J = 3.3 Hz, 3H), 7.12 – 7.05 (m, 2H), 6.43 (dd, J = 17.3, 1.5 Hz, 1H), 6.15 (dd, J = 17.3, 10.4 Hz, 1H), 5.84 (dd, J = 10.4, 1.4 Hz, 1H), 4.39 – 4.34 (m, 2H), 4.26 – 4.21 (m, 2H), 3.94 – 3.89 (m, 2H), 3.86 – 3.81 (m, 2H); ^{13}C NMR (126 MHz, $CDCl_3$) δ = 166.17, 162.34,

155.66, 147.77, 144.68, 133.87, 132.33, 131.30, 131.23, 129.40, 128.24, 124.35, 117.08, 115.45, 69.48, 67.80, 63.58.

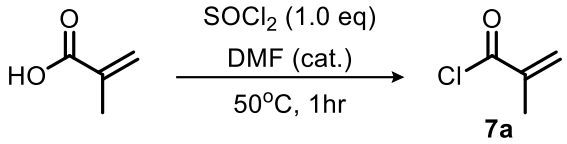

7a

To a flame-dried 50.0 mL round-bottom flask under N_2 equipped with a magnetic stir bar was added 8.85 mL (14.5 g, 122 mmol, 1.05 equiv) thionyl chloride ($SOCl_2$) and one drop of DMF. While stirring under N_2 at room temperature, 9.8 mL (10.0 g, 116.2 mmol, 1.00 equiv) methacrylic acid was added dropwise. The reaction was heated to 50°C, and after one hour of stirring, a short path distillation head was attached to the round-bottom flask. The oil bath temperature was increased to 130°C and the product distilled at 72°C (probe temp, ambient temperature) to afford 6.3 g (52% yield) of methacryloyl chloride (**7a**) as a clear liquid which was used directly in the next step with no further purifications.

Methacryloyl chloride (7a): Clear liquid; 52% yield; R_f = 0.67 (TLC conditions: 50% ethyl acetate/hexanes); ^{1}H NMR (500 MHz, $CDCl_3$) δ = 6.50 (s, 1H), 6.04 (s, 1H), 2.02 (s, 3H); ^{13}C NMR (126 MHz, $CDCl_3$) δ = 168.82, 140.71, 133.38, 18.54.

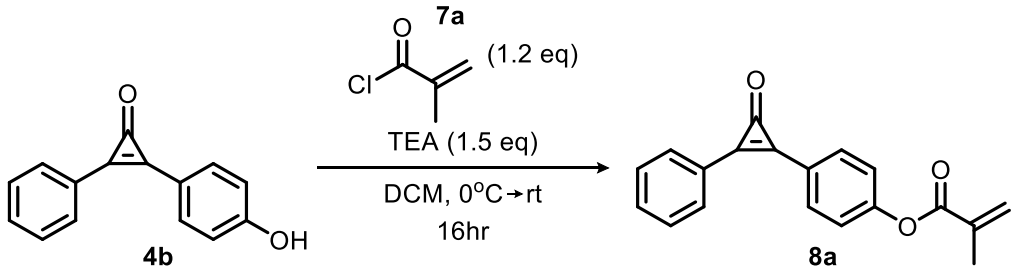

4b **8a**

To a flame-dried 100 mL round-bottom flask under N_2 equipped with a magnetic stir bar was added 1.50 g (6.75 mmol, 1.0 equiv) of **DPCP-OH** (**4b**) which was diluted with 22.5 mL anhydrous DCM (0.30M). To this solution was added 1.41 mL (1.02 g, 10.1 mmol, 1.50 equiv) triethylamine (TEA), the reaction was cooled to 0°C and was allowed to stir for 5 minutes before adding 847 mg (8.1 mmol, 1.20 equiv) **methacryloyl chloride** (**7a**) dropwise. The reaction was allowed to warm to room temperature while stirring overnight. Following this period, the volatiles were removed under reduced pressure to yield a crude residue which was purified by column chromatography eluting with 40% acetone/hexanes. Evaporation of the fractions containing the desired compound under reduced pressure yielded 1.21 g (62% yield) of the title compound as yellow powder.

0-PEG methacrylated DPCP (8a): Yellow powder; 62% yield; R_f = 0.58 (TLC conditions: 50% acetone/hexanes); ^{1}H NMR (500 MHz, $CDCl_3$) δ = 8.06 – 7.94 (m, 4H), 7.64 – 7.55 (m, 3H), 7.37 (d, *J* = 8.2 Hz, 2H), 6.40 (s, 1H), 5.83 (s, 1H), 2.08 (s, 3H); ^{13}C NMR (126 MHz, $CDCl_3$) δ = 165.17, 155.49, 154.15, 148.00, 147.45, 135.45, 132.93, 132.77, 131.45, 129.44, 128.15, 124.06, 122.85, 121.63, 18.32.

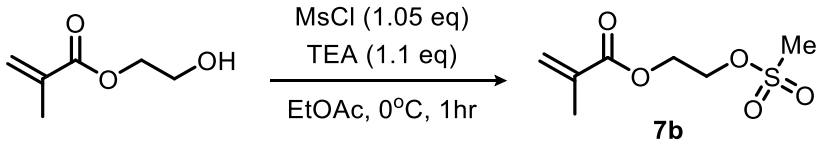

7b

To a 100 mL flame-dried round-bottom flask under N_2 equipped with a magnetic stir bar was added 932 μL (1.00 g, 20.0 mmol, 1.00 equiv) 2-hydroxyethyl methacrylate, which was diluted with 7.69 mL ethyl acetate (1.00 M). To this solution was added 1.18 mL (856 mg, 8.46 mmol, 1.10 equiv) triethylamine (TEA) and the reaction mixture was

cooled to 0°C. This reaction mixture was allowed to stir for 5 minutes before adding 625 µL (925 mg, 8.07 mmol, 1.05 equiv) methanesulfonyl chloride (MsCl) dropwise. This reaction was allowed to stir at 0°C for 1 hour before water (~50 mL) was added, the biphasic mixture was transferred to a 250 mL separatory funnel, and the aqueous layer was extracted with ethyl acetate (~30 mL). The combined organics were washed with water (~100 mL), dried over sodium sulfate, filtered, and 4.41 mgs (1000 ppm) butylated hydroxytoluene (BHT) was added to the organic layer. The volatiles were removed under reduced pressure to yield 1.60 g (100% yield) of the title compound as a clear liquid that was used in the next step with no further purifications.

1-PEG methacrylated mesylate (7b): Clear liquid; 100% yield; R_f = 0.54 (TLC conditions: 50% ethyl acetate/hexanes); ^{1}H NMR (500 MHz, $CDCl_3$) δ = 6.19 (s, 1H), 5.65 (s, 1H), 4.51 – 4.40 (m, 4H), 3.07 (s, 3H), 1.98 (s, 3H); ^{13}C NMR (126 MHz, $CDCl_3$) δ = 166.89, 135.64, 126.60, 67.14, 62.08, 37.79, 18.23.

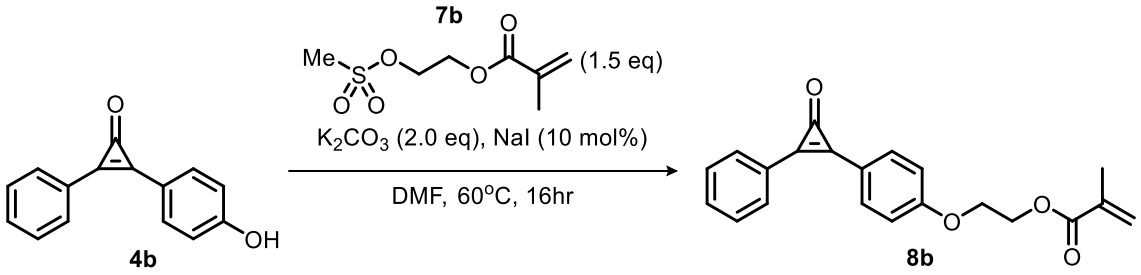

To a flame-dried 20 mL microwave vial under N_2 equipped with a magnetic stir bar was added 750 mg (3.38 mmol, 1.00 equiv) of **DPCP-OH** (**4b**) which was diluted with 6.75 mL of DMF (0.50 M). To this solution was added 1.05 g (5.07 mmol, 1.50 equiv) of **1-PEG methacrylated mesylate** (**7b**) via syringe followed by 51.0 mg (0.34 mmol, 0.10

equiv) sodium iodide (NaI). Finally, 934 mg (6.76 mmol, 2.00 equiv) potassium carbonate was added to the reaction mixture, the round-bottom flask was equipped with a reflux condenser, and the reaction was heated to 60°C for 16 hours. After this period, the flask was cooled to room temperature and the reaction mixture was transferred to a 500 mL separatory funnel. The reaction was diluted with ethyl acetate (~100 mL), washed with water (~150 mL), washed with brine (~150 mL), dried over sodium sulfate, filtered, and submitted to column chromatography (20% acetone/hexanes → 50% acetone/hexanes). Evaporation of the fractions containing the desired material yielded 768 mg (68% yield) of the title compound as a yellow solid.

1-PEG methacrylated DPCP (8b): Yellow flakes; 68% yield; R_f = 0.56 (TLC conditions: 50% acetone/hexanes); ^{1}H NMR (500 MHz, $CDCl_3$) δ = 8.00 – 7.94 (m, 4H), 7.64 – 7.57 (m, 3H), 7.11 (d, *J* = 8.3 Hz, 2H), 6.18 (s, 1H), 5.63 (s, 1H), 4.57 (t, *J* = 4.8 Hz, 2H), 4.35 (t, *J* = 4.8 Hz, 2H), 1.98 (s, 3H); ^{13}C NMR (126 MHz, $CDCl_3$) δ = 167.32, 162.14, 155.66, 147.78, 145.00, 135.97, 133.92, 132.40, 131.34, 129.44, 126.37, 124.40, 117.38, 115.50, 66.33, 62.78, 18.38.

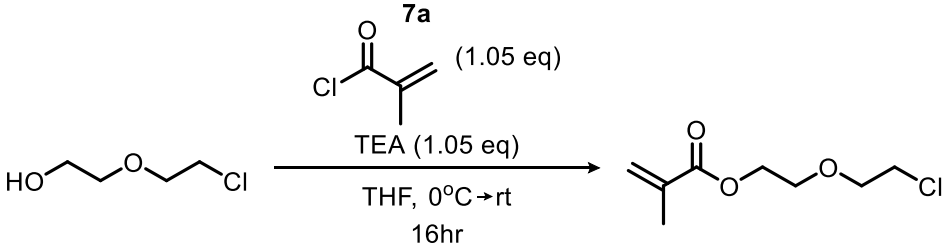

To a 50.0 mL round-bottom flask under N_2 equipped with a magnetic stir bar was added 1.27 mL (1.50 g, 12.04 mmol, 1.00 equiv) 2-(2-chloroethoxy)ethanol, which was diluted with 15.0 mL anhydrous THF (0.80 M). To this solution was added 1.76 mL (1.28

g, 12.6 mmol, 1.05 equiv) triethylamine (TEA). The reaction mixture was cooled to 0°C before adding 1.31 g (12.6 mmol, 1.05 equiv) **methacryloyl chloride** (**7a**) dropwise via syringe. The reaction was allowed to warm to room temperature while stirring overnight. After this period, the volatiles were removed under reduced pressure to yield a crude residue that was diluted in ethyl acetate (~100 mL), transferred to a 250 mL separatory funnel, washed with water (150 mL), washed with brine (~150 mL), dried over sodium sulfate, filtered, and purified by column chromatography (20% EtOAc/hexanes). Evaporation of the fractions containing the desired material yielded 1.59 g (69% yield) of the title compound as a clear liquid.

2-PEG methacrylated chloro: Clear liquid; 69% yield; R_f = 0.35 (TLC conditions: 10% EtOAc/hexanes); ^{1}H NMR (500 MHz, $CDCl_3$) δ = 6.16 (s, 1H), 5.60 (s, 1H), 4.33 (t, *J* = 5.8 Hz, 2H), 3.80 – 3.79 (m, 4H), 3.65 (t, *J* = 5.8 Hz, 2H), 1.97 (s, 3H); ^{13}C NMR (126 MHz, $CDCl_3$) δ = 167.32, 136.10, 125.84, 71.27, 69.18, 63.69, 42.66, 18.28.

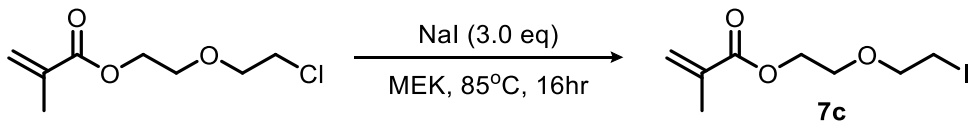

7c

To a 100 mL round-bottomed flask equipped with a magnetic stir bar was added 250 mg (1.30 mmol, 1.00 equiv) of **2-PEG methacrylated chloro** and this was diluted with 4.3 mLs (0.30 M) of reagent grade methyl ethyl ketone (MEK). To this solution was added 585 grams (3.9 mmol, 3.00 equiv) of sodium iodide (NaI), the flask was equipped to a reflux condenser, heated to 85°C, and refluxed at this temperature overnight. After this time, the reaction mixture was concentrated under reduced pressure and the resultant crude

residue was dissolved in of EtOAc (~100 mLs), transferred to a 250 mL separatory funnel, and the organic layer was washed with water (~100 mLs), a saturated solution of $Na_2S_2O_3$ (~100 mLs), and brine (~100 mLs). The combined organics were then dried over sodium sulfate, filtered, and concentrated under reduced pressure to yield 298 mg (81% yield) of the title compound as a clear liquid that was used in the next step with no further purifications.

2-PEG methacrylated iodo (7c): Clear liquid; 81% yield; R_f = 0.37 (TLC conditions: 10% EtOAc/hexanes); ^{1}H NMR (500 MHz, $CDCl_3$) δ = 6.15 (s, 1H), 5.59 (s, 1H), 4.33 (t, *J* = 5.9 Hz, 2H), 3.80 – 3.68 (m, 4H), 3.26 (t, *J* = 6.0 Hz, 2H), 1.96 (s, 3H); ^{13}C NMR (126 MHz, $CDCl_3$) δ = 167.32, 136.11, 125.88, 71.83, 68.73, 63.73, 18.33, 2.57.

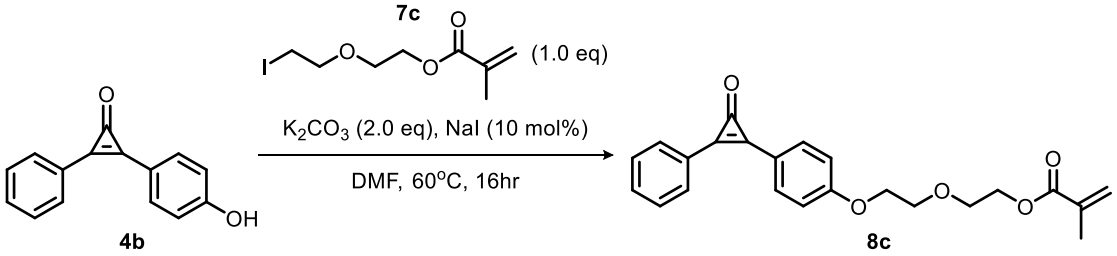

To a flame-dried 100 mL round-bottom flask under N_2 equipped with a magnetic stir bar was added 1.00 g (4.50 mmol, 1.00 equiv) of **DPCP-OH** (**4b**) which was diluted with 9.00 mL DMF (0.50M). To this solution was added 1.27 g (4.50 mmol, 1.00 equiv) of **2-PEG methacrylated iodo** (**7c**) via syringe followed by 68.0 mg (1.13 mmol, 0.10 equiv) sodium iodide (NaI). Finally, 1.25 g (9.0 mmol, 2.00 equiv) potassium carbonate (K_2CO_3) was added to the reaction mixture, the flask was equipped with a reflux condenser, and the reaction was heated to 60°C for 16 hours. After this period, the reaction was cooled to room temperature and transferred to a 500 mL separatory funnel. The reaction was

diluted with ethyl acetate (~200 mL), washed with water (~250 mL), washed with brine (~250 mL), dried over sodium sulfate, filtered, and submitted to column chromatography (20% acetone/hexanes → 50% acetone/hexanes). Evaporation of the fractions containing the desired material yielded 1.45 g (84% yield) of the title compound as a light brown solid. **2-PEG methacrylated DPCP (8c):** Light brown solid; 84% yield; R_f = 0.40 (TLC conditions: 50% acetone/hexanes); ^{1}H NMR (500 MHz, $CDCl_3$) δ = 7.91 – 7.85 (m, 4H), 7.53 – 7.48 (m, 3H), 7.01 (d, *J* = 8.3 Hz, 2H), 6.06 (s, 1H), 5.50 (s, 1H), 4.28 (t, *J* = 4.8 Hz, 2H), 4.16 (t, *J* = 4.7 Hz, 2H), 3.85 (t, *J* = 4.7 Hz, 2H), 3.77 (t, *J* = 4.8 Hz, 2H), 1.88 (s, 3H); ^{13}C NMR (126 MHz, $CDCl_3$) δ = 167.13, 162.12, 155.39, 147.55, 144.45, 135.93, 133.60, 132.06, 131.04, 129.14, 125.64, 124.13, 116.85, 115.21, 77.16, 76.91, 76.65, 69.25, 67.60, 63.52, 18.11.

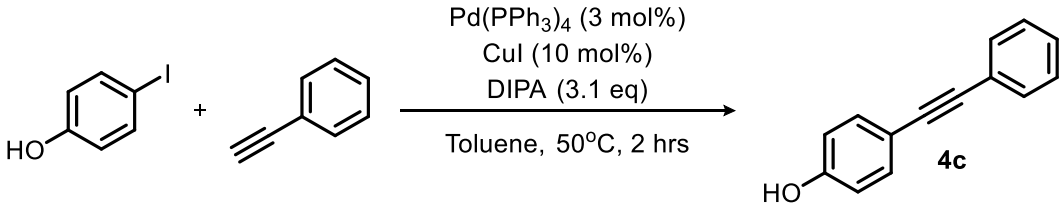

To a flame-dried 50.0 mL round bottom flask under N_2 equipped with a magnetic stir bar was added 1.18 g 4-iodophenol (5.36 mmol, 1.00 equiv) which was diluted with 18 mL (0.3M) toluene. To this solution was added 1.10 mL (1.02 g, 10.0 mmol, 1.87 equiv) of phenylacetylene before degassing with N_2 for 30 minutes. After this time, 184 mg (0.16 mmol, 0.03 equiv, 3.00 mol%) of tetrakis(triphenylphosphine)palladium(0) ($Pd(PPh_3)_4$) and 95.0 mg (0.50 mmol, 0.10 equiv, 10.0 mol%) of copper(I)-iodide were added to the solution. Finally, 2.34 mL (1.68 g, 16.6 mmol, 3.1 equiv) of diisopropylamine (DIPA) was

added and the solution was heated to 50°C. After 2 hours, thin layer chromatography indicated that the reaction had gone to completion. After cooling to room temperature, the solvent was removed under reduced pressure and the reaction mixture was diluted with ethyl acetate (50 mL). The. The organic layer was transferred to a 250 mL separatory funnel and washed with 1M HCl (50 mL), brine (100 mL), dried over sodium sulfate, filtered, and submitted to column chromatography (5% EtOAc/hexanes → 25% EtOAc/hexanes). Evaporation of the fractions containing the desired material yielded 1.45 g (95% yield) of the title compound as a light brown solid.

DPA-OH (4c): Light brown solid; 95% yield; R_f = 0.24 (TLC conditions: 10% EtOAc/hexanes); ^{1}H NMR (500 MHz, $CDCl_3$) δ = 7.57 – 7.49 (m, 2H), 7.46 (d, *J* = 8.1 Hz, 2H), 7.42 – 7.31 (m, 3H), 6.84 (d, *J* = 8.1 Hz, 2H); ^{13}C NMR (126 MHz, $CDCl_3$) δ = 155.63, 133.34, 131.51, 128.38, 128.06, 123.54, 115.72, 115.59, 89.31, 88.18.

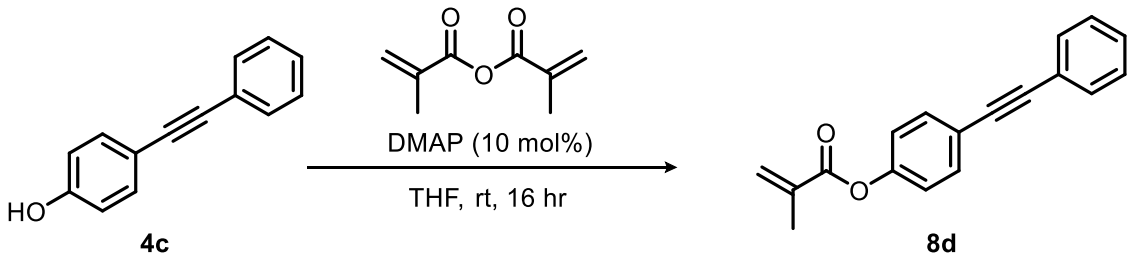

4c **8d**

To a flame-dried 50.0 mL round-bottom flask under N_2 was added 575 mg **DPA-OH** (**4c**) (2.96 mmol, 1.0 equiv), which was diluted with 14.8 mL dry THF (0.20M). To this solution was added 462 μL (479 mg, 3.11 mmol, 1.05 equiv) of methacrylic anhydride and 36.0 mg 4-dimethylaminopyridine (0.29 mmol, 0.10 equiv, 10.0 mol%). The reaction was allowed to stir at room temperature overnight before removing the THF under reduced

pressure. The crude mixture was diluted with ethyl acetate (50 mL), washed with 1M HCl (50 mL), a saturated aqueous solution of sodium bicarbonate ($NaHCO_3$) (50 mL), brine (100 mL), dried with sodium sulfate, filtered, and submitted to column chromatography (2% EtOAc/hexanes → 10% EtOAc/hexanes). Evaporation of the fractions containing the desired material yielded 582 mg (75% yield) of the title compound as a white powder.

0-PEG methacrylated DPA (8d): White solid; 75% yield; R_f = 0.62 (TLC conditions: 20% EtOAc/hexanes); ^{1}H NMR (500 MHz, $CDCl_3$) δ = 7.59 – 7.50 (m, 4H), 7.34 (td, *J* = 4.9, 2.3 Hz, 3H), 7.16 – 7.10 (m, 2H), 6.36 (s, 1H), 5.77 (s, 1H), 2.07 (s, 3H); ^{13}C NMR (126 MHz, $CDCl_3$) δ = 165.55, 150.78, 135.75, 132.75, 131.62, 128.37, 128.33, 127.51, 123.17, 121.76, 120.88, 89.44, 88.63, 18.37.

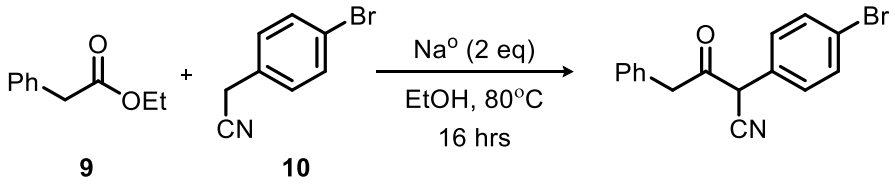

9 **10**

To a 250 mL two-necked round-bottom flask equipped with a reflux condenser and an addition funnel was added 68.0 mL of ethanol (1.50M) and 4.69 g (204 mmol, 2.00 equiv) of sodium metal (Na°). After stirring for 10-20 minutes at 80°C the sodium metal completely dissolved and a light brown solution formed. While refluxing, a mixture of 20.0 g (102 mmol, 1.00 equiv) of 4-bromophenylacetonitrile (**9**) and 20.8 g (126.5 mmol, 1.24 equiv) of ethyl phenylacetate (**10**) was added through the addition funnel as a viscous liquid over a period of 1 hour and the solution was refluxed overnight. The solution was cooled to room temperature, poured into ice water (300 mL) and the solution was transferred to a

separatory funnel. The aqueous alkaline mixture was extracted with ether (~150 mL, 2X) and the ether layer was discarded. The aqueous solution was acidified with 1M HCl and extracted with ethyl acetate (~100 mL, 3X). The ethyl acetate solution was washed with water (~100 mL, 1X), sodium bicarbonate (~100 mL, 2X), brine (~200 mL, 1X), dried over Na_2SO_4, filtered, and concentrated. The product was triturated in cold hexanes (~50 mL) to afford 26.3 g (82% yield) of α-(4-bromophenyl)-γ-phenylacetoacetonitrile as an off-white powder.

Beta-ketonitrile: off-white powder; 82% yield; R_f = 0.29 (TLC conditions: 50% EtOAc/hexanes); ^{1}H NMR (500 MHz, DMSO) δ =7.65 (d, *J* = 8.1 Hz, 2H), 7.51 (d, *J* = 8.4 Hz, 2H), 7.46 – 7.02 (m, 5H), 3.90 (s, 2H); ^{13}C NMR (126 MHz, DMSO) δ = 172.53, 136.66, 132.99, 131.10, 128.57, 128.47, 128.38, 126.75, 121.67, 118.15, 85.08, 41.72.

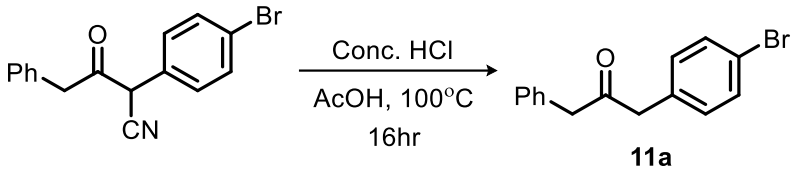

11a

To a thick-walled 100 mL pressure vessel equipped with a football shaped magnetic stir bar was added 10.1 g (32.3 mmol, 1.00 equiv) of beta-ketonitrile as a solid. At room temperature, this material was then diluted with 10.8 mL of glacial acetic acid followed by 21.5 mL of concentrated (12.1 N) HCl (overall concentration 0.30 M, ratio of acetic acid:conc. HCl of 1:2) and the pressure vessel was capped tightly with a screw on PTFE cap. It was noted that upon the addition of solvents a suspension was formed, and the bulk of the material was out of solution. The pressure vessel was then lowered into a room temperature oil bath, stirred at 750 RPM and heated to 100°C over the course of several

minutes. *Note: this reaction was done behind a blast shield in an isolated fume hood.* After 16 hours at 100^{o}C, the reaction mixture had cleared to form a suspended red oil (when stirring was halted it was observed that the red oil would settle to the bottom, forming a biphasic reaction mixture). After this period the reaction vessel was removed from the heat and allowed to reach room temperature. The vessel was then placed into an ice bath, cooled to 0^{o}C over the course of several minutes and the lid was slowly and carefully opened to release pressure. The reaction was then diluted with 100 mL of hexanes, stirred until the red oil dissolved in the organic layer and the contents were transferred to a 500 mL separatory funnel. The organic layer was separated, and the aqueous layer was additionally extracted with portions of hexanes (50.0 mL, 2X). The combined organics were then washed with water (200 mL, 1X), brine (200 mL, 1X), dried over Na_2SO_4, filtered, and concentrated to yield a red solid that was submitted to column chromatography (2.5% → 5% EtOAc/hexanes). Evaporation of the fractions containing the desired material yielded 7.7 g (83% yield) of the title compound as a white solid which was used in the next step with no further purification.

Ketone (11a): White solid; 83% yield; R_f = 0.52 (TLC conditions: 20% EtOAc/hexanes); ^{1}H NMR (500 MHz, $CDCl_3$) δ = 7.35 (d, *J* = 8.4 Hz, 2H), 7.28 – 7.17 (m, 3H), 7.09 (d, *J* = 6.8 Hz, 2H), 6.92 (d, *J* = 8.2 Hz, 2H), 3.62 (d, *J* = 25.9 Hz, 4H); ^{13}C NMR (126 MHz, $CDCl_3$) δ = 204.97, 133.81, 132.99, 131.79, 131.30, 129.55, 128.88, 127.27, 121.14, 49.52, 48.15.

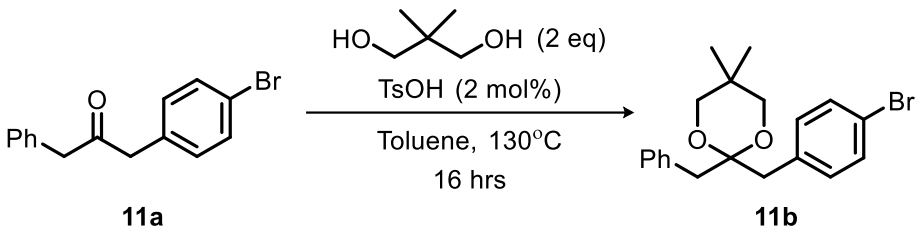

11a **11b**

To a 250 mL round-bottom flask equipped with a reflux condenser and a Dean-Stark apparatus was added 10.0 g (34.6 mmol, 1.0 equiv) of **ketone** (**11a**) as a solid followed by 7.20 g (69.2 mmol, 2.0 equiv) of neopentyl glycol. The solids were diluted with toluene (70 mL; 0.5M) before adding 0.13 g (0.69 mmol, 0.02 equiv, 2.00 mol%) of *p*-toluenesulfonic acid while stirring at 750 RPM. The reaction mixture was then lowered into a room temperature oil bath and heated to 130°C over the course of several minutes. After 16 hours at 130°C, the solution was cooled to room temperature, diluted with hexanes (150 mL), and transferred to a 500 mL separatory funnel. The organic solution was washed with aqueous sodium bicarbonate (200 mL, 1X), brine (200 mL, 1X), dried over Na_2SO_4, filtered, and concentrated to yield 12.9 g (97% yield) of the title compound as a white solid which was used in the next step with no further purification.

Acetal (11b): White solid, 97% yield; R_f = 0.65 (TLC conditions: 20% EtOAc/hexanes); ^{1}H NMR (500 MHz, $CDCl_3$) δ = 7.39 (d, *J* = 8.4 Hz, 1H), 7.32 – 7.20 (m, 5H), 7.09 (d, *J* = 8.4 Hz, 2H), 3.64 (dd, *J* = 11.3 Hz, 4H), 3.01 (s, 2H), 2.86 (s, 2H), 0.78 (d, *J* = 4.4 Hz, 6H); ^{13}C NMR (126 MHz, $CDCl_3$) δ = 136.80, 135.90, 132.76, 130.82, 130.71, 128.04, 126.43, 120.28, 99.78, 70.69, 40.60, 39.35, 29.85, 22.63, 22.53.

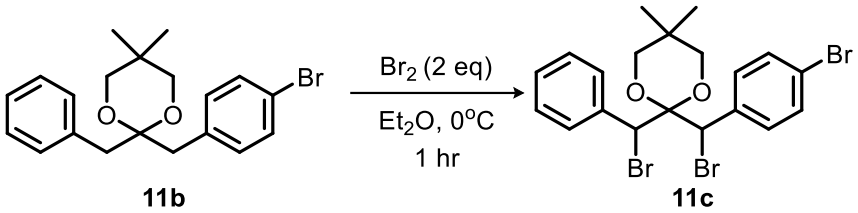

To a 100 mL round-bottom flask under N_2 was added 10.0 g (26.7 mmol; 1.00 equiv) of **acetal** (**11b**) and this was diluted with 27.0 mLs of diethyl ether (Et_2O, 1.00 M). The solution was cooled to 0°C before adding 2.74 mL (53.4 mmol, 2.00 equiv) of bromine (Br_2) dropwise. After stirring at 0°C for 1 hour, the solution was warmed to room temperature. The diethyl ether was removed under reduced pressure to afford 14.2 g (100% yield) of the title compound as a red foam, which was used in the next step with no further purifications.

Dibromo acetal (11c): Red foam, 100% yield; R_f = 0.48 (TLC conditions: 20% EtOAc/hexanes); ^{1}H NMR (500 MHz, $CDCL_3$) δ = 7.48 – 7.41 (m, 4H), 7.40 – 7.30 (m, 5H), 5.37 (s, 1H), 5.11 (s, 1H), 4.03 (d, *J* = 11.4 Hz, 1H), 3.93 (d, *J* = 11.4 Hz, 1H), 1.10 (s, 3H), 0.97 (s, 3H); ^{13}C NMR (125 MHz, $CDCl_3$) δ = 137.22, 136.72, 132.28, 131.98, 131.07, 130.87, 130.35, 130.17, 128.03, 98.47, 71.41, 70.98, 54.37, 53.27, 29.22, 23.57.

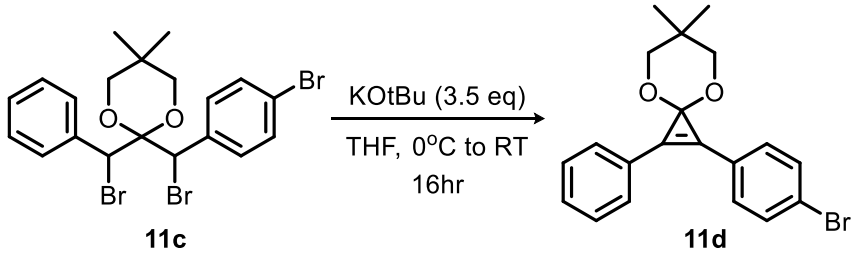

To a 250 mL round-bottom flask under N_2 was added 14.1 g (26.7 mmol, 1.0 equiv) of **dibromo acetal** (**11c**) and this was diluted with 89.0 mLs of THF (0.30 M) and the

solution was cooled to 0°C. While vigorously stirring, 10.5 g (93.45 mmol, 3.50 equiv) of potassium *tert*-butoxide (KO*t*Bu) was added in a single portion. After warming to room temperature overnight, the volatiles were removed under reduced pressure and the mixture was redissolved in ethyl acetate (100 mL). The organic solution was washed with water (100 mL, 2x), brine (100 mL, 1X), dried over Na_2SO_4, filtered, and concentrated to yield a thick orange solid. The solid was triturated with cold hexanes (~50 mL) to yield 7.20 g (72% yield) of the title compound as an off-white solid which was used in the next step with no further purification.

Cyclopropenone acetal (11d): Off-white solid, 72% yield; R_f = 0.56 (TLC conditions: 20% EtOAc/hexanes); ^{1}H NMR (500 MHz, $CDCl_3$) δ = 7.75 (d, *J* = 6.9 Hz, 2H), 7.62 (q, *J* = 8.7 Hz, 4H), 7.52 – 7.46 (m, 2H), 7.45 – 7.38 (m, 1H), 3.87 (q, *J* = 10.8 Hz, 4H), 1.18 (d, *J* = 27.1 Hz, 6H); ^{13}C NMR (126 MHz, $CDCl_3$) δ = 132.33, 131.41, 130.21, 129.87, 129.15, 127.68, 126.90, 126.09, 124.98, 123.78, 83.25, 79.03, 77.41, 30.61, 22.66, 22.55.

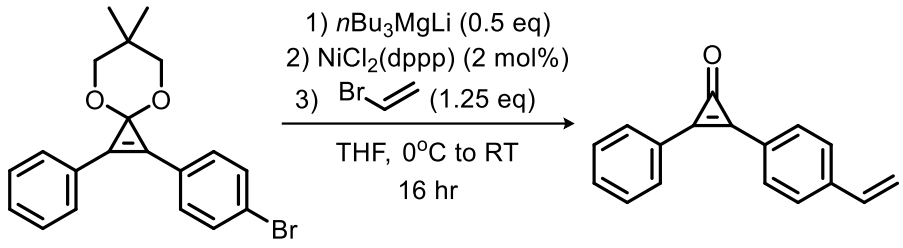

To a 100 mL round-bottom flask under N_2 equipped with a magnetic stir bar was added 3.37 mL (6.73 mmol, 0.50 equiv) of *n*-butyl magnesium chloride and 16.8 mL THF (0.80M). This solution was cooled to 0°C before adding 5.40 mL (13.47 mmol, 1.00 equiv) of n-butyl lithium. This mixture was stirred for 5 minutes at 0°C before it was added dropwise to a solution of 5.00 g (13.47 mmol, 1.00 equiv) of **cyclopropenone acetal** (**11d**)

in THF (33.5 mL). After 5 minutes, this mixture was cooled to 0^{o}C and added dropwise to a THF (16.8 mL) solution containing 16.84 mL (16.84 mmol, 1.25 equiv) of vinyl bromide and 0.15 g (0.27 mmol, 0.02 equiv, 2.00 mol%) of $NiCl_2$(dppp). The reaction mixture was warmed to room temperature and stirred for 16 hours. After this period the reaction was quenched with an aqueous solution of ammonium chloride (NH_4Cl). To this solution was added 70 mL aqueous hydrochloric acid (1M) which stirred for 30 minutes to remove the ketal protecting group. The reaction was then diluted with 200 mL of ethyl acetate and transferred to a 500 mL separatory funnel. The combined organics were then washed with water (200 mL, 1X), brine (200 mL, 1X), dried over Na_2SO_4, filtered, and concentrated to yield an orange solid that was submitted to column chromatography (20% → 50% EtOAc/hexanes). Evaporation of the fractions containing the desired material yielded 1.70 g (55% yield) of the title compound as a yellow solid.

Sty-DPCP (12a): Yellow solid, 55% yield; R_f = 0.56 (TLC conditions: 20% EtOAc/hexanes); ^{1}H NMR (500 MHz, $CDCl_3$) δ = 8.05 – 7.94 (m, 4H), 7.62 (ddd, *J* = 7.2, 5.0, 2.0 Hz, 5H), 6.81 (dd, *J* = 17.6, 10.8 Hz, 1H), 5.95 (d, *J* = 17.6 Hz, 1H), 5.48 (d, *J* = 10.9 Hz, 1H); ^{13}C NMR (126 MHz, $CDCl_3$) δ = 155.77, 147.85, 147.65, 141.77, 135.79, 132.73, 132.66, 131.86, 131.51, 131.48, 129.40, 127.08, 124.15, 123.07, 117.27.

3.3 Polymerization

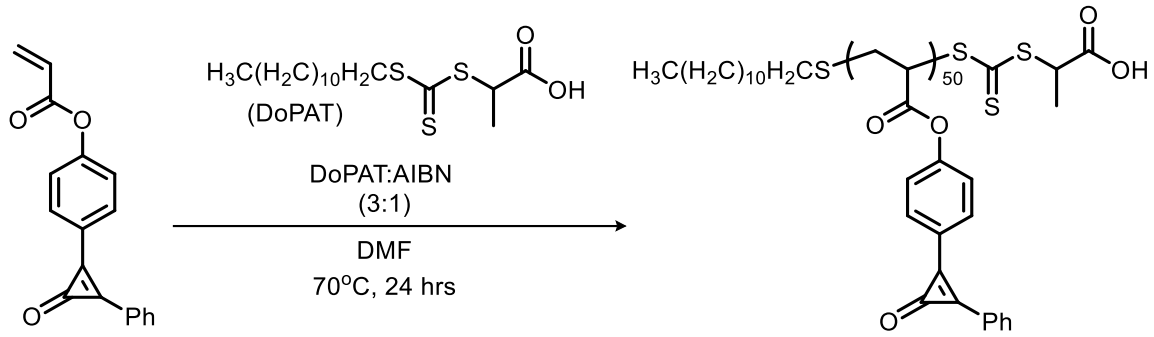

To a 2.00 mL ampoule was added 50.0 mg (0.181 mmol, 1.00 equiv), of **0-PEG acrylated DPCP** (**6a**) before diluting with 50.0 μL of DMF containing 1.20 mg DoPAT (3.44 μmol, 0.02 equiv) followed by 50.0 μL DMF containing 0.187 mg AIBN (1.14 μmol; 0.006 equiv). Finally, 50.0 μL DMF was added to dilute the mixture to 300 wt% with respect to **6a.** The mixture was stirred until its contents dissolved and was deoxygenated by three freeze-pump-thaw cycles. The ampoule was carefully flame sealed using a blow torch. Polymerization was initiated by immersion of the ampoule in a preheated 70°C oil bath. After 24 hours at this temperature, the polymerization was quenched by scoring and cracking the ampoule, exposing the reaction mixture to air. An aliquot of the crude product was taken to determination the conversion by ^{1}H NMR analysis. The polymer was precipitated in 30.0 mL of stirring cold methanol (0°C) followed by stirring for 15 minutes, filtration, and drying under high vacuum to yield 26.0 mg (56% yield) of name as a light yellow powder.

Poly-DPCP Acrylate (50-mer): Light yellow powder; 56% conversion; 52% yield; ^{1}H NMR (500 MHz, $CDCl_3$) δ = 7.95 – 7.51 (4H), 7.32 (5H), 3.24 – 2.91 (1H), 2.68 – 1.76 (2H), 1.70 – 0.98 (2H).

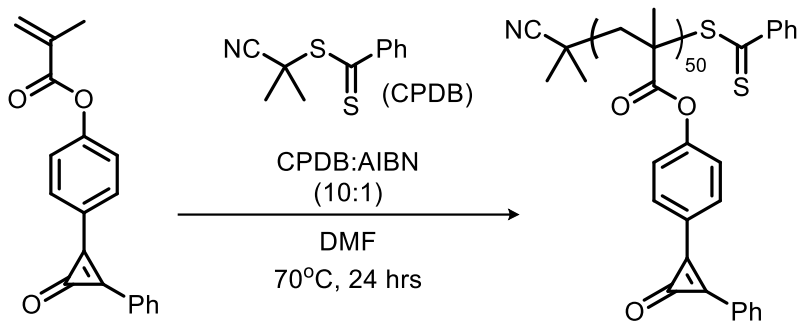

To a 2.00 mL ampoule was added 380 mg (1.31 mmol, 1.0 equiv) of **0-PEG methacrylated DPCP (8a)**, before the addition of 200 μL of a DMF solution containing 5.79 mg (0.026 mmol, 0.02 equiv) of CPDB followed by 100 μL of DMF containing 0.43 mg AIBN (2.62 μmol, 0.002 equiv). Finally, 840 μL DMF was added to dilute the mixture to 300 wt% with respect to **8a.** The mixture was stirred until its contents dissolved and the reaction was deoxygenated by three freeze-pump-thaw cycles. The ampoule was carefully flame sealed using a blow torch. Polymerization was initiated by immersion of the ampoule into a preheated 70°C oil bath. After 24 h, the polymerization was quenched by scoring and cracking the ampoule, exposing the reaction mixture to air. An aliquot of the crude product was taken to determination the conversion by ^{1}H NMR analysis. The polymer was precipitated in 60.0 mL of cold stirring methanol (0°C) followed by stirring for 15 minutes, filtration, and drying under vacuum to yield 346 mg (91% yeidl) of the title polymer as a light pink powder.

***Poly*-DPCP Methacrylate (50-mer):** Light pink powder; 98% conversion; 91% yield; ^{1}H NMR (500 MHz, $CDCl_3$) δ = 8.18 – 7.59 (4H), 7.60 – 7.27 (5H), 2.38 (2H), 2.11 – 1.15 (5H).

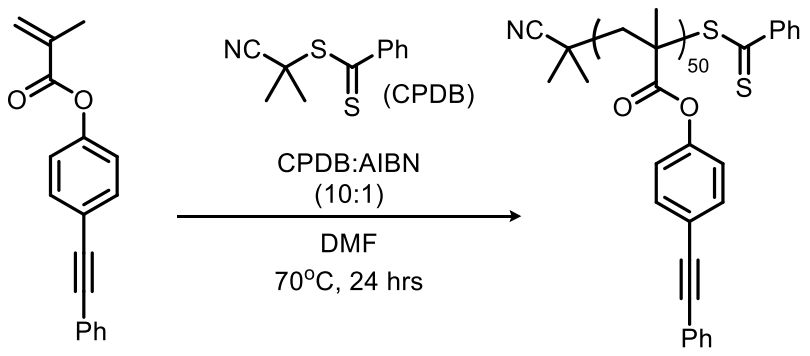

To a 2.00 mL ampoule was added 150 mg (0.572 mmol, 1.00 equiv) of **0-PEG methacrylated DPA** (**8d**) before diluting with 100 μL DMF containing 2.53 mg (0.0114 mmol, 0.02 equiv) of CPDB followed by 100 μL DMF containing 0.188 mg (1.14 μmol, 0.002 equiv) of AIBN. Finally, 250 μL DMF was added to dilute the mixture to 300 wt% with respect to **8d.** The mixture was stirred until its contents dissolved and was deoxygenated by three freeze-pump-thaw cycles. The ampoule was carefully flame sealed using a blow torch. Polymerization was initiated by immersion of the ampoule into a preheated 70°C oil bath. After 24 hours at this temperature, the polymerization was quenched by scoring and cracking the ampoule, exposing the reaction mixture to air. An aliquot of the crude product was taken to determination the conversion by ^{1}H NMR analysis. The polymer was precipitated in 40.0 mL of cold stirring methanol (0°C) followed by stirring for 15 minutes, filtration, and drying under vacuum to yield 106 mg (71% yield) of the title polymer as a white powder.

***Poly*-DPA Methacrylate (50-mer):** White powder; 96% conversion; 71% yield; ^{1}H NMR (500 MHz, $CDCl_3$) δ = 7.60 – 7.35 (4H), 7.32 – 7.16 (3H), 7.12 – 6.94 (2H), 2.86 – 2.01 (2H), 2.06 – 1.17 (4H).

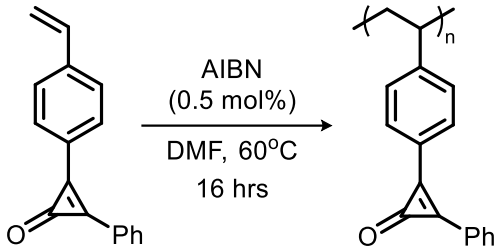

12a **12b**

To a 6.00 mL microwave vial was added 100 mg (0.43 mmol, 1.00 equiv) of ***sty*-DPCP** (**12a**) which was diluted with 430 μL of a DMF solution containing 0.35 mg AIBN (2.15 μmol, 0.50 mol%) (1M). The microwave vial was sealed with a Teflon cap and the solution was sparged with N_2 gas for 15 minutes before polymerization was initiated by immersion of the vial in a pre-heated 60°C oil bath. After 24 h, the polymerization was quenched by removing the Teflon cap, exposing the reaction mixture to air. The polymer was precipitated in 40.0 mL of cold stirring methanol (0°C) followed by stirring for 15 minutes, filtration, and drying under vacuum to yield a yellow powder.

***Poly*-Sty-DPCP (12b):** Yellow powder; ^{1}H NMR (500 MHz, $CDCl_3$) δ 8.05 – 7.06 (m, 7H), 6.95 – 6.23 (m, 2H), 2.53 – 1.88 (m, 1H), 1.82 – 1.34 (m, 2H).

References

(1) Blumenthal, I. Carbon Monoxide Poisoning. *J R Soc Med* **2001**, *94* (6), 270–272.

(2) Ruan, H.-L.; Deng, W.-S.; Wang, Y.; Chen, J.-B.; Hong, W.-L.; Ye, S.-S.; Hu, Z.-J. Carbon Monoxide Poisoning: A Prediction Model Using Meteorological Factors and Air Pollutant. *BMC Proc* **2021**, *15* (S1), 1. https://doi.org/10.1186/s12919-021-00206-7.

(3) Graber, J. M.; Macdonald, S. C.; Kass, D. E.; Smith, A. E.; Anderson, H. A. Carbon Monoxide: The Case for Environmental Public Health Surveillance. *Public Health Rep* **2007**, *122* (2), 138–144. https://doi.org/10.1177/003335490712200202.

(4) Weinstock, B.; Niki, H. Carbon Monoxide Balance in Nature. *Science* **1972**, *176* (4032), 290–292. https://doi.org/10.1126/science.176.4032.290.

(5) Voiland, A. Fourteen Years of Carbon Monoxide from MOPITT, 2022.

(6) Bierhals, J. Carbon Monoxide. In *Ullmann's Encyclopedia of Industrial Chemistry*; Wiley-VCH Verlag GmbH & Co. KGaA, Ed.; Wiley-VCH Verlag GmbH & Co. KGaA: Weinheim, Germany, 2001; p a05_203. https://doi.org/10.1002/14356007.a05_203.

(7) Motterlini, R.; Otterbein, L. E. The Therapeutic Potential of Carbon Monoxide. *Nat Rev Drug Discov* **2010**, *9* (9), 728–743. https://doi.org/10.1038/nrd3228.

(8) Chiodi, H. Respiratory and Circulatory Responses to Acute Carbon Monoxide Poisoning. *Am. J. Physiol.* **1941**, *134*, 683–693.

(9) Ryter, S. W.; Alam, J.; Choi, A. M. K. Heme Oxygenase-1/Carbon Monoxide: From Basic Science to Therapeutic Applications. *Physiological Reviews* **2006**, *86* (2), 583–650. https://doi.org/10.1152/physrev.00011.2005.

(10) Hayashi, S.; Omata, Y.; Sakamoto, H.; Higashimoto, Y.; Hara, T.; Sagara, Y.; Noguchi, M. Characterization of Rat Heme Oxygenase-3 Gene. Implication of Processed Pseudogenes Derived from Heme Oxygenase-2 Gene. *Gene* **2004**, *336* (2), 241–250. https://doi.org/10.1016/j.gene.2004.04.002.

(11) Wu, L.; Wang, R. Carbon Monoxide: Endogenous Production, Physiological Functions, and Pharmacological Applications. *Pharmacol Rev* **2005**, *57* (4), 585–630. https://doi.org/10.1124/pr.57.4.3.

(12) Mahan, V. L. Neuroprotective, Neurotherapeutic, and Neurometabolic Effects of Carbon Monoxide. *Medical Gas Research* **2012**, *2* (1), 32. https://doi.org/10.1186/2045-9912-2-32.

(13) Woo, J.-I.; Kil, S.-H.; Oh, S.; Lee, Y.-J.; Park, R.; Lim, D. J.; Moon, S. K. IL-10/HMOX1 Signaling Modulates Cochlear Inflammation via Negative Regulation of MCP-1/CCL2 Expression in Cochlear Fibrocytes. *J. Immunol.* **2015**, *194* (8), 3953. https://doi.org/10.4049/jimmunol.1402751.

(14) Otterbein, L. E.; Bach, F. H.; Alam, J.; Soares, M.; Tao Lu, H.; Wysk, M.; Davis, R. J.; Flavell, R. A.; Choi, A. M. K. Carbon Monoxide Has Anti-Inflammatory Effects Involving the Mitogen-Activated Protein Kinase Pathway. *Nat Med* **2000**, *6* (4), 422–428. https://doi.org/10.1038/74680.

(15) Kozma, F.; Johnson, R. A.; Zhang, F.; Yu, C.; Tong, X.; Nasjletti, A. Contribution of Endogenous Carbon Monoxide to Regulation of Diameter in Resistance Vessels. *American Journal of Physiology-Regulatory, Integrative and Comparative Physiology* **1999**, *276* (4), R1087–R1094. https://doi.org/10.1152/ajpregu.1999.276.4.R1087.

(16) Johnson, R. A.; Lavesa, M.; Askari, B.; Abraham, N. G.; Nasjletti, A. A Heme Oxygenase Product, Presumably Carbon Monoxide, Mediates a Vasodepressor Function in Rats. *Hypertension* **1995**, *25* (2), 166–169. https://doi.org/10.1161/01.HYP.25.2.166.

(17) *Carbon Monoxide Expedites Metabolic Exhaustion to Inhibit Tumor Growth | Cancer Research*. https://cancerres.aacrjournals.org/content/73/23/7009 (accessed 2021-10-03).

(18) Mann, B. E. CO-Releasing Molecules: A Personal View. *Organometallics* **2012**, *31* (16), 5728–5735. https://doi.org/10.1021/om300364a.

(19) Ling, K.; Men, F.; Wang, W.-C.; Zhou, Y.-Q.; Zhang, H.-W.; Ye, D.-W. Carbon Monoxide and Its Controlled Release: Therapeutic Application, Detection, and Development of Carbon Monoxide Releasing Molecules (CORMs). *J. Med. Chem.* **2018**, *61* (7), 2611–2635. https://doi.org/10.1021/acs.jmedchem.6b01153.

(20) Motterlini, R.; Clark, J. E.; Foresti, R.; Sarathchandra, P.; Mann, B. E.; Green, C. J. Carbon Monoxide-Releasing Molecules. *Circulation Research* **2002**, *90* (2), e17–e24. https://doi.org/10.1161/hh0202.104530.

(21) Ferrandiz, M. L.; Maicas, N.; Garcia-Arnandis, I.; Terencio, M. C.; Motterlini, R.; Devesa, I.; Joosten, L. A. B.; van den Berg, W. B.; Alcaraz, M. J. Treatment with a CO-Releasing Molecule (CORM-3) Reduces Joint Inflammation and Erosion in Murine Collagen-Induced Arthritis. *Annals of the Rheumatic Diseases* **2007**, *67* (9), 1211–1217. https://doi.org/10.1136/ard.2007.082412.

(22) Guo, Y.; Stein, A. B.; Wu, W.-J.; Tan, W.; Zhu, X.; Li, Q.-H.; Dawn, B.; Motterlini, R.; Bolli, R. Administration of a CO-Releasing Molecule at the Time of Reperfusion Reduces Infarct Size in Vivo. *American Journal of Physiology-Heart and Circulatory Physiology* **2004**, *286* (5), H1649–H1653. https://doi.org/10.1152/ajpheart.00971.2003.

(23) Chen, B.; Guo, L.; Fan, C.; Bolisetty, S.; Joseph, R.; Wright, M. M.; Agarwal, A.; George, J. F. Carbon Monoxide Rescues Heme Oxygenase-1-Deficient Mice from Arterial Thrombosis in Allogeneic Aortic Transplantation. *The American Journal of Pathology* **2009**, *175* (1), 422–429. https://doi.org/10.2353/ajpath.2009.081033.

(24) Nobre, L. S.; Seixas, J. D.; Romão, C. C.; Saraiva, L. M. Antimicrobial Action of Carbon Monoxide-Releasing Compounds. *Antimicrob Agents Chemother* **2007**, *51* (12), 4303–4307. https://doi.org/10.1128/AAC.00802-07.

(25) Wegiel, B.; Larsen, R.; Gallo, D.; Chin, B. Y.; Harris, C.; Mannam, P.; Kaczmarek, E.; Lee, P. J.; Zuckerbraun, B. S.; Flavell, R.; Soares, M. P.; Otterbein, L. E. Macrophages Sense and Kill Bacteria through Carbon Monoxide–Dependent Inflammasome Activation. *J. Clin. Invest.* **2014**, *124* (11), 4926–4940. https://doi.org/10.1172/JCI72853.

(26) Porshneva, K.; Papiernik, D.; Psurski, M.; Łupicka-Słowik, A.; Matkowski, R.; Ekiert, M.; Nowak, M.; Jarosz, J.; Banach, J.; Milczarek, M.; Goszczyński, T. M.; Sieńczyk, M.; Wietrzyk, J. Temporal Inhibition of Mouse Mammary Gland Cancer Metastasis by CORM-A1 and DETA/NO Combination Therapy. *Theranostics* **2019**, *9* (13), 3918–3939. https://doi.org/10.7150/thno.31461.

(27) Shao, L.; Liu, C.; Wang, S.; Liu, J.; Wang, L.; Lv, L.; Zou, Y. The Impact of Exogenous CO Releasing Molecule CORM-2 on Inflammation and Signaling of Orthotopic Lung Cancer. *Oncol Lett* **2018**. https://doi.org/10.3892/ol.2018.9022.

(28) Clark, J. E.; Naughton, P.; Shurey, S.; Green, C. J.; Johnson, T. R.; Mann, B. E.; Foresti, R.; Motterlini, R. Cardioprotective Actions by a Water-Soluble Carbon Monoxide–Releasing Molecule. *Circulation Research* **2003**, *93* (2). https://doi.org/10.1161/01.RES.0000084381.86567.08.

(29) Zobi, F.; Degonda, A.; Schaub, M. C.; Bogdanova, A. Yu. CO Releasing Properties and Cytoprotective Effect of *Cis* - *Trans* - $[Re^{II}(CO)_2Br_2L_2]^n$ Complexes. *Inorg. Chem.* **2010**, *49* (16), 7313–7322. https://doi.org/10.1021/ic100458j.

(30) Juszczak, M.; Kluska, M.; Wysokiński, D.; Woźniak, K. DNA Damage and Antioxidant Properties of CORM-2 in Normal and Cancer Cells. *Scientific Reports* **2020**, *10* (1), 12200. https://doi.org/10.1038/s41598-020-68948-6.

(31) Pierri, A. E.; Pallaoro, A.; Wu, G.; Ford, P. C. A Luminescent and Biocompatible PhotoCORM. *J. Am. Chem. Soc.* **2012**, *134* (44), 18197–18200. https://doi.org/10.1021/ja3084434.

(32) Hasegawa, U.; van der Vlies, A. J.; Simeoni, E.; Wandrey, C.; Hubbell, J. A. Carbon Monoxide-Releasing Micelles for Immunotherapy. *J. Am. Chem. Soc.* **2010**, *132* (51), 18273–18280. https://doi.org/10.1021/ja1075025.

(33) Nguyen, D.; Nguyen, T.-K.; Rice, S. A.; Boyer, C. CO-Releasing Polymers Exert Antimicrobial Activity. *Biomacromolecules* **2015**, *16* (9), 2776–2786. https://doi.org/10.1021/acs.biomac.5b00716.

(34) Nguyen, D.; Adnan, N. N. M.; Oliver, S.; Boyer, C. The Interaction of CORM-2 with Block Copolymers Containing Poly(4-Vinylpyridine): Macromolecular Scaffolds for Carbon Monoxide Delivery in Biological Systems. *Macromolecular Rapid Communications* **2016**, *37* (9), 739–744. https://doi.org/10.1002/marc.201500755.

(35) Brückmann, N. E.; Wahl, M.; Reiß, G. J.; Kohns, M.; Wätjen, W.; Kunz, P. C. Polymer Conjugates of Photoinducible CO-Releasing Molecules. *European Journal of Inorganic Chemistry* **2011**, *2011* (29), 4571–4577. https://doi.org/10.1002/ejic.201100545.

(36) Berends, H.-M.; Kurz, P. Investigation of Light-Triggered Carbon Monoxide Release from Two Manganese PhotoCORMs by IR, UV–Vis and EPR Spectroscopy. *Inorganica Chimica Acta* **2012**, *380*, 141–147. https://doi.org/10.1016/j.ica.2011.10.047.

(37) Antony, L. A. P.; Slanina, T.; Šebej, P.; Šolomek, T.; Klán, P. Fluorescein Analogue Xanthene-9-Carboxylic Acid: A Transition-Metal-Free CO Releasing

Molecule Activated by Green Light. *Org. Lett.* **2013**, *15* (17), 4552–4555. https://doi.org/10.1021/ol4021089.

(38) Peng, P.; Wang, C.; Shi, Z.; Johns, V. K.; Ma, L.; Oyer, J.; Copik, A.; Igarashi, R.; Liao, Y. Visible-Light Activatable Organic CO-Releasing Molecules (PhotoCORMs) That Simultaneously Generate Fluorophores. *Org. Biomol. Chem.* **2013**, *11* (39), 6671. https://doi.org/10.1039/c3ob41385c.

(39) Anderson, S. N.; Richards, J. M.; Esquer, H. J.; Benninghoff, A. D.; Arif, A. M.; Berreau, L. M. A Structurally-Tunable 3-Hydroxyflavone Motif for Visible Light-Induced Carbon Monoxide-Releasing Molecules (CORMs). *ChemistryOpen* **2015**, *4* (5), 590–594. https://doi.org/10.1002/open.201500167.

(40) Potts, K. T.; Baum, J. S. Chemistry of Cyclopropenones. *Chem. Rev.* **1974**, *74* (2), 189–213. https://doi.org/10.1021/cr60288a003.

(41) Breslow, R.; Haynie, R.; Mirra, J. THE SYNTHESIS OF DIPHENYLCYCLOPROPENONE. *J. Am. Chem. Soc.* **1959**, *81* (1), 247–248. https://doi.org/10.1021/ja01510a060.

(42) Shih, H.-W.; Prescher, J. A. A Bioorthogonal Ligation of Cyclopropenones Mediated by Triarylphosphines. *J. Am. Chem. Soc.* **2015**, *137* (32), 10036–10039. https://doi.org/10.1021/jacs.5b06969.

(43) Row, R. D.; Shih, H.-W.; Alexander, A. T.; Mehl, R. A.; Prescher, J. A. Cyclopropenones for Metabolic Targeting and Sequential Bioorthogonal Labeling. *J. Am. Chem. Soc.* **2017**, *139* (21), 7370–7375. https://doi.org/10.1021/jacs.7b03010.

(44) Row, R. D.; Nguyen, S. S.; Ferreira, A. J.; Prescher, J. A. Chemically Triggered Crosslinking with Bioorthogonal Cyclopropenones. *Chem. Commun.* **2020**, *56* (74), 10883–10886. https://doi.org/10.1039/D0CC04600K.

(45) Vennekate, H. Photodecarbonylation of Diphenylcyclopropenone – a Direct Pathway to Electronically Excited Diphenylacetylene? *Zeitschrift für Physikalische Chemie* **2011**, *225* (9–10), 1089–1104. https://doi.org/10.1524/zpch.2011.0164.

(46) Aghaei, S. Topical Immunotherapy of Severe Alopecia Areata with Diphenylcyclopropenone (DPCP): Experience in an Iranian Population. *BMC Dermatol* **2005**, *5* (1), 6. https://doi.org/10.1186/1471-5945-5-6.

(47) Nowicka, D.; Maj, J.; Jankowska-Konsur, A.; Hryncewicz-Gwóźdź, A. Efficacy of Diphenylcyclopropenone in Alopecia Areata: A Comparison of Two Treatment Regimens. *pdia* **2018**, *35* (6), 577–581. https://doi.org/10.5114/ada.2018.77608.

(48) Kuin, R. A.; Spuls, P. I.; Limpens, J.; van Zuuren, E. J. Diphenylcyclopropenone in Patients with Alopecia Areata. A Critically Appraised Topic. *Br J Dermatol* **2015**, *173* (4), 896–909. https://doi.org/10.1111/bjd.14040.

(49) Kuzmanich, G.; Natarajan, A.; Chin, K. K.; Veerman, M.; Mortko, C. J.; Garcia-Garibay, M. A. Solid-State Photodecarbonylation of Diphenylcyclopropenone: A Quantum Chain Process Made Possible by Ultrafast Energy Transfer. *J. Am. Chem. Soc.* **2008**, *130* (4), 1140–1141. https://doi.org/10.1021/ja078301x.

(50) Kuzmanich, G.; Gard, M. N.; Garcia-Garibay, M. A. Photonic Amplification by a Singlet-State Quantum Chain Reaction in the Photodecarbonylation of Crystalline

Diarylcyclopropenones. *J. Am. Chem. Soc.* **2009**, *131* (32), 11606–11614. https://doi.org/10.1021/ja9043449.

(51) Shao, C.; Duan, H.; Min, Y.; Zhang, X. Diphenyl Cyclopropenone-Centered Polymers for Site-Specific CO-Releasing and Chain Dissociation. *Chinese Chemical Letters* **2020**, *31* (1), 299–302. https://doi.org/10.1016/j.cclet.2019.03.053.

(52) Nielsen, A.; Kuzmanich, G.; Garcia-Garibay, M. A. Quantum Chain Reaction of Tethered Diarylcyclopropenones in the Solid State and Their Distance-Dependence in Solution Reveal a Dexter S2–S2 Energy-Transfer Mechanism. *J. Phys. Chem. A* **2014**, *118* (10), 1858–1863. https://doi.org/10.1021/jp501216z.

(53) Noy, J.-M.; Li, Y.; Smolan, W.; Roth, P. J. Azide– *Para* -Fluoro Substitution on Polymers: Multipurpose Precursors for Efficient Sequential Postpolymerization Modification. *Macromolecules* **2019**, *52* (8), 3083–3091. https://doi.org/10.1021/acs.macromol.9b00109.

(54) Chiefari, J.; Chong, Y. K. (Bill); Ercole, F.; Krstina, J.; Jeffery, J.; Le, T. P. T.; Mayadunne, R. T. A.; Meijs, G. F.; Moad, C. L.; Moad, G.; Rizzardo, E.; Thang, S. H. Living Free-Radical Polymerization by Reversible Addition−Fragmentation Chain Transfer: The RAFT Process. *Macromolecules* **1998**, *31* (16), 5559–5562. https://doi.org/10.1021/ma9804951.

(55) Perrier, S. 50th Anniversary Perspective: RAFT Polymerization—A User Guide. *Macromolecules* **2017**, *50* (19), 7433–7447. https://doi.org/10.1021/acs.macromol.7b00767.

(56) Moad, G.; Rizzardo, E.; Thang, S. H. Radical Addition–Fragmentation Chemistry in Polymer Synthesis. *Polymer* **2008**, *49* (5), 1079–1131. https://doi.org/10.1016/j.polymer.2007.11.020.

(57) Moad, G. Reversible Addition-Fragmentation Chain Transfer (Co)Polymerization of Conjugated Diene Monomers: Butadiene, Isoprene and Chloroprene: RAFT (Co)Polymerization of Conjugated Diene Monomers. *Polym. Int.* **2017**, *66* (1), 26–41. https://doi.org/10.1002/pi.5173.

(58) Siljanovska Petreska, G.; van Sluijs, C.; Auschra, C.; Paulis, M. Design of Waterborne Asymmetric Block Copolymers as Thermoresponsive Materials. *Polymers* **2020**, *12* (6), 1253. https://doi.org/10.3390/polym12061253.

(59) Benaglia, M.; Chiefari, J.; Chong, Y. K.; Moad, G.; Rizzardo, E.; Thang, S. H. Universal (Switchable) RAFT Agents. *J. Am. Chem. Soc.* **2009**, *131* (20), 6914–6915. https://doi.org/10.1021/ja901955n.

(60) Derboven, P.; Van Steenberge, P. H. M.; Vandenbergh, J.; Reyniers, M.-F.; Junkers, T.; D'hooge, D. R.; Marin, G. B. Improved Livingness and Control over Branching in RAFT Polymerization of Acrylates: Could Microflow Synthesis Make the Difference? *Macromol. Rapid Commun.* **2015**, *36* (24), 2149–2155. https://doi.org/10.1002/marc.201500357.

(61) Rizzardo, E.; Chen, M.; Chong, B.; Moad, G.; Skidmore, M.; Thang, S. H. RAFT Polymerization: Adding to the Picture. *Macromol. Symp.* **2007**, *248* (1), 104–116. https://doi.org/10.1002/masy.200750211.

(62) Tanaka, K.; Shigematsu, Y.; Sukekawa, M.; Hoshino, Y.; Honda, K. Regioselective One-Pot Synthesis of 2,3-Diaryl-2H-1-Benzopyrans via Brønsted Acid-Catalyzed [4+2] Cycloaddition of Salicylaldehydes with Diarylacetylenes. *Tetrahedron Letters* **2016**, *57* (52), 5914–5918. https://doi.org/10.1016/j.tetlet.2016.11.076.

(63) Coan, S. B.; Becker, E. I. α-(4-Chlorophenyl)-γ-Phenylacetoacetonitrile: Acetoacetonitrile, 2-(*p* -Chlorophenyl)-4-Phenyl-. In *Organic Syntheses*; John Wiley & Sons, Inc., Ed.; John Wiley & Sons, Inc.: Hoboken, NJ, USA, 2003; pp 30–30. https://doi.org/10.1002/0471264180.os035.10.

(64) 1-(p-CHLOROPHENYL)-3-PHENYL-2-PROPANONE. *Org. Synth.* **1955**, *35*, 32. https://doi.org/10.15227/orgsyn.035.0032.

(65) *Geometric enantiomerism in cyclic compounds: Chiral dibrominated 1,3-dioxanes - Cismaş - 2011 - Chirality - Wiley Online Library*. https://onlinelibrary.wiley.com/doi/10.1002/chir.20895 (accessed 2021-10-03).

(66) Ando, R.; Sakaki, T.; Jikihara, T. Convenient Synthesis of 2-Phenylcyclopropenone Acetals. *J. Org. Chem.* **2001**, *66* (10), 3617–3618. https://doi.org/10.1021/jo001722b.

(67) Lau, S. Y. W.; Hughes, G.; O'Shea, P. D.; Davies, I. W. Magnesiation of Electron-Rich Aryl Bromides and Their Use in Nickel-Catalyzed Cross-Coupling Reactions. *Org. Lett.* **2007**, *9* (11), 2239–2242. https://doi.org/10.1021/ol070841b.

(68) Nakamura, M.; Isobe, H.; Nakamura, E. Cyclopropenone AcetalsSynthesis and Reactions. *Chem. Rev.* **2003**, *103* (4), 1295–1326. https://doi.org/10.1021/cr0100244.

(69) Gigmes, D.; Dufils, P.-E.; Glé, D.; Bertin, D.; Lefay, C.; Guillaneuf, Y. Intermolecular Radical 1,2-Addition of the BlocBuilder MA Alkoxyamine onto Activated Olefins: A Versatile Tool for the Synthesis of Complex Macromolecular Architecture. *Polym. Chem.* **2011**, *2* (8), 1624. https://doi.org/10.1039/c1py00057h.

(70) Matyjaszewski, K. Atom Transfer Radical Polymerization (ATRP): Current Status and Future Perspectives. *Macromolecules* **2012**, *45* (10), 4015–4039. https://doi.org/10.1021/ma3001719.

Appendix A

Spectra:

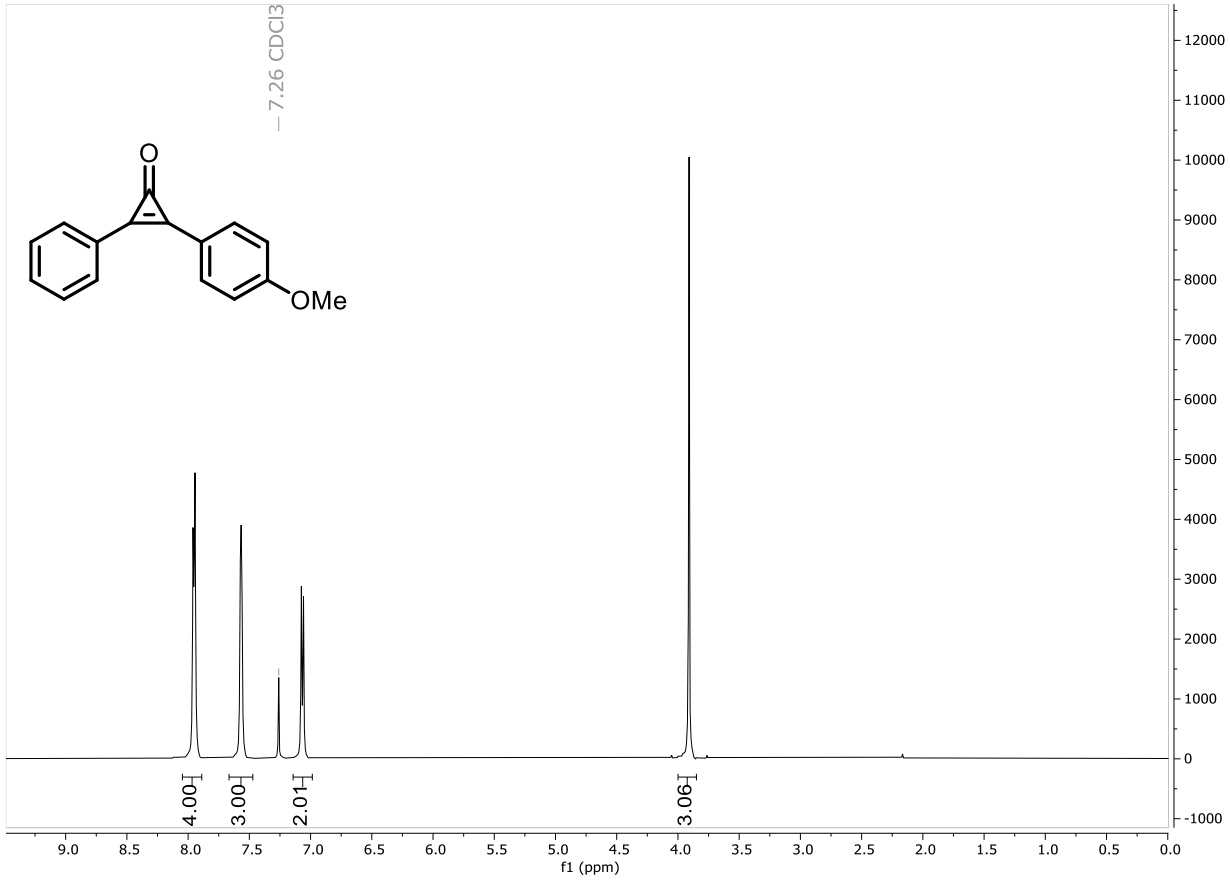

163.13
155.56
147.77
144.46
133.82
132.23
131.20
129.32
124.30
116.80
114.83
77.16 CDCl3
55.61
O
OMe
f1 (ppm)

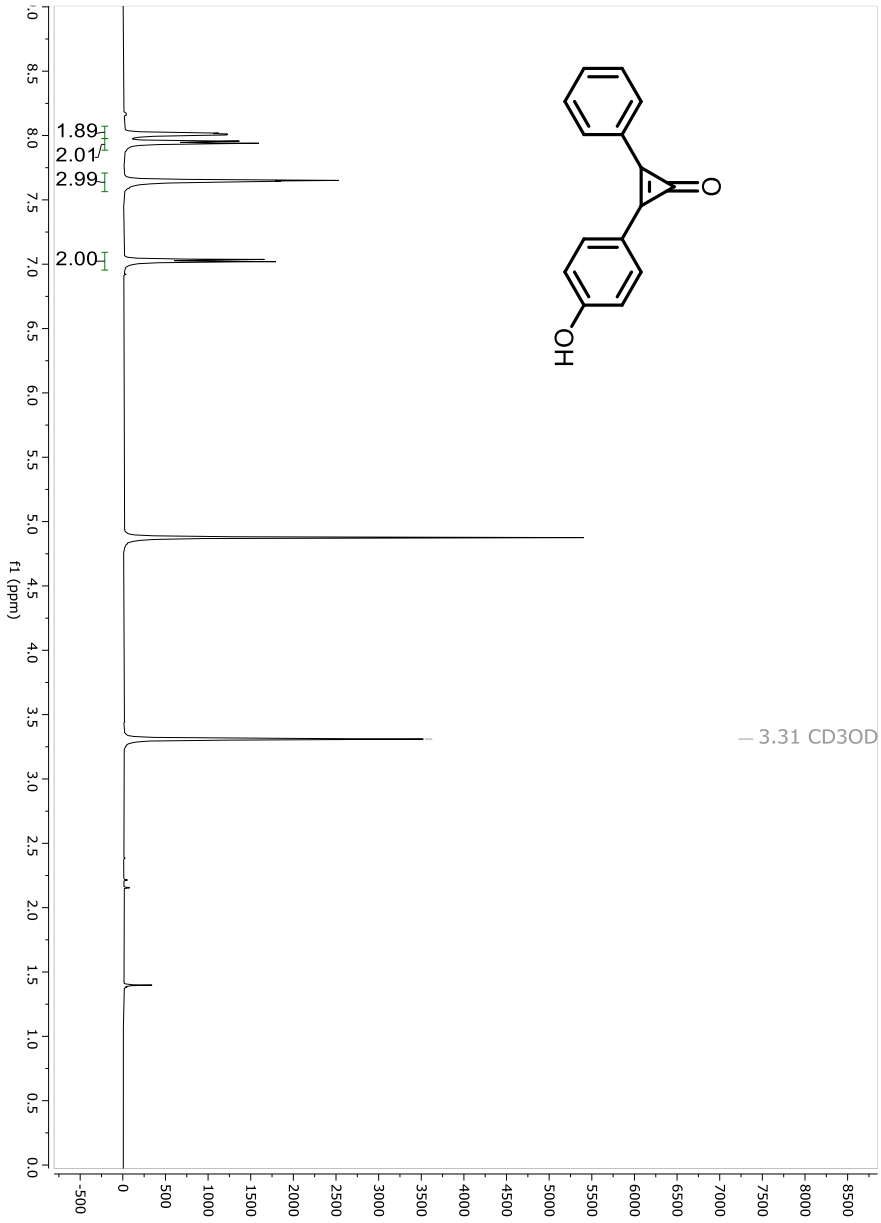
1.89
2.01
2.99
2.00
3.31 CD3OD
OH
O
f1 (ppm)

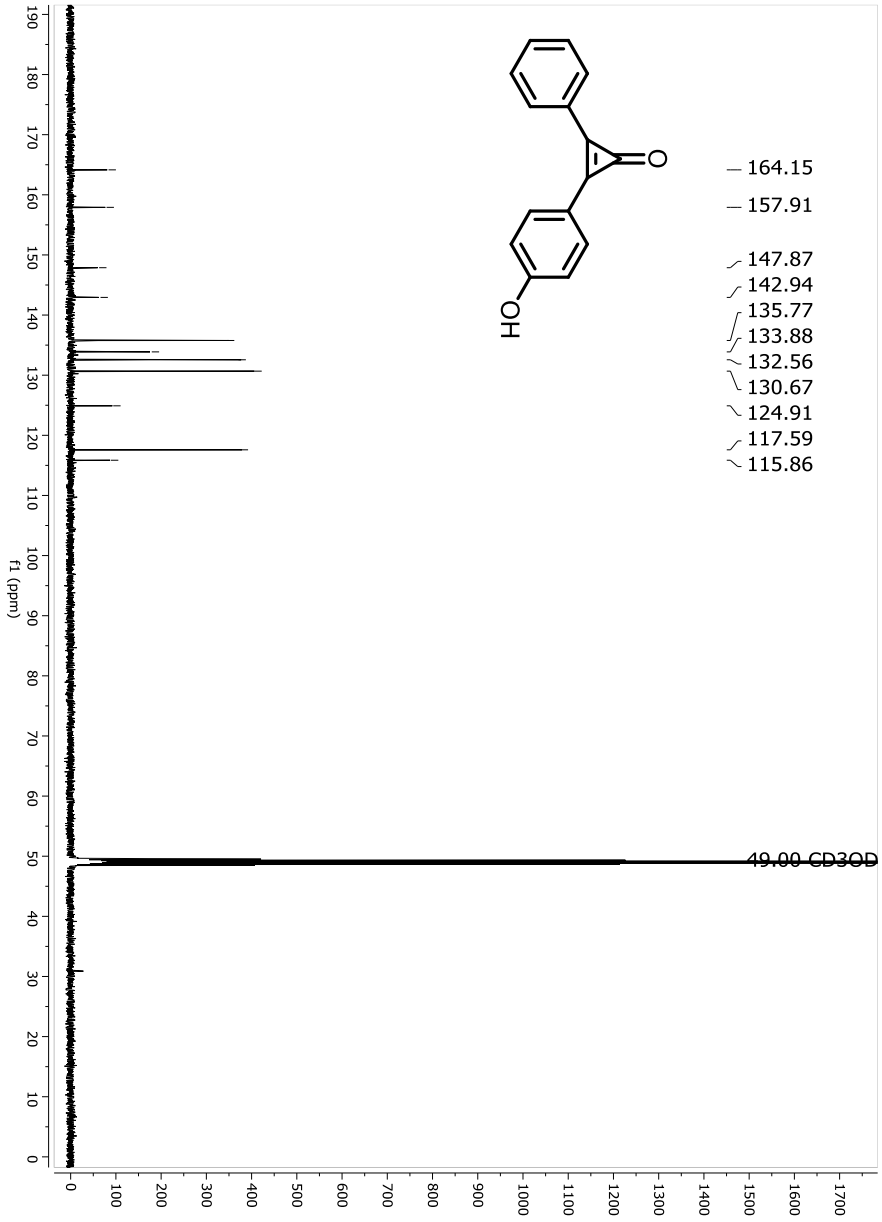
164.15
157.91
147.87
142.94
135.77
133.88
132.56
130.67
124.91
117.59
115.86
49.00 CD3OD
O
OH
f1 (ppm)

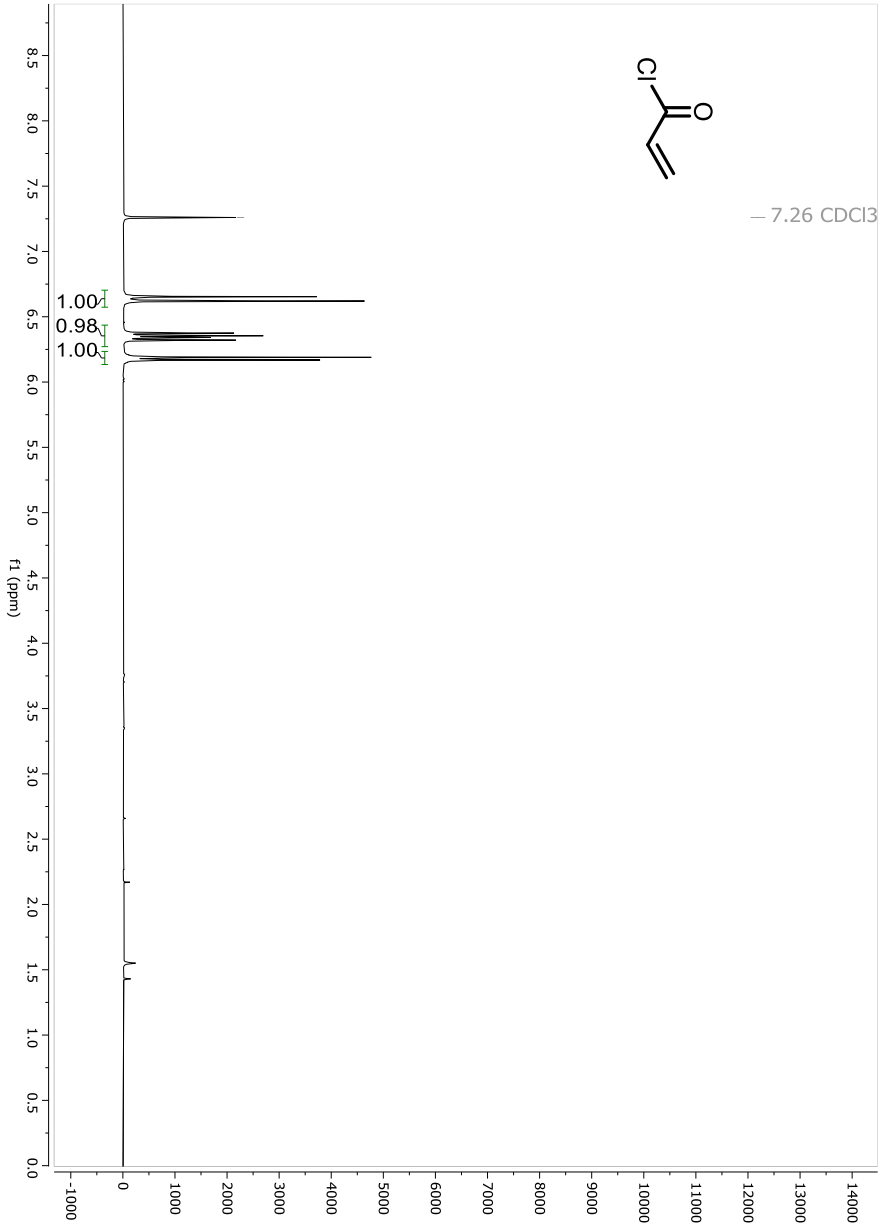
Cl
O
7.26 CDCl3
1.00
0.98
1.00
f1 (ppm)

166.46
136.74
133.17
77.16 CDCl3
O
Cl
f1 (ppm)

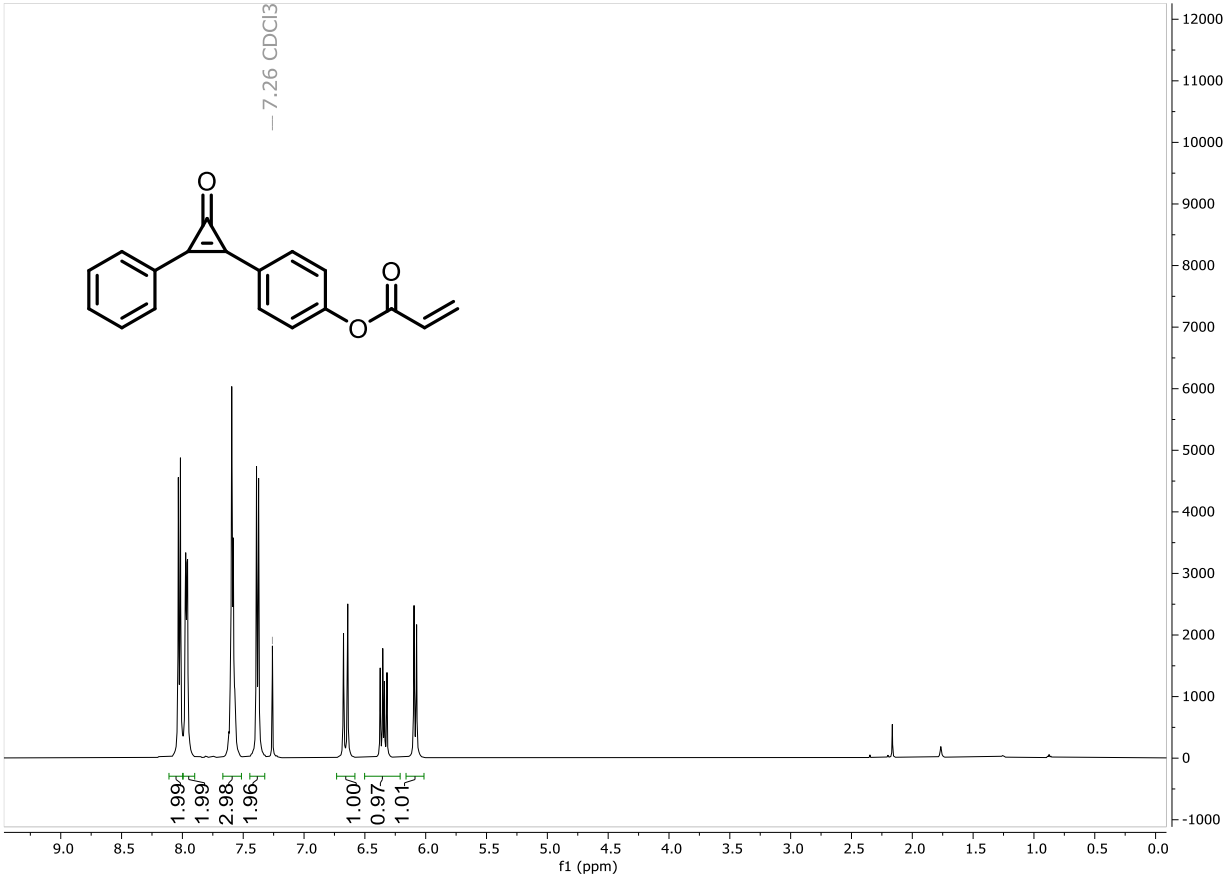
7.26 CDCl3
O
O
O
1.99
1.99
2.98
1.96
1.00
0.97
1.01
12000
11000
10000
9000
8000
7000
6000
5000
4000
3000
2000
1000
0
-1000
9.0
8.5
8.0
7.5
7.0
6.5
6.0
5.5
5.0
4.5
4.0
3.5
3.0
2.5
2.0
1.5
1.0
0.5
0.0
f1 (ppm)

163.90
155.52
153.81
148.14
147.44
133.69
133.01
132.88
131.53
129.52
127.49
124.07
122.84
121.79
77.16 CDCl3
O
O
O
f1 (ppm)

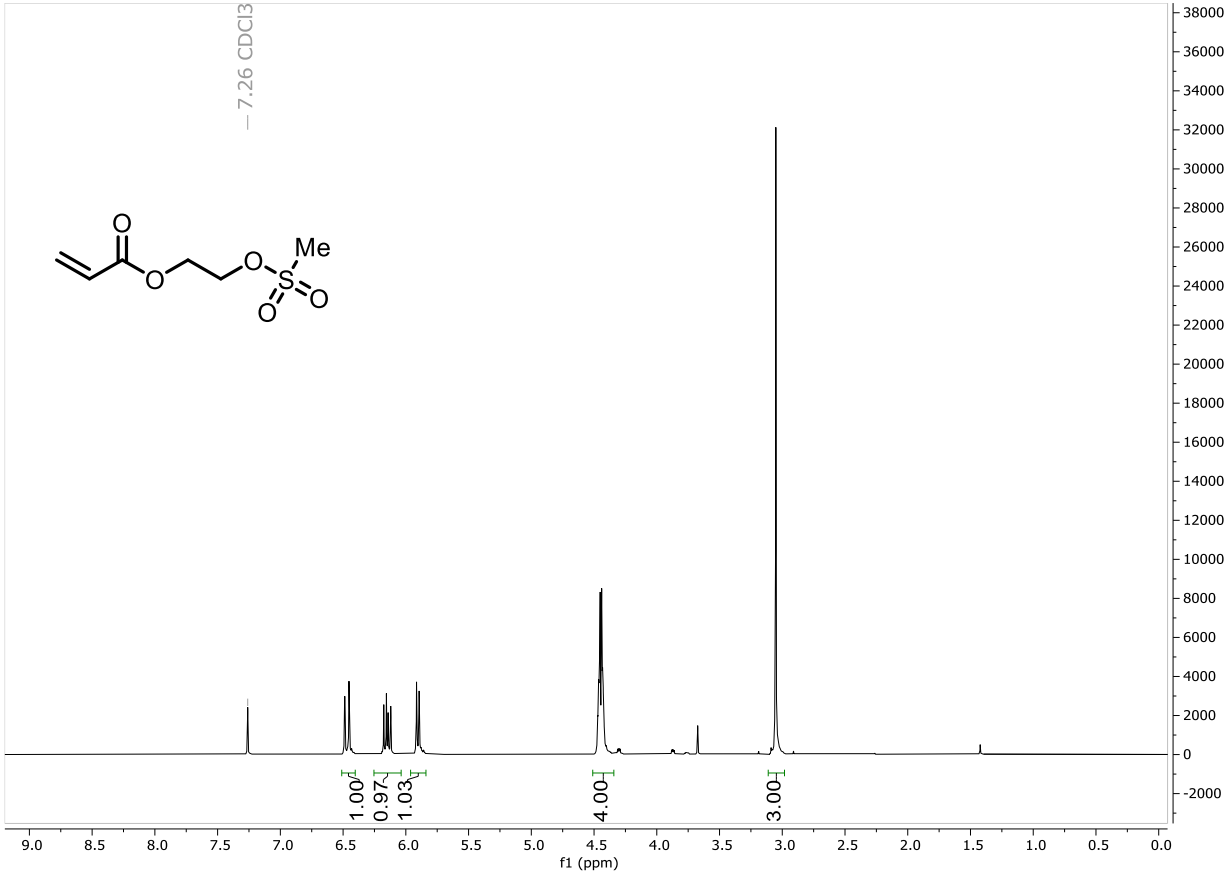
7.26 CDCl3
Me
O
O
O
S
O
O
1.00
0.97
1.03
4.00
3.00
f1 (ppm)

165.65
132.05
127.66
77.16 CDCl3
67.22
61.98
37.75
O
O
O
S
Me
O
O
4400
4200
4000
3800
3600
3400
3200
3000
2800
2600
2400
2200
2000
1800
1600
1400
1200
1000
800
600
400
200
0
190
180
170
160
150
140
130
120
110
100
90
80
70
60
50
40
30
20
10
0
f1 (ppm)

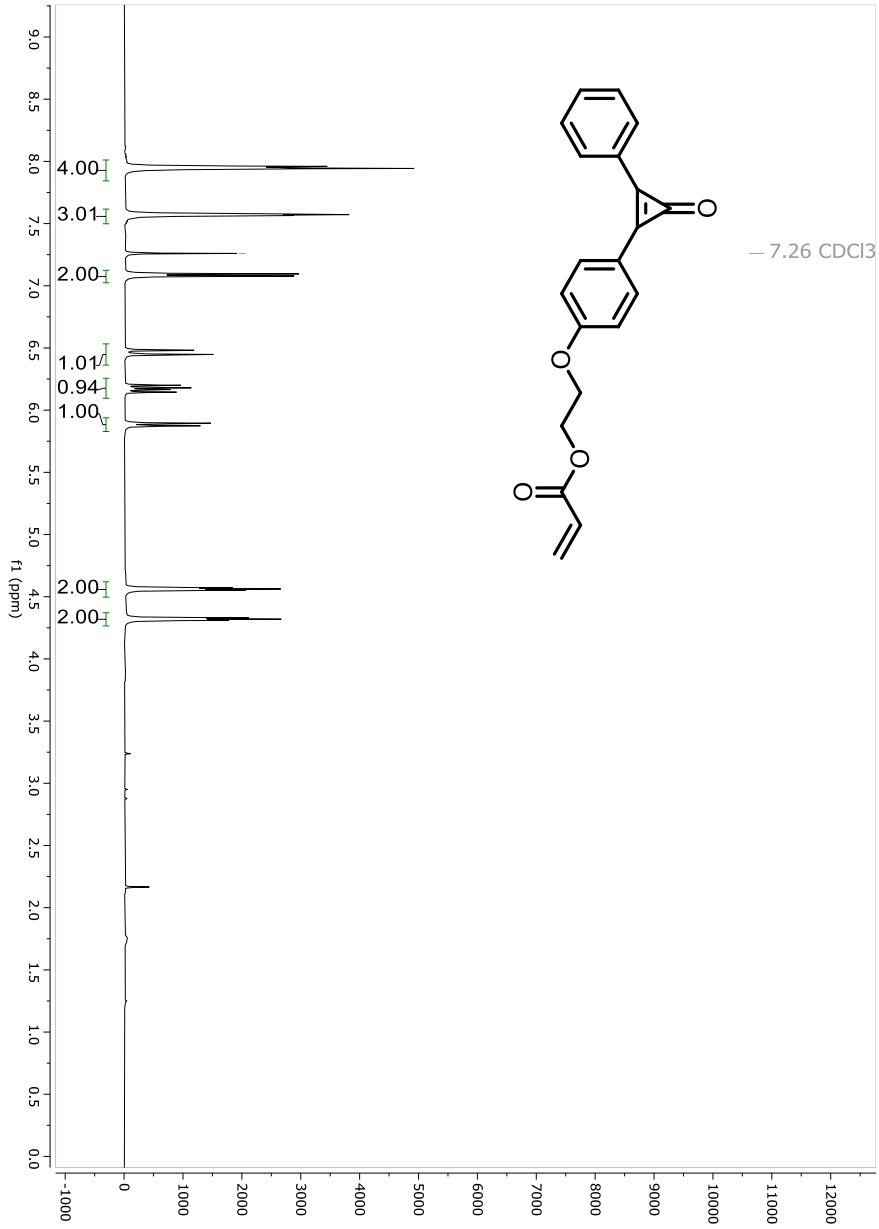
4.00
3.01
2.00
1.01
0.94
1.00
2.00
2.00
f1 (ppm)
7.26 CDCl3

166.08
162.03
155.65
147.74
145.00
133.93
132.41
131.75
131.35
129.44
127.99
124.37
117.38
115.44
77.16 CDCl3
66.26
62.59
O
O
O
O
1000
900
800
700
600
500
400
300
200
100
0
190
180
170
160
150
140
130
120
110
100
90
80
70
60
50
40
30
20
10
0
f1 (ppm)

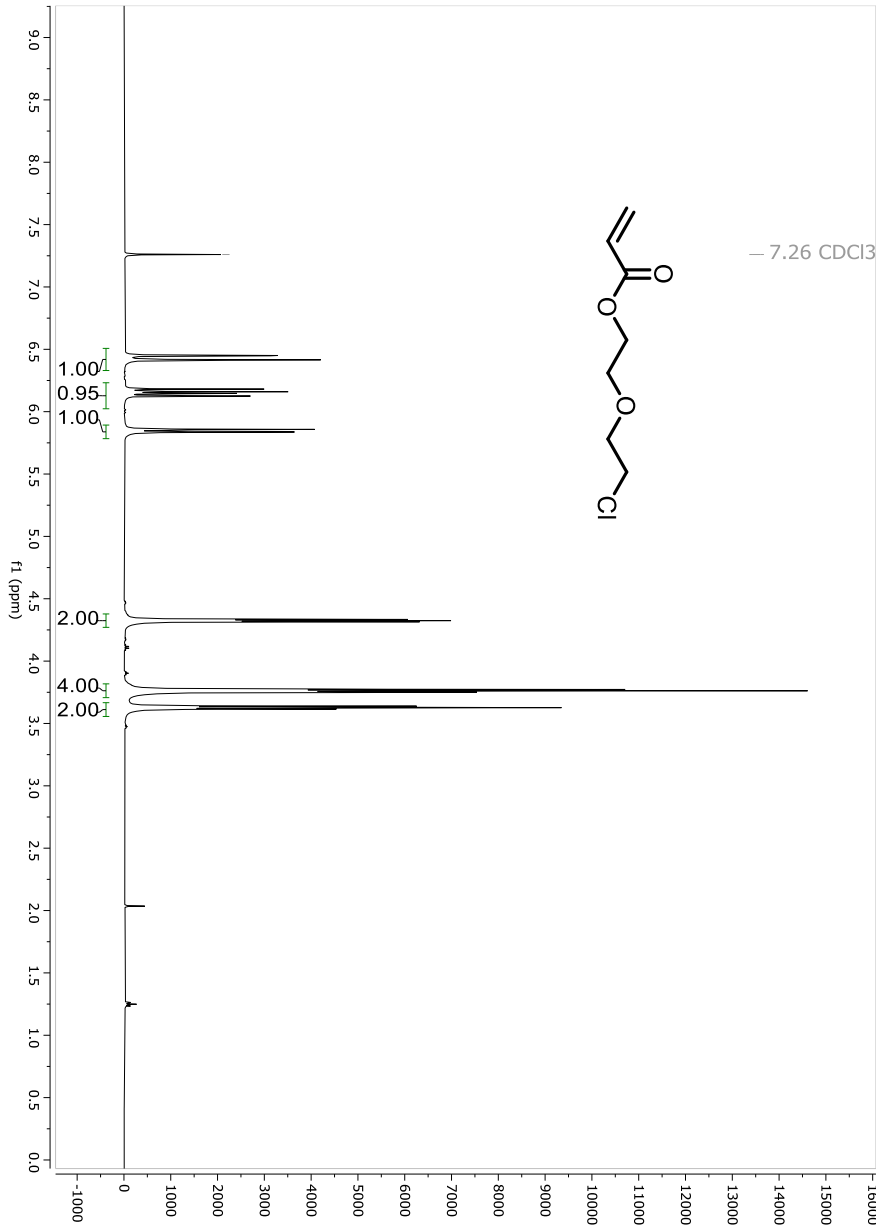
7.26 CDCl3
1.00
0.95
1.00
2.00
4.00
2.00
f1 (ppm)
O
O
O
Cl

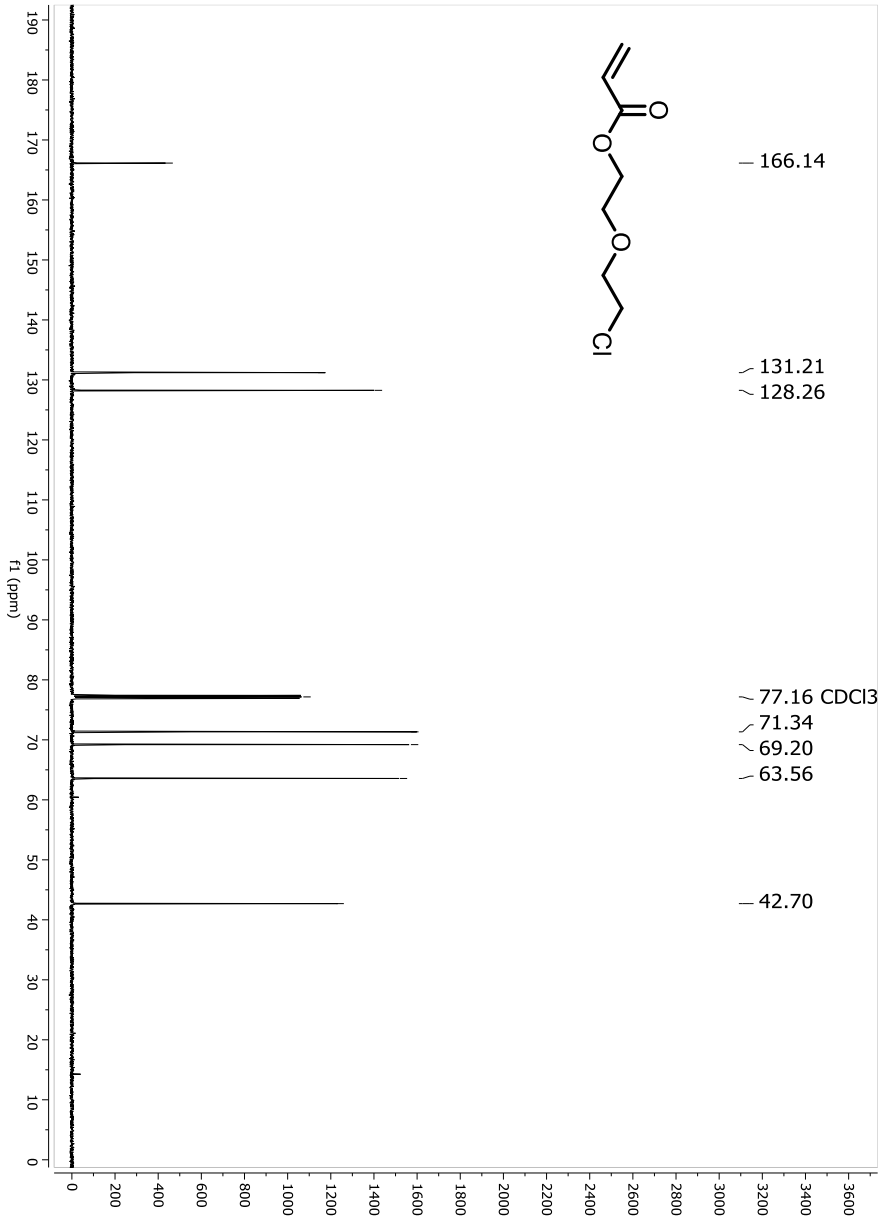
166.14
131.21
128.26
77.16 CDCl3
71.34
69.20
63.56
42.70
f1 (ppm)
O
O
O
Cl

7.26 CDCl3
O
O
O
I
10000
9000
8000
7000
6000
5000
4000
3000
2000
1000
0
1.00
0.97
1.04
2.00
4.00
2.00
9.0
8.5
8.0
7.5
7.0
6.5
6.0
5.5
5.0
4.5
4.0
3.5
3.0
2.5
2.0
1.5
1.0
0.5
0.0
f1 (ppm)

166.23
131.33
128.32
77.16 CDCl3
71.98
68.81
63.65
2.61
O
O
O
I
f1 (ppm)

7.26 CDCl3
O
O
O
O
4.00
3.00
2.00
0.99
0.96
1.00
2.04
2.02
1.99
2.02
9.0
8.5
8.0
7.5
7.0
6.5
6.0
5.5
5.0
4.5
4.0
3.5
3.0
2.5
2.0
1.5
1.0
0.5
0.0
f1 (ppm)
7000
6500
6000
5500
5000
4500
4000
3500
3000
2500
2000
1500
1000
500
0
-500

166.17
162.34
155.66
147.77
144.68
133.87
132.33
131.30
131.23
129.40
128.24
124.35
117.08
115.45
77.16 CDCl3
69.48
67.80
63.58
O
O
O
O
f1 (ppm)

7.26 CDCl3
O
Cl
1.00
1.00
3.00
50000
45000
40000
35000
30000
25000
20000
15000
10000
5000
0
7.5
7.0
6.5
6.0
5.5
5.0
4.5
4.0
3.5
3.0
2.5
2.0
1.5
f1 (ppm)

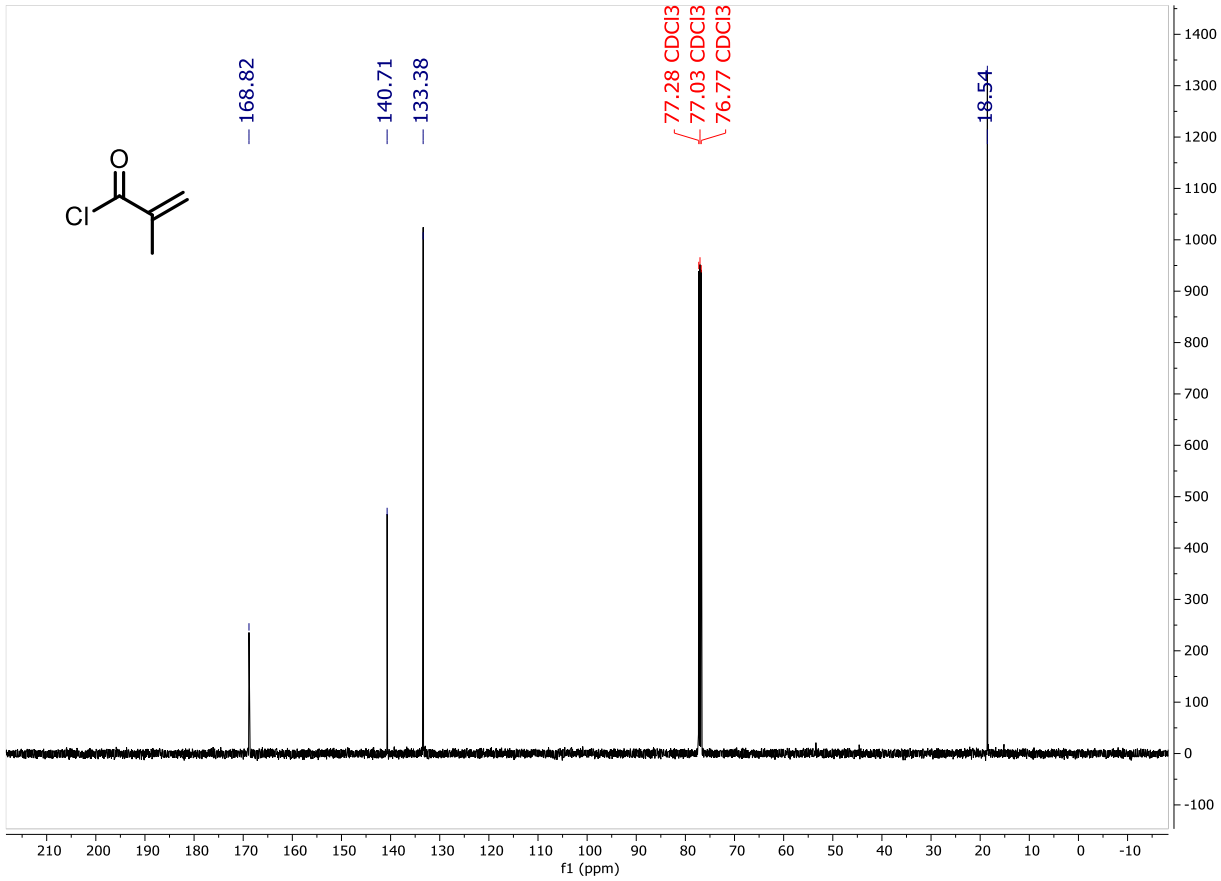
168.82
140.71
133.38
77.28 CDCl3
77.03 CDCl3
76.77 CDCl3
18.54
O
Cl
f1 (ppm)

7.26 CDCl3
O
O
O
4.00
3.00
2.00
1.00
1.00
3.00
f1 (ppm)

165.17
155.49
154.15
148.00
147.45
135.45
132.93
132.77
131.45
129.44
128.15
124.06
122.85
121.63
77.28 CDCl3
77.03 CDCl3
76.77 CDCl3
18.32
O
O
O
f1 (ppm)

7.26 CDCl3
Me
1.00
1.00
4.00
3.00
3.00
f1 (ppm)

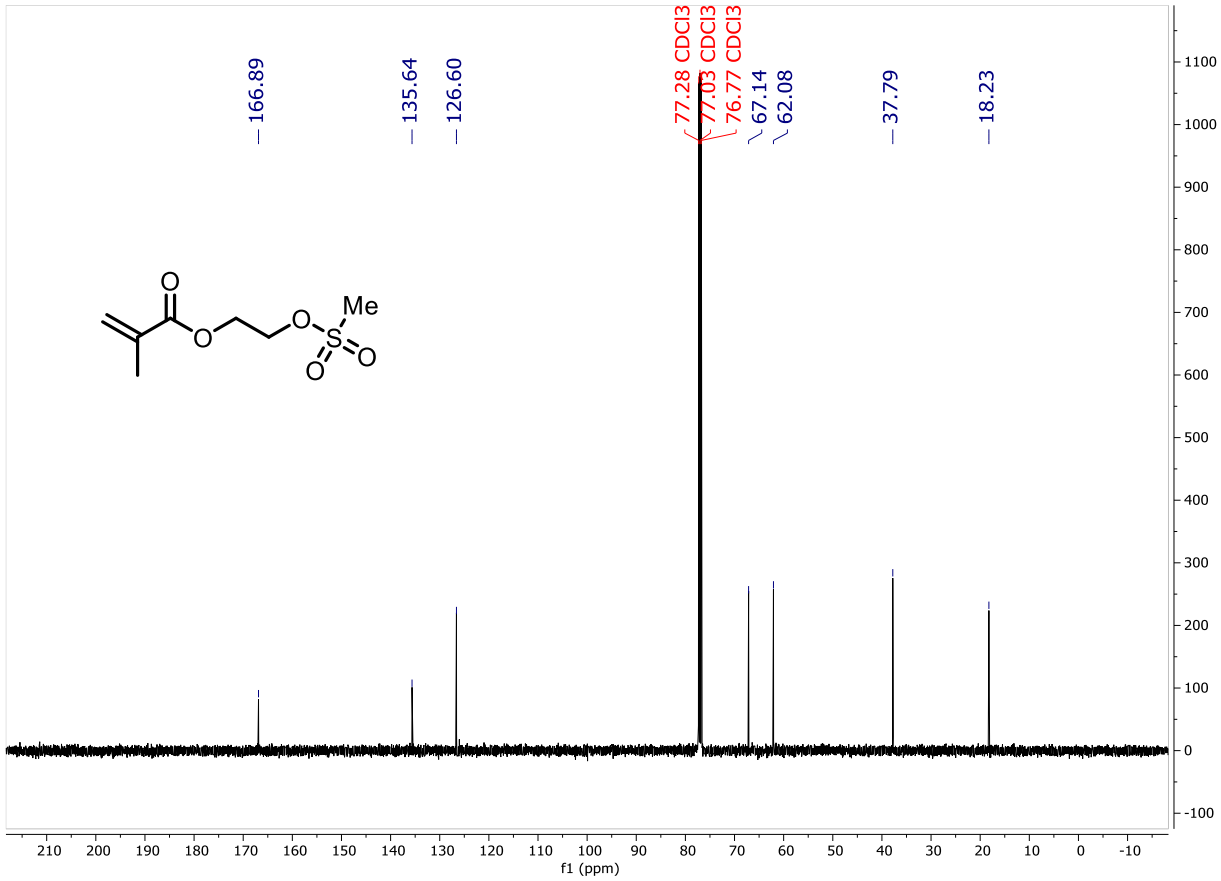
166.89
135.64
126.60
77.28 CDCl3
77.03 CDCl3
76.77 CDCl3
67.14
62.08
37.79
18.23
Me
f1 (ppm)

7.26 CDCl3
O
O
O
O
4.00
3.00
2.00
1.00
1.00
2.00
2.00
3.00
11000
10000
9000
8000
7000
6000
5000
4000
3000
2000
1000
0
-1000
8.5
8.0
7.5
7.0
6.5
6.0
5.5
5.0
4.5
4.0
3.5
3.0
2.5
2.0
1.5
1.0
f1 (ppm)

167.32
162.14
155.66
147.78
145.00
135.97
133.92
132.40
131.34
129.44
126.37
124.40
117.38
115.50
77.16 CDCl3
66.33
62.78
18.38
O
O
O
O
f1 (ppm)

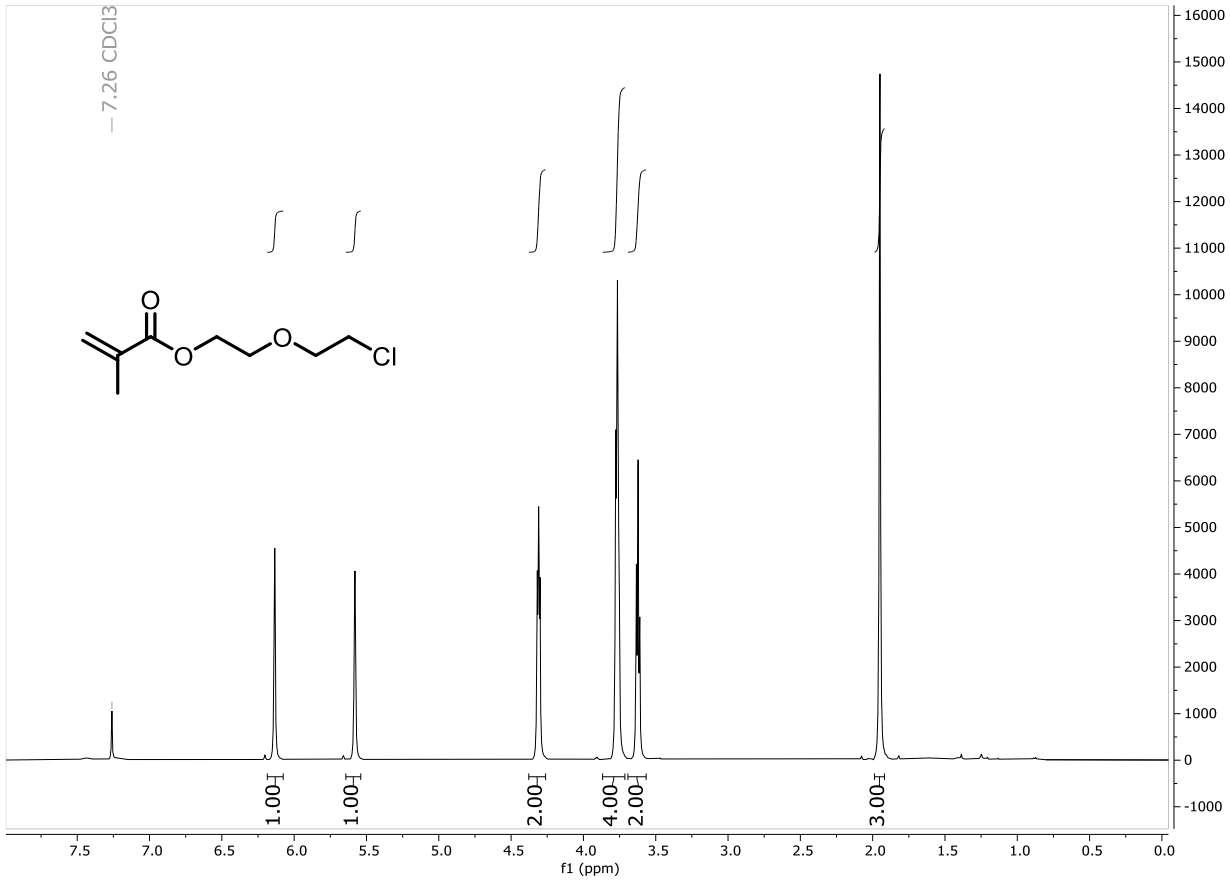
7.26 CDCl3
O
O
O
Cl
1.00
1.00
2.00
4.00
2.00
3.00
16000
15000
14000
13000
12000
11000
10000
9000
8000
7000
6000
5000
4000
3000
2000
1000
0
-1000
7.5
7.0
6.5
6.0
5.5
5.0
4.5
4.0
3.5
3.0
2.5
2.0
1.5
1.0
0.5
0.0
f1 (ppm)

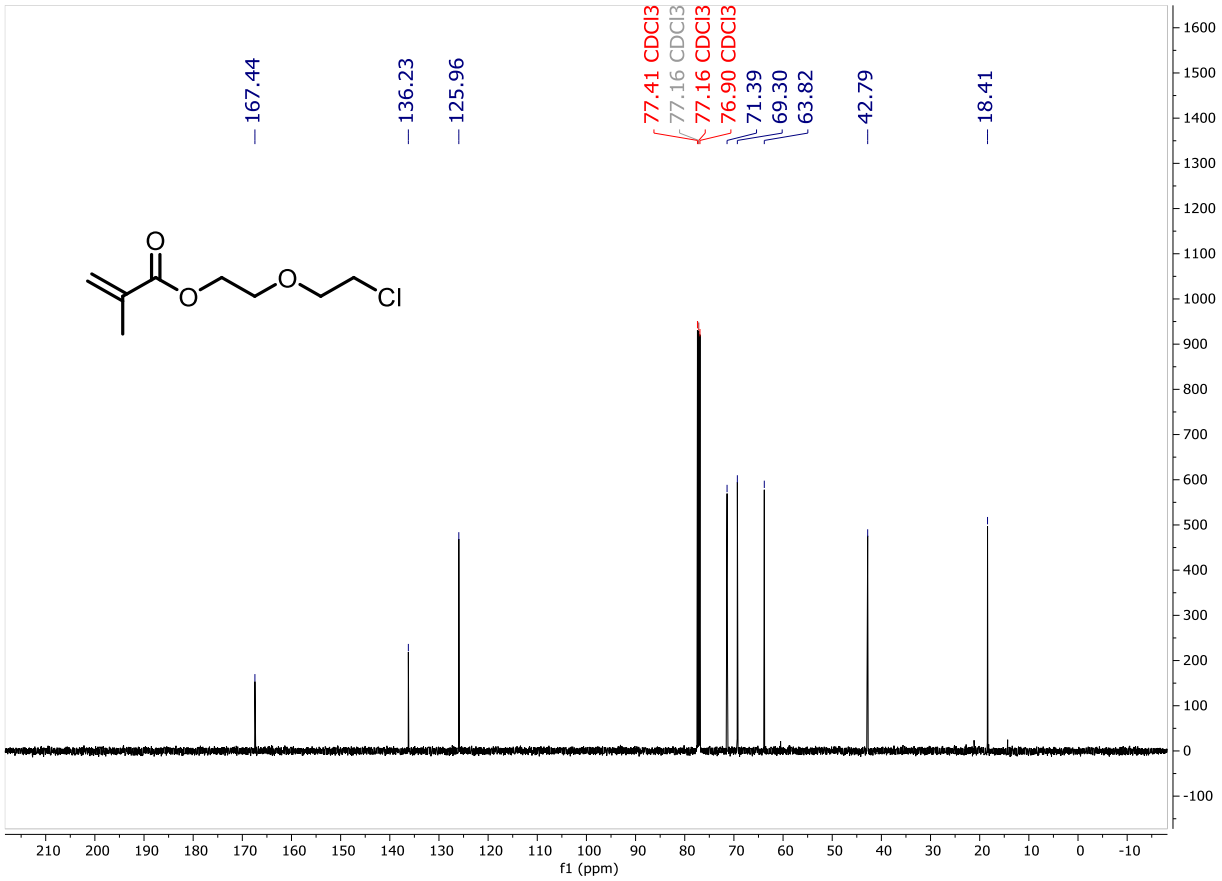
167.44
136.23
125.96
77.41 CDCl3
77.16 CDCl3
77.16 CDCl3
76.90 CDCl3
71.39
69.30
63.82
42.79
18.41
O
O
O
Cl
f1 (ppm)

7.26 CDCl3
O
O
O
I
1.00
1.00
2.00
4.00
1.96
3.00
f1 (ppm)

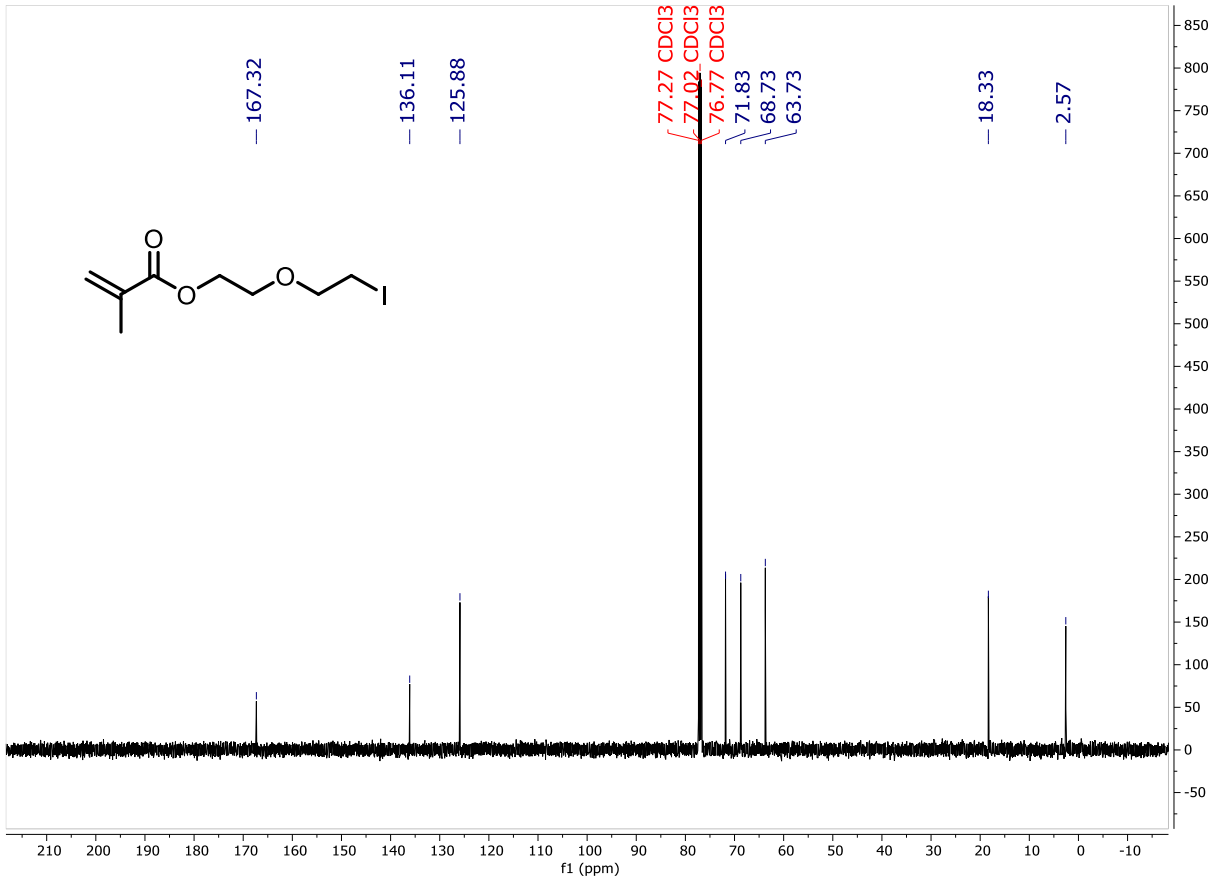
167.32
136.11
125.88
77.27 CDCl3
77.02 CDCl3
76.77 CDCl3
71.83
68.73
63.73
18.33
2.57
O
O
O
I
f1 (ppm)

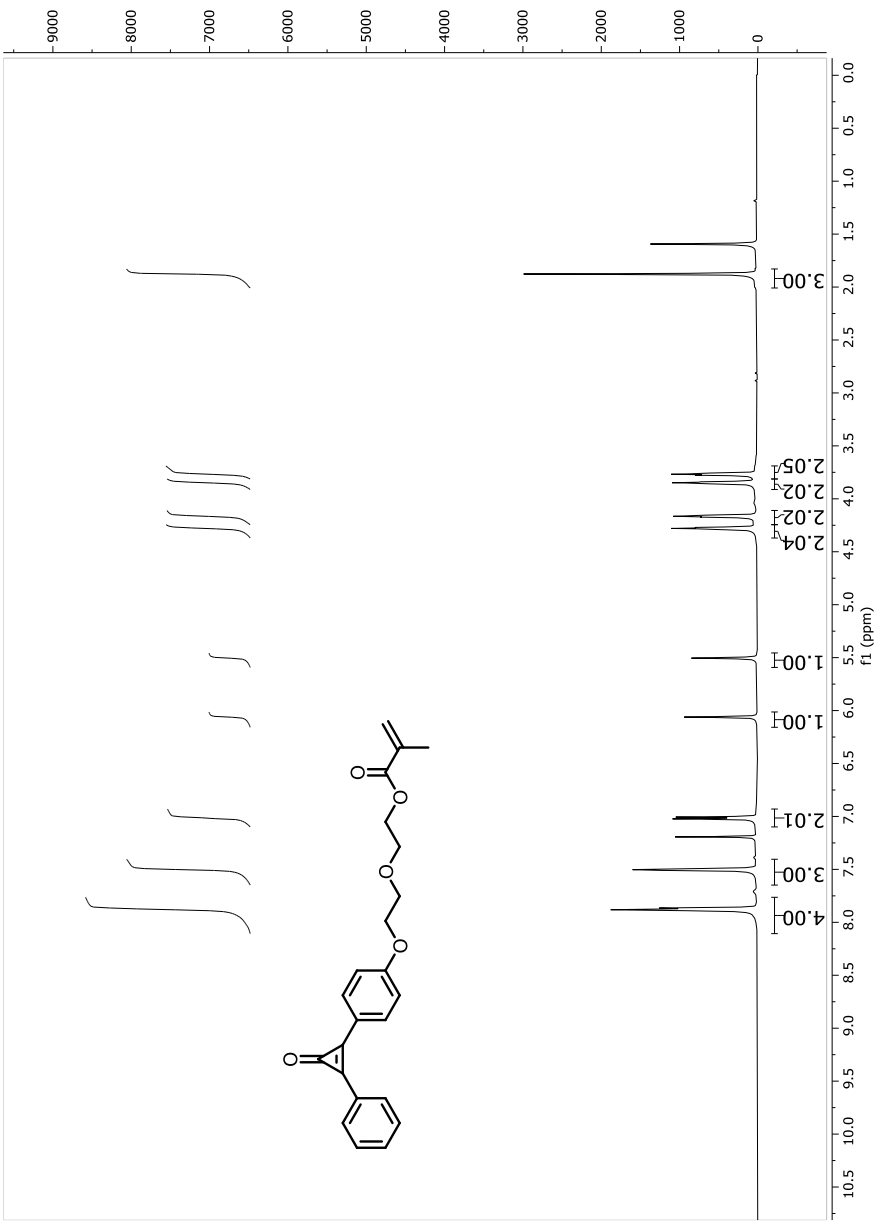
9000
8000
7000
6000
5000
4000
3000
2000
1000
0
0.0
0.5
1.0
1.5
2.0
2.5
3.0
3.5
4.0
4.5
5.0
5.5
6.0
6.5
7.0
7.5
8.0
8.5
9.0
9.5
10.0
10.5
f1 (ppm)
4.00
3.00
2.01
1.00
1.00
2.04
2.02
2.02
2.05
3.00
O
O
O
O
O
O

167.13
162.12
155.39
147.55
144.45
135.93
133.60
132.06
131.04
129.14
125.64
124.13
116.85
115.21
77.16 CDCl3
77.16 CDCl3
76.91 CDCl3
76.65 CDCl3
69.25
67.60
63.52
18.11
O
O
O
O
O
f1 (ppm)

7.26 CDCl3
HO
2.00
1.97
2.98
2.01
0.98
f1 (ppm)

155.63
133.34
131.51
128.38
128.06
123.54
115.72
115.59
89.31
88.18
77.34 CDCl3
77.08 CDCl3
76.83 CDCl3
HO
f1 (ppm)

7.26 CDCl3
3.95
2.90
2.00
1.00
1.00
3.00
f1 (ppm)

165.55
150.78
135.75
132.75
131.62
128.37
128.33
127.51
123.17
121.76
120.88
89.44
88.63
77.28 CDCl3
77.02 CDCl3
76.77 CDCl3
18.37
O
O
f1 (ppm)

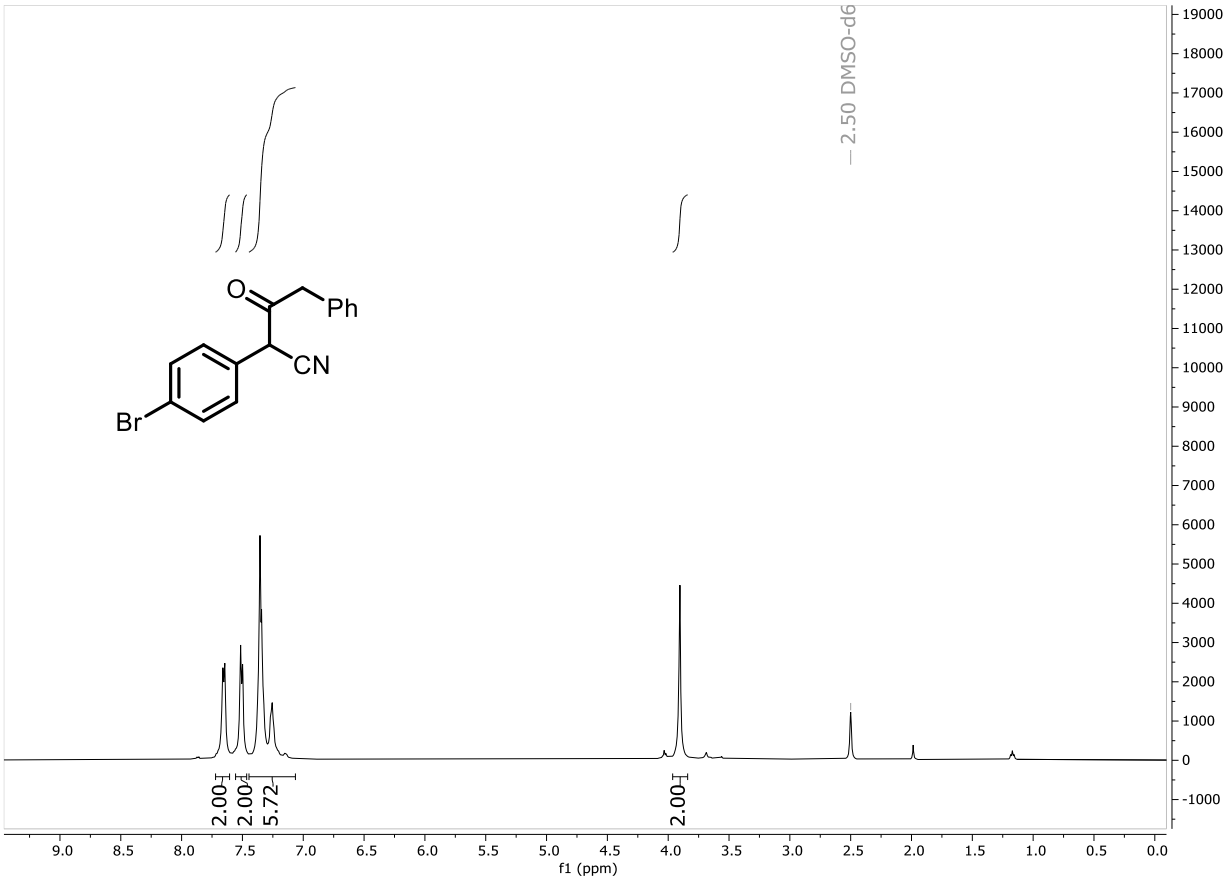
2.50 DMSO-d6
O
Ph
CN
Br
2.00
2.00
5.72
2.00
f1 (ppm)

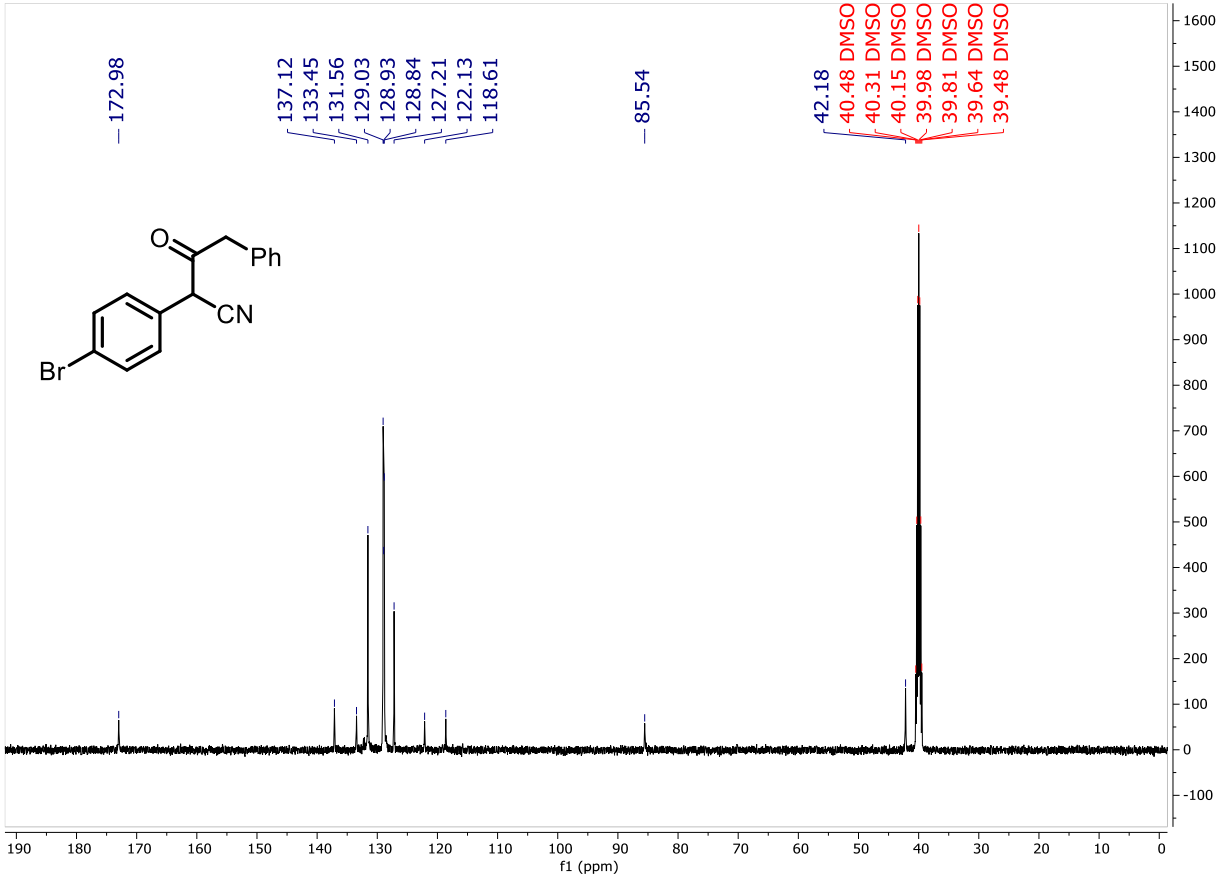
172.98
137.12
133.45
131.56
129.03
128.93
128.84
127.21
122.13
118.61
85.54
42.18
40.48 DMSO
40.31 DMSO
40.15 DMSO
39.98 DMSO
39.81 DMSO
39.64 DMSO
39.48 DMSO
O
Ph
CN
Br
f1 (ppm)

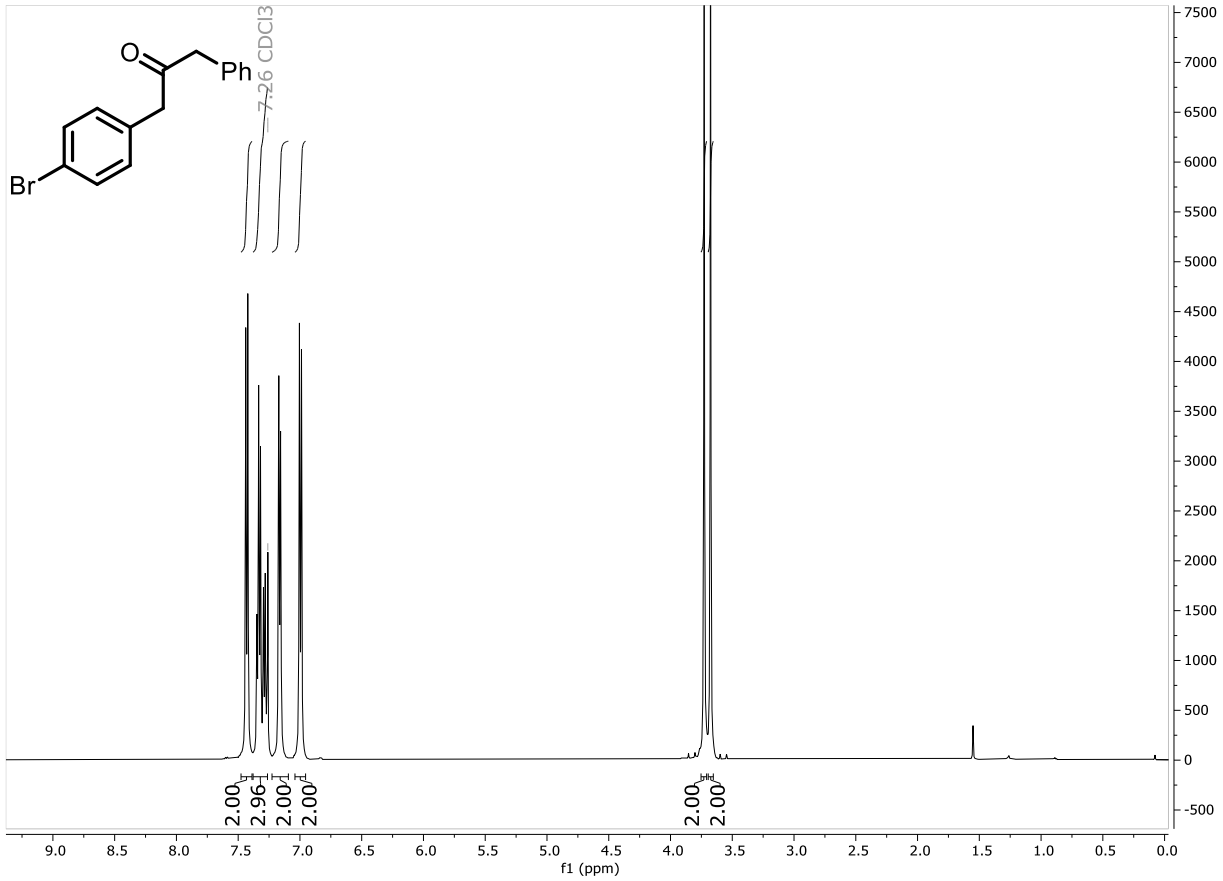
O
Ph
Br
7.26 CDCl3
2.00
2.96
2.00
2.00
2.00
2.00
f1 (ppm)

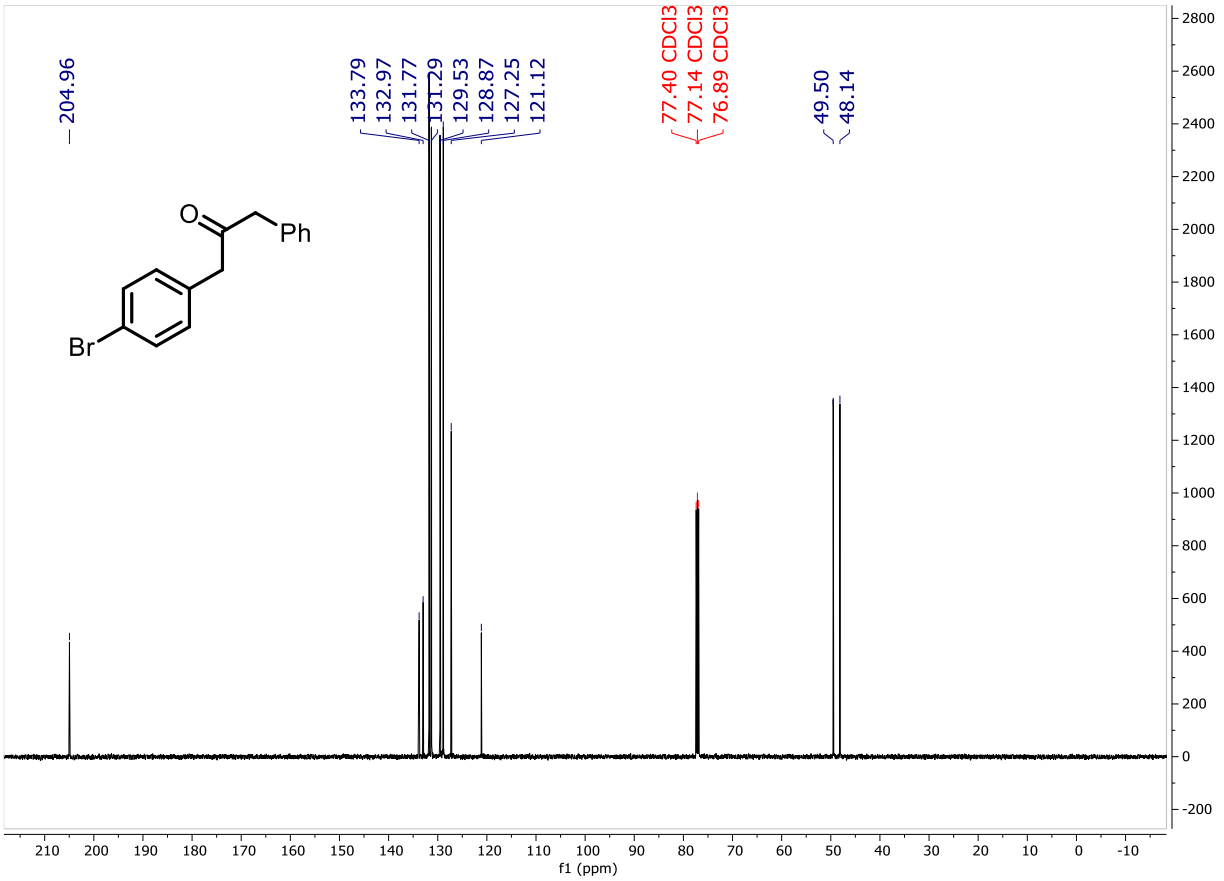
204.96
133.79
132.97
131.77
131.29
129.53
128.87
127.25
121.12
77.40 CDCl3
77.14 CDCl3
76.89 CDCl3
49.50
48.14
O
Ph
Br
f1 (ppm)

7.26 CDCl3
Br
O
O
2.00
5.28
1.98
2.01
2.02
2.02
2.01
5.99
f1 (ppm)

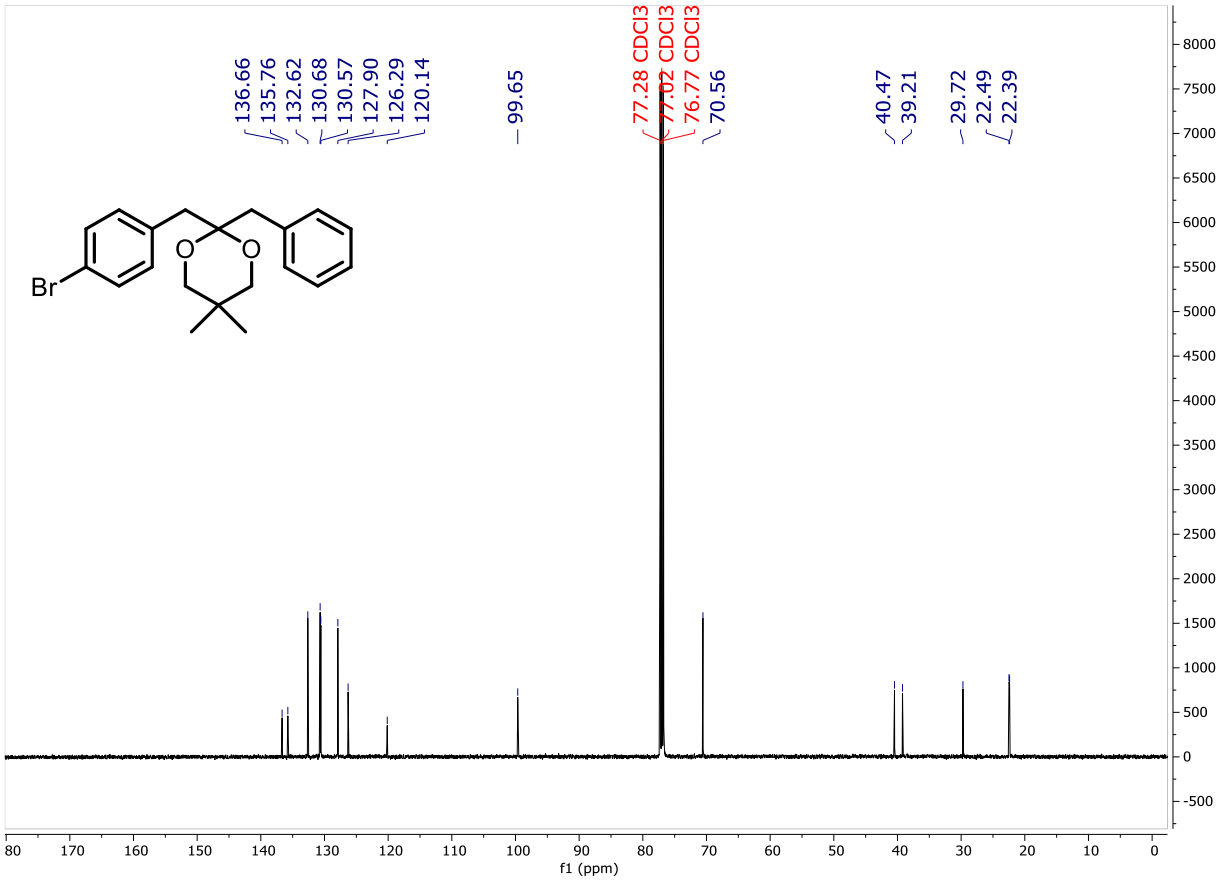
136.66
135.76
132.62
130.68
130.57
127.90
126.29
120.14
99.65
77.28 CDCl3
77.02 CDCl3
76.77 CDCl3
70.56
40.47
39.21
29.72
22.49
22.39
Br
O
O
f1 (ppm)

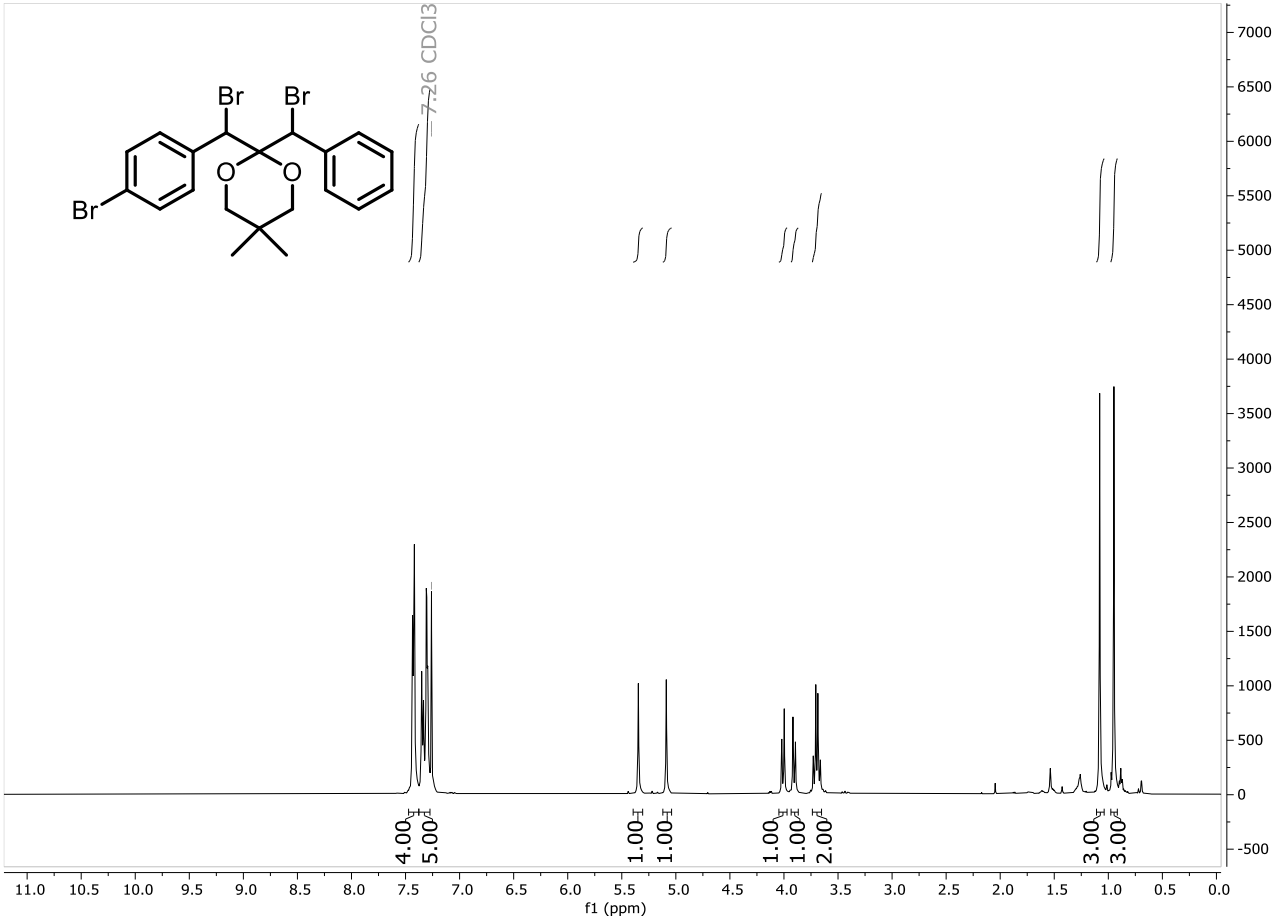
Br
Br
Br
O
O
7.26 CDCl3
4.00
5.00
1.00
1.00
1.00
1.00
2.00
3.00
3.00
f1 (ppm)

137.22
136.72
132.28
131.98
131.07
130.87
130.35
130.17
128.03
98.47
77.16 CDCl3
71.90
71.41
70.98
54.37
53.27
29.22
23.57
Br
Br
Br
O
O
4500
4000
3500
3000
2500
2000
1500
1000
500
0
-500
210
200
190
180
170
160
150
140
130
120
110
100
90
80
70
60
50
40
30
20
10
0
-10
f1 (ppm)

7.26 CDCl3
Br
O
O
2.00
4.00
2.00
1.00
4.00
6.00
f1 (ppm)

132.22
131.30
130.10
129.76
129.04
127.57
126.79
125.98
124.87
123.67
83.14
78.91
77.30 CDCl3
77.05 CDCl3
76.79 CDCl3
30.50
22.55
22.43
O
O
Br
f1 (ppm)

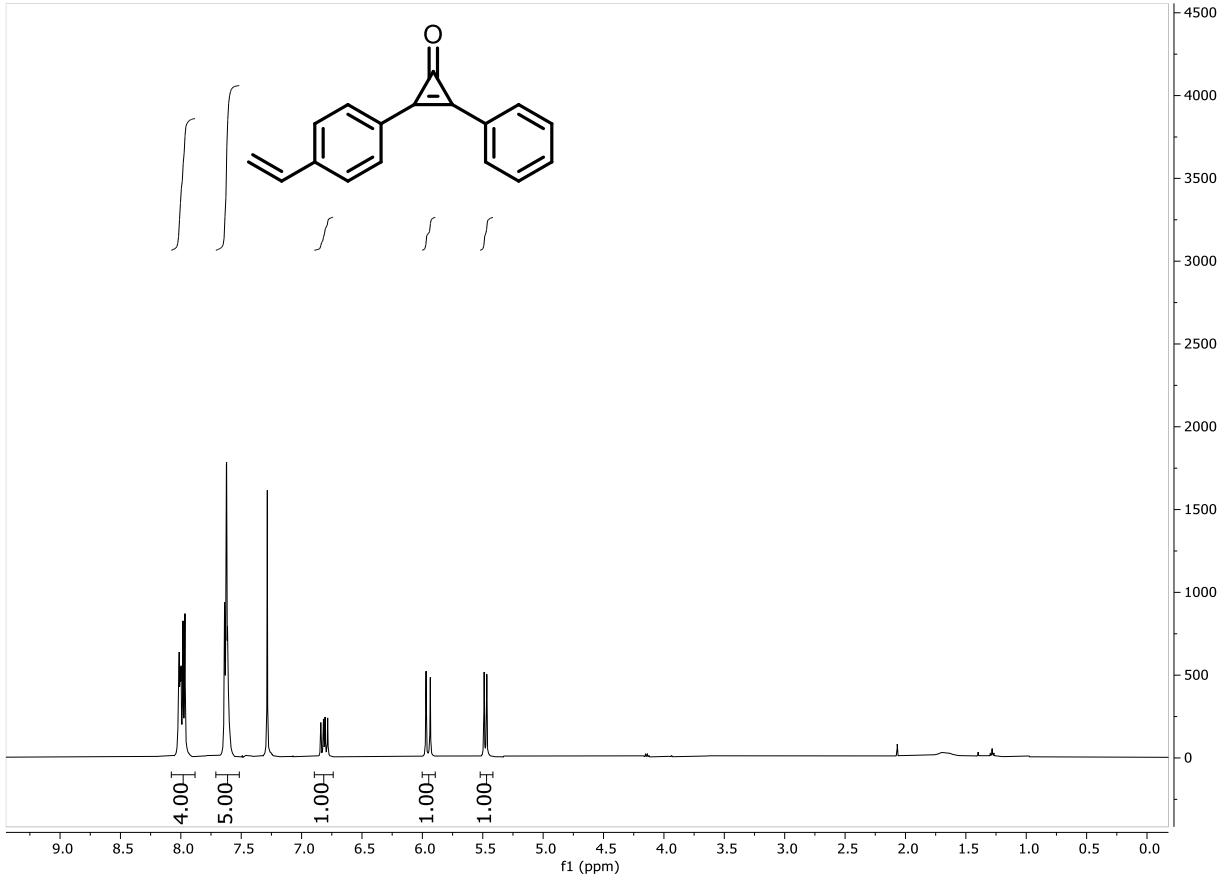
O
4.00
5.00
1.00
1.00
1.00
9.0
8.5
8.0
7.5
7.0
6.5
6.0
5.5
5.0
4.5
4.0
3.5
3.0
2.5
2.0
1.5
1.0
0.5
0.0
f1 (ppm)
4500
4000
3500
3000
2500
2000
1500
1000
500
0

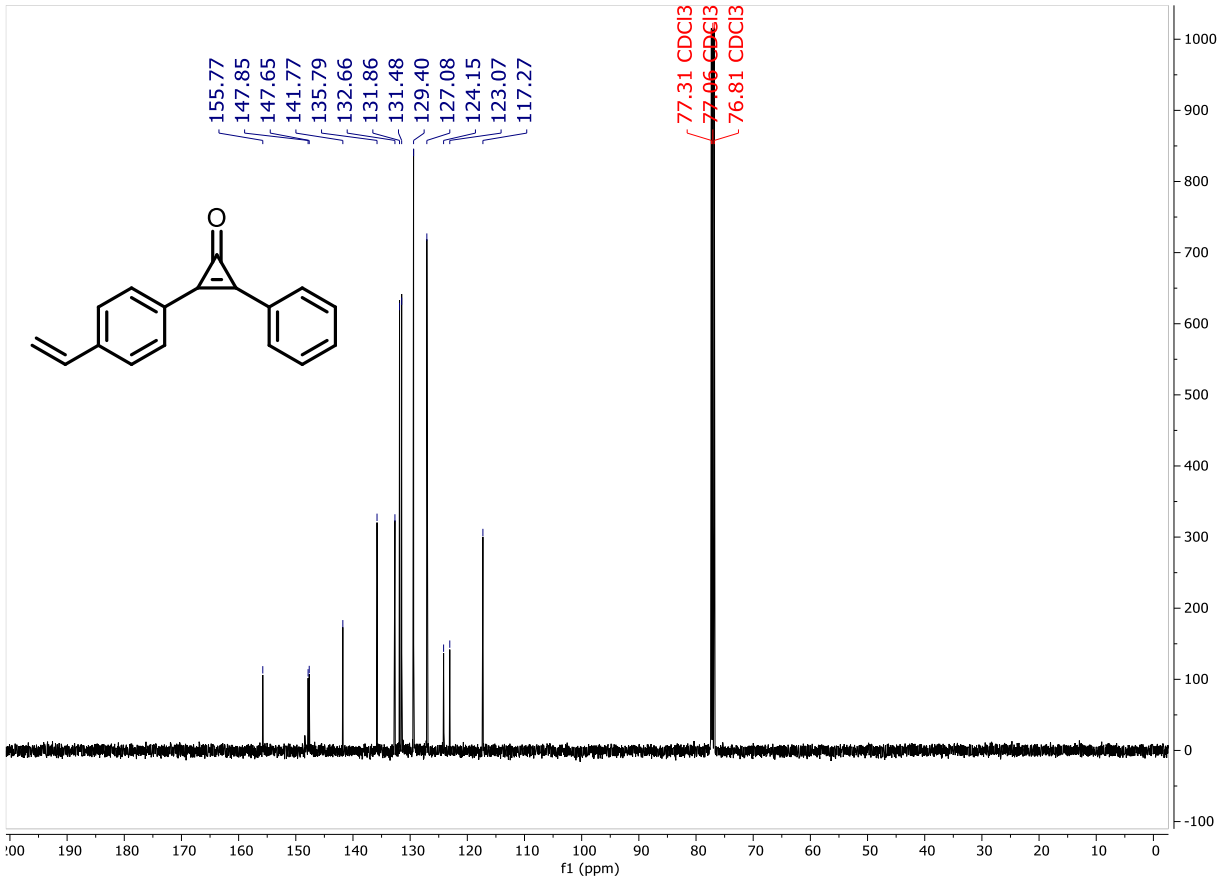
155.77
147.85
147.65
141.77
135.79
132.66
131.86
131.48
129.40
127.08
124.15
123.07
117.27
77.31 CDCl3
77.06 CDCl3
76.81 CDCl3
O
1000
900
800
700
600
500
400
300
200
100
0
-100
190
180
170
160
150
140
130
120
110
100
90
80
70
60
50
40
30
20
10
0
f1 (ppm)

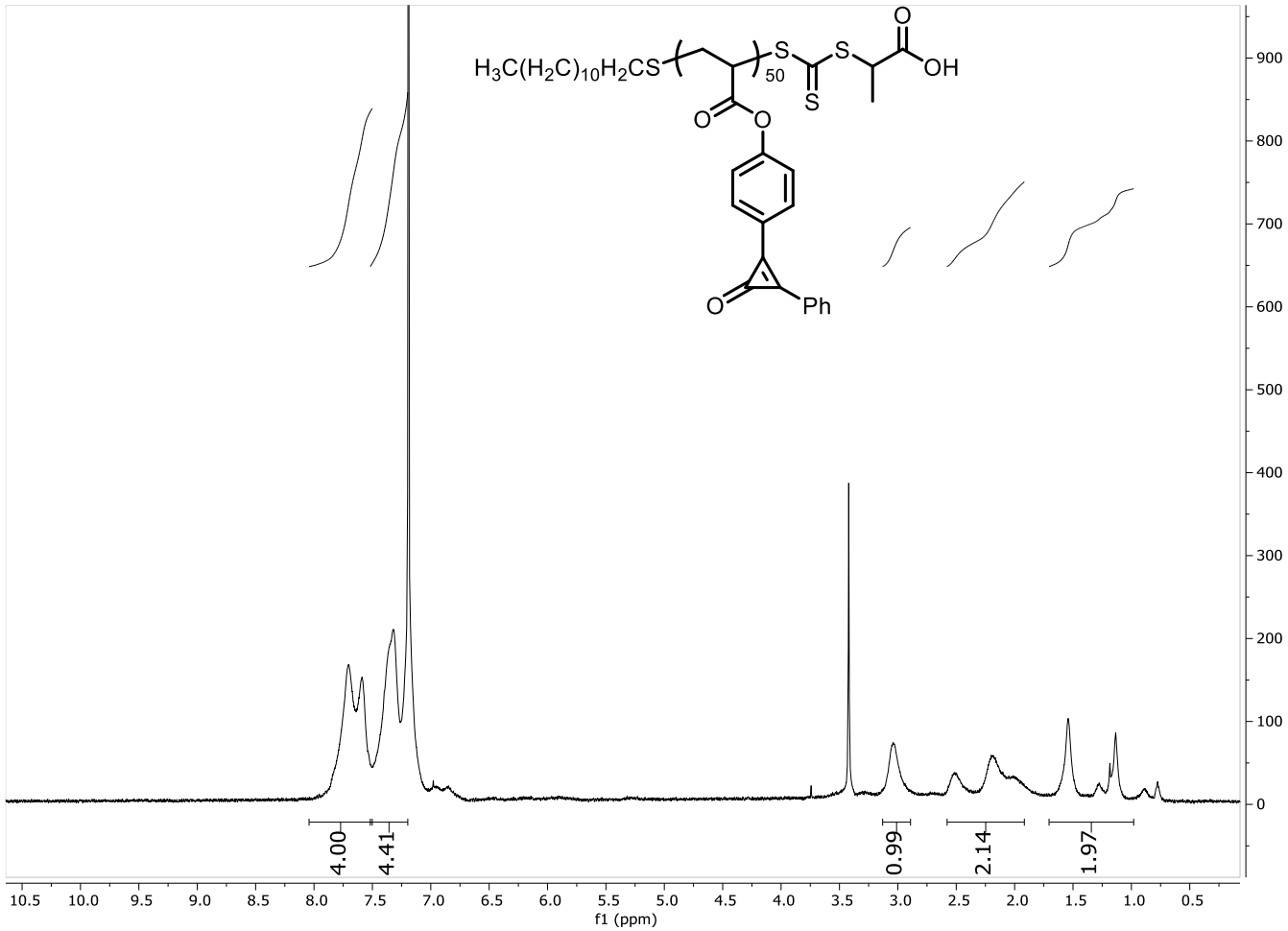
H3C(H2C)10H2CS
50
S
S
S
O
OH
O
O
O
Ph
4.00
4.41
0.99
2.14
1.97
f1 (ppm)

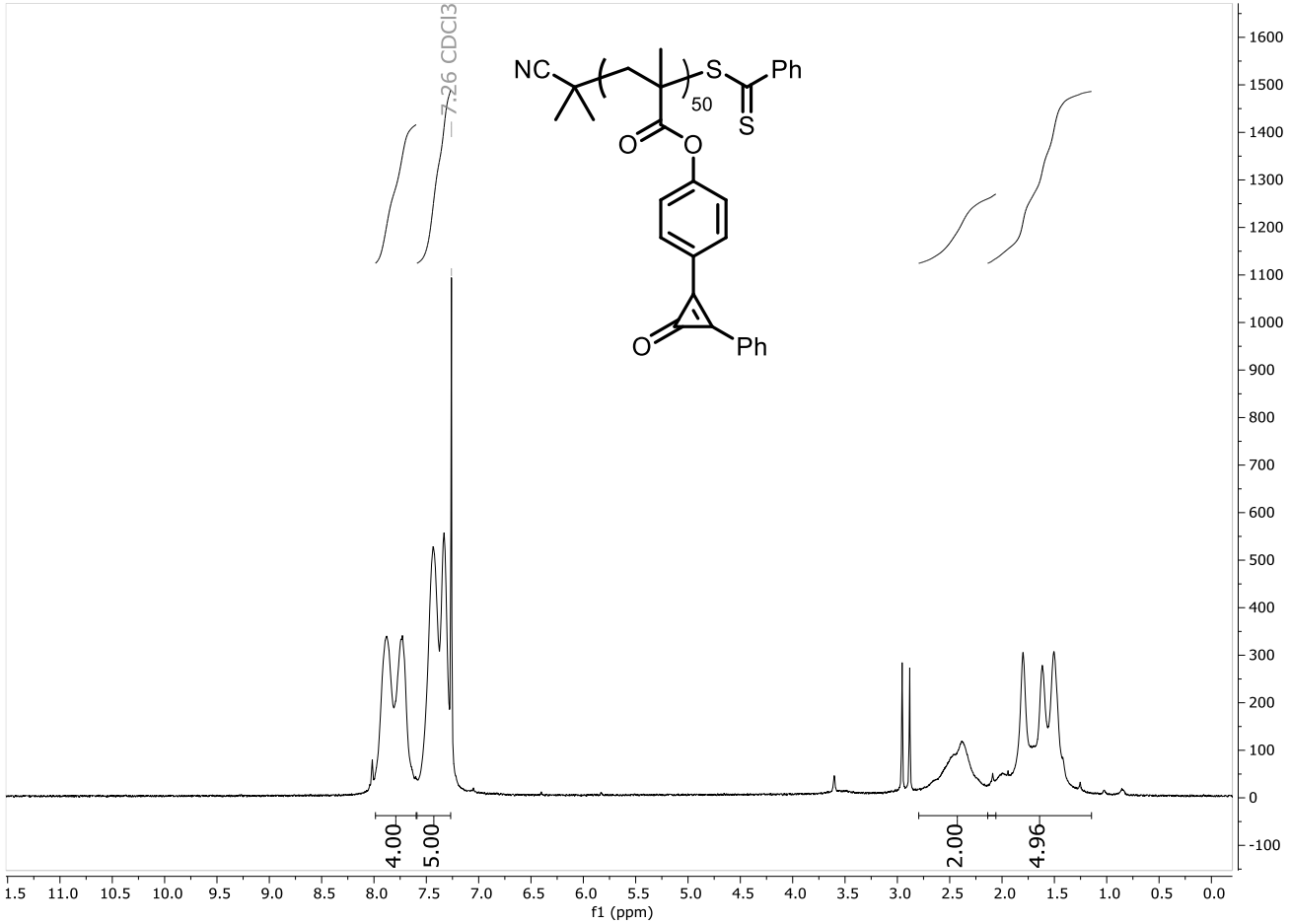
7.26 CDCl3
NC
S
Ph
50
S
O
O
O
Ph
4.00
5.00
2.00
4.96
f1 (ppm)

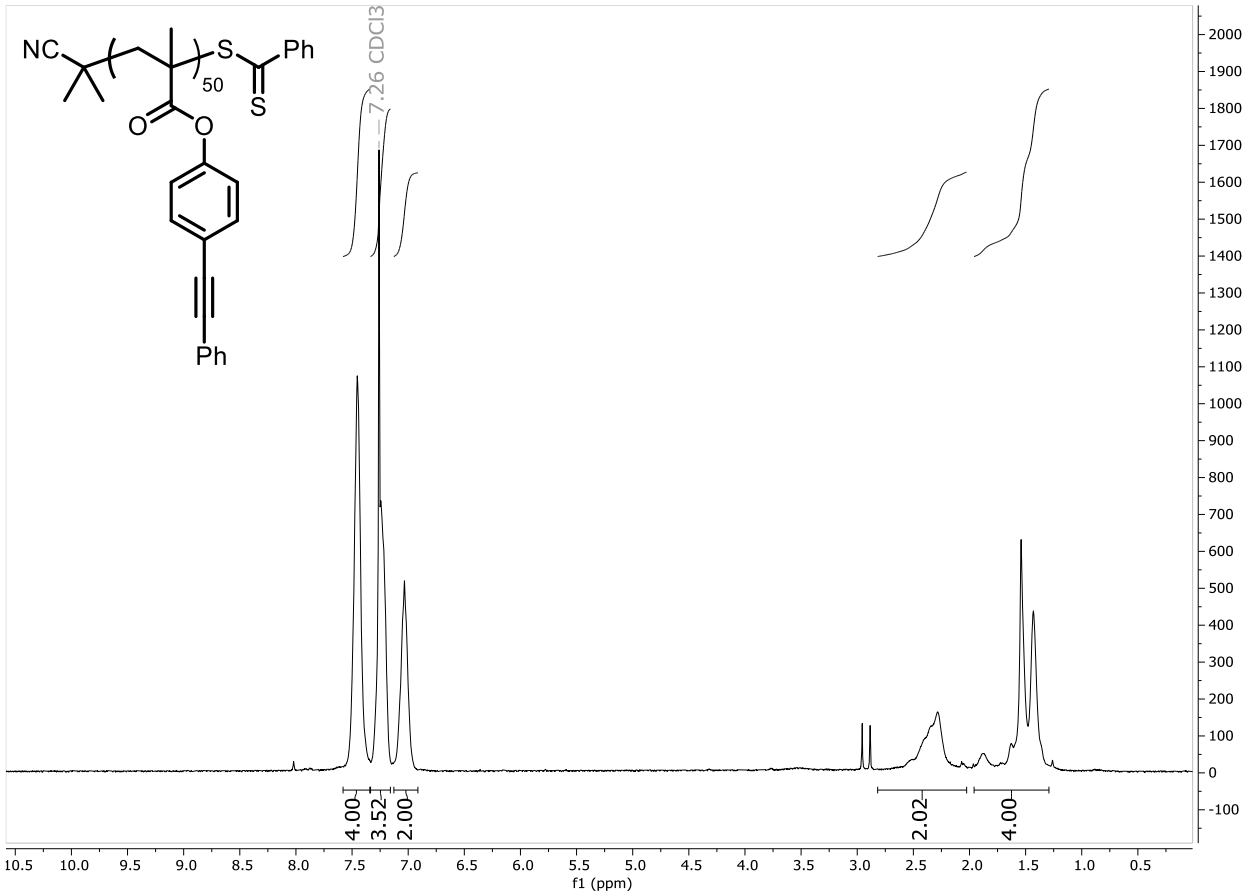
NC
S
Ph
50
S
O
O
Ph
7.26 CDCl3
4.00
3.52
2.00
2.02
4.00
f1 (ppm)

n
O
Ph
7.26 CDCl3
7.00
2.00
1.00
2.31
f1 (ppm)